UNIVERSIDAD NACIONAL DE COLOMBIA-SEDE MANIZALES

Tesis de maestría en Ingeniería _ Ingeniería Química

ESQUEMA DE ANÁLISIS PARA EL CÁLCULO DEL EQUILIBRIO LÍQUIDO VAPOR DE SISTEMAS BINARIOS ASIMÉTRICOS QUE CONTIENEN DIÓXIDO DE CARBONO A ALTAS PRESIONES

SCHEMATIC ANALYSIS FOR THE CALCULATION OF VAPOR LIQUID EQUILIBRIUM FOR ASYMMETRIC BINARY SYSTEMS CONTAINING CARBON DIOXIDE AT HIGH PRESSURES

Víctor Manuel Trejos Montoya

Director: Carlos Ariel Cardona Alzate

Manizales, Colombia 2010

Copyright © Víctor Manuel Trejos Montoya, 2010
Printed by Book Partner, National University of Colombia at Manizales, Colombia

To my brother

Cristian David Trejos

And to my parents,

Víctor M. Trejos and Dolly M. Jaramillo

PREFACE

The thesis is submitted in partial fulfillment of the requirements for the M.Sc. degree at the National University of Colombia at Manizales. This work has been carried out from September 2008 to April 2010 at the Department of Chemical Engineering of National University of Colombia at Manizales under the supervision of Professor Carlos A. Cardona. The project has been financed by the program “Scholarship of Academic Excellence”, from the National University of Colombia at Manizales in the framework of a grant entitled: “*Schematic analysis for the calculation of vapor liquid equilibrium for asymmetric binary systems containing carbon dioxide at high pressures*”.

Víctor Manuel Trejos Montoya

April 6, 2010

ACKNOWLEDGMENTS

I would like to thank to numerous people that played a key role in my M.Sc. studies and contributed positively in one way or another:

- Professor Carlos A. Cardona, my advisor for gave me the opportunity to be a member of the PQCB research group and to develop this interesting project.

- Jimmy A. López, my friend for the immense help and support that he has provided me, as well as their great guidance and their ability to transfer their enthusiasm and knowledge to the people he is working with.

- The National University of Colombia at Manizales, for the financial support through the program "Scholarship of Academic Excellence", which made possible this work.

- Professors Miguel A. Gómez and Javier Fontalvo for their great advice and their inspiration to develop once work good during my stay in the University of Colombia at Manizales.

- My special friend and adviser Paula A. Giraldo for being always there whenever I had a disadvantage. Thank you for have great affection for me.

- My good friends Crsitian F. Triana (Negris), Alexandra Duarte (May), Raúl bedoya, Jorge H. Ramirez, Juan A. Díez (Cazquivano), Julian Silva (Tieso), Alejo Naranjo (Roncho), Monica J. Olaya, Juan Carlos (Muelitas), Ana I. Ramos, Angélica Alzate (Angie), J. Adrian (Adriancito), Jorge A. Moncada (Monky), Jorge I. Rosero (The Saint), Jhon A. Posada, Luis E. (Rolo), Oscar D. Hernández and other good friends who have contributed positively in one way or another in my personal and professional training. Finally, many thank to my family especially my cousin Maritza Montoya and my aunt Sandra Montoya.

CONTENTS

Preface ***i***

Acknowledgments ***ii***

Summary ***vi***

1. INTRODUCTION **1**

2. SUPERCRITICAL FLUIDS: THEIR PROPERTIES, ADVANTAGES AND APLICATIONS **4**

2.1. Introduction…….4

2.2. Applications and advantages of supercritical fluids (SCF)…….5

2.2.1. Supercritical Fluid Extraction (SFE)……6

2.2.2. Applications and advantages of Carbon Dioxide ……8

2.3. Fluid Phase behavior using Supercritical Carbon Dioxide…….……...12

2.3.1. Experimental data for mixtures at high pressure…….16

2.4. Conclusions……..…….…….16

Acronyms……16

References……...17

3. OBJECTIVE FUNCTIONS ANALYSIS IN THE MINIMIZATION OF BINARY VLE DATA FOR MIXTURES CONTAINING CO_2 **22**

3.1. Introduction……22

3.2. Equation of state and mixing rules…….24

3.3. Asymmetric binary mixtures……..26

3.4. Objective functions……28

3.5. Results and discussion……30
3.6. Conclusions……37
List of symbols……38
References……...39

4. MIXING RULES COMBINING AN EQUATION OF STATE WITH FREE ENERGY MODELS (EOS-G^{ex}) FOR ASYMMETRIC MIXTURES CONTAINING CO_2 43
4.1. Introduction……43
4.2. Phase equilibrium using EOS approach……45
4.3. Combined equation of state and excess Gibbs energy model……..……..45
4.3.1 The original Huron-Vidal (HVO) model…...……46
4.3.2 The Michelsen-Huron-Vidal (MHV1) model……48
4.3.3 The Michelsen-Huron-Vidal (MHV2) model……49
4.3.4 Orbey-Sandler modification of the Huron-Vidal mixing rules (HVOS).50
4.3.5 The Wong-Sandler (WS) model……..50
4.4. Results and discussion……54
4.5. Conclusions……61
References……..61

5. PARAMETERS ESTIMATION AND VLE CALCULATION IN BINARY MIXTURES CONTAINING CARBON DIOXIDE + *n*-ALKANES AND *n*-ALKANOLS 63
5.1. Introduction……63
5.2. Equation of state and mixing rules……65
5.2.1. Parameters optimization……66
5.3. Results and discussion……68
5.4. Conclusions……76
List of symbols……...77
References……..78

6. THERMODYNAMIC CONSISTENCY OF EXPERIMENTAL VLE DATA FOR ASYMMETRIC BINARY MIXTURES CONTAINING CO2 AT HIGH PRESSURES 80

6.1. Introduction……80

6.2. Thermodynamic consistency model ……..…….82

6.3. Equation of state and mixing rules…….83

6.4. Asymmetric binary mixtures……..85

6.5. Thermodynamic consistency criteria……..87

6.6. Results and discussion……...88

6.7. Conclusions……99

References……100

List of Captions…….102

APPENDIX A Optimal parameters and deviations……...……105

APPENDIX B Summary of algebraic details for the various mixing rules…...……108

ABSTRACT

The present work provides a framework of vapor-liquid equilibrium analysis for asymmetric binary mixtures containing carbon dioxide at high pressures. The scheme integrates fitted parameters of vapor liquid equilibrium, objective functions, the combination of equations of state models with excess free energy models (EOS-G^{ex}) and the thermodynamic consistency analysis of asymmetric binary mixtures containing carbon dioxide at high pressures, in order to improve the design stages and set ups of equipment operating with supercritical fluids.

RESUMEN

El presente trabajo establece el desarrollo de un esquema de análisis del equilibrio líquido vapor de sistemas binarios asimétricos que contienen dióxido de carbono a altas presiones. Dicho esquema integra el ajuste de parámetros del equilibrio líquido vapor, análisis de funciones objetivo, reglas de mezclado EOS-G^{ex} y consistencia termodinámica de este tipo de mezclas con el fin de mejorar las etapas de diseño y la puesta en marcha de equipos que operan con fluidos supercríticos.

CHAPTER 1

INTRODUCTION

Predicting and correlating thermodynamic properties, as well as the appropriate description of phase equilibria with equations of state (EOS), remains a crucial step in the design of chemical processes such as supercritical fluid extraction (SFE), and petrochemical processes involving asymmetric mixtures. Chemical industry continues developing new products of high added value such as functional materials, paints, detergents, pharmaceuticals and others. The design of processes involving mixtures containing carbon dioxide at high pressures requires thermodynamic models increasingly accurate to allow good exactitude that describe the properties of the systems of interest.

Recently, EOS have been of great importance to calculate physical and thermodynamic properties of pure fluids and fluid mixtures. The calculation of these properties plays a vital role in plant design and process economics. Thermodynamic models for describing the vapor liquid equilibrium (VLE) have increased. Many EOS have been reported in the literature to describe the VLE and the thermodynamic properties of fluid and fluid mixtures. Generally, cubic EOS, provide reliable results for mixtures of hydrocarbons and they have been widely used in the petrochemical industry. However, these EOS exhibit deficiencies for the prediction of thermodynamic properties near the critical point, and do not model the VLE for asymmetric mixtures at high pressures showing high deviations in bubble point and vapor phase concentration.

Furthermore, to analyze the feasibility of supercritical processes extraction, capture and store processes, to design new processes, to analyze and simulate existing processes using carbon dioxide as a solvent in a supercritical state, it is necessary to know the properties and the fluid phase equilibria of the mixtures. Evaluating analysis diagram for accurately predicting the ELV for mixtures containing carbon dioxide at high pressures will improve the design stages and implementation of equipment operating with supercritical fluids. In the same way, it is necessary to generate an integrated analysis diagram that includes the analysis of thermodynamic models, mixing rules, objective functions and thermodynamic consistency for the calculation of VLE for asymmetric binary systems containing carbon dioxide at high pressures.

The thesis is accordingly divided into the following chapters:

- **Chapter 2:** *Supercritical fluids: their properties, advantages and applications*

  This chapter intends to introduce the reader with the properties, advantages, applications and fluid phase equilibrium of supercritical fluids. The structures of the supercritical fluids are discussed taking into account the properties of carbon dioxide. The special solvent properties of supercritical fluids are explained within the framework of binary fluid phase diagrams. Different aspects related to solvent properties, environmental utilities make supercritical fluids desirable agents in the chemical process industry.

- **Chapter 3:** *Objective functions analysis in the minimization of binary VLE data for mixtures containing CO_2*

  This chapter is intended to introduce the reader with the importance of the objective functions analysis in the minimization of binary vapor liquid equilibria (VLE) data for asymmetric mixtures containing carbon dioxide. In this chapter five different objective functions were studied with the purpose of analyzing their performance for parameters estimation of vapor–liquid equilibrium models for asymmetric binary mixtures containing carbon dioxide at high pressures.

  (J.A. López, V.M. Trejos, C.A. Cardona, Objective functions analysis in the minimization of binary VLE data for asymmetric mixtures at high pressures, Fluid Phase Equilibria 248 (2006) 147–157.)

- **Chapter 4:** *Mixing rules combining an equation of state with free energy models (EOS-G^{ex}) for asymmetric mixtures containing CO_2*

  In this chapter is presented the summary for a collection of mixing rules that combine activity coefficient (or excess free energy of mixing) models with equations of state. The original Huron-Vidal (HVO), the modified Michelsen-Huron-Vidal first-order (MHV1), the modified Michelsen-Huron-Vidal second-order (MHV2), the Wong-Sandler (WS), and the modified Orbey-Sandler (HVOS) mixing rules were used for phase equilibrium calculation of asymmetric mixtures containing carbon dioxide.

- **Chapter 5:** *Parameters estimation and VLE calculation in binary mixtures containing carbon dioxide + n-alkanes and n-alkanols*

  In the present chapter, vapor–liquid equilibrium for binary mixtures (CO_2 + *n*-alkane, from methane to 1-decane and CO_2 + *n*-alkanol, from methanol to 1-decanol) was calculated using the binary interaction parameter k_{12} of the second virial coefficient and non-random two liquid model parameters τ_{12} and τ_{21}.

(J.A. López, V.M. Trejos, C.A. Cardona, Parameters Estimation and VLE Calculation in Asymmetric Binary Mixtures Containing Carbon Dioxide + *n*-Alkanols, Fluid Phase Equilibria 275 (2008) 1-7.)

- **Chapter 6:** *Thermodynamic consistency of experimental VLE data for asymmetric binary mixtures containing CO_2 at high pressures*

  In this chapter, the thermodynamic consistency of isothermal vapor-liquid equilibrium data of asymmetric mixtures containing carbon dioxide at high pressures has been evaluated. A method based on the isothermal Gibbs-Duhem equation was used for the test of thermodynamic consistency using an Φ–Φ approach.

  (V.M. Trejos, J.A. López, C.A. Cardona, Thermodynamic consistency of experimental VLE data for asymmetric binary mixtures at high pressures. Fluid phase equilibria, Vol. 230, pp. 1-10, (2010).)

CHAPTER 2

SUPERCRITICAL FLUIDS: THEIR PROPERTIES, ADVANTAGES AND APLICATIONS

This chapter intends to introduce the reader with the properties, advantages, applications and fluid phase equilibrium of supercritical fluids. The structures of the supercritical fluids are discussed taking into account the properties of carbon dioxide. The special solvent properties of supercritical fluids are explained within the framework of binary fluid phase diagrams. Different aspects related to solvent properties, environmental utilities make supercritical fluids desirable agents in the chemical process industry. This chapter will focus on advantages and applications, for example as a media reaction of food and other products and fluid phase using carbon dioxide. The basic knowledge and terminology required for understand the following chapters will be introduced at an elementary level.

2.1. Introduction

One fluid is defined like supercritical when its temperature and pressure exceed its critical temperature and pressure, respectively, while its temperature not far from its critical state. In the Fig. 2.1a, is showed the region when the behavior of the fluid is denominated supercritical state. In *P-T* space, we see only two remarkable features: the vapor pressure curve, indicating the conditions under which the vapor and liquid coexist, and the critical point, at which the distinction between vapor and liquid disappears. In the Fig. 2.1b, is showed the same fluid in a pressure-volume representation. The region corresponding to the supercritical states in Fig. 2.1a is cross hatched in the Fig. 2.1b and 2.1c. The volume, as well as density, enthalpy, energy and entropy are very different variables compared with the temperature and pressure in order to the first figure is very different from the whole of figures. In the Fig. 2.1a, were indicated the critical isotherm $T=T_c$ and the critical isobar $P=P_c$. In the case of a liquid is heated in a partially filled closed vessel the pressure increases, the vapor phase becomes more dense and the liquid less dense. At the critical point the two phases become identical and the phase boundary disappears. Above the critical temperature a liquid phase will not appear regardless of how much the pressure is increased. The critical point is where the difference between the two phases vapor and liquid disappears. The critical isotherm indicated in the Fig. 2.1b, is first isotherm to reach zero slope, indication of infinite isothermal compressibility and incipient stability. The critical isobar in the Fig. 2.1c is the first isobar to reach zero slopes.

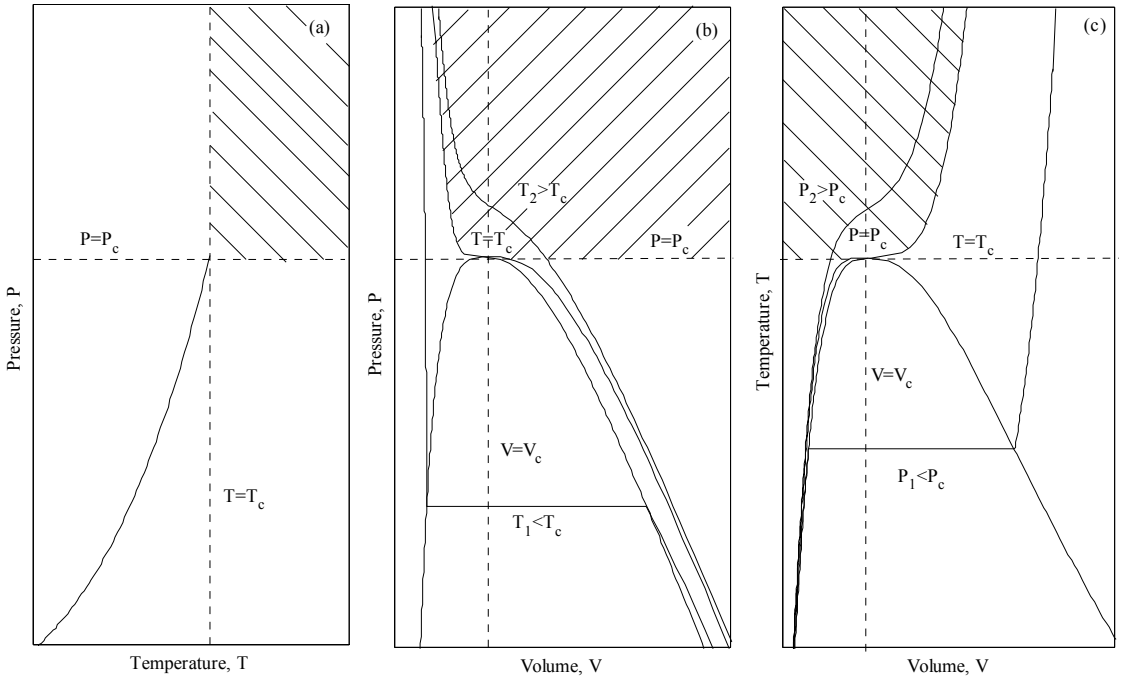

Fig. 2.1 (a). *P-T* phase diagram of a one-component fluid, with the vapor pressure curve and critical point. (b). Same diagram in *P-V* space coexistence curve and several isotherms. (c). Same diagram in *T-V* space coexistence curve and several isobar. The cross-hatched region is considered supercritical.

In summary, a fluid is critical when the difference between coexisting liquid and vapor phases disappears. At this point the isothermal compressibility of the one phase fluid becomes infinite. In the supercritical region, a state of liquid-like density can transform into one of vapor-like density by tuning the pressure or the temperature without appearance of an interface.

2.2. Applications and advantages of supercritical fluids (SCFs)

In the last two decades numerous researchers have investigated the fundamentals and process applications of SCFs. Preliminary studies reveal that SCF extraction is a potential separation technology, which requires lower energy and has other advantages over traditional separation processes [1]. During the same period SCFs technology, mainly based on carbon dioxide, have found applications in many fields, such as separations, chemical reactions, particle micronization and materials processing, due to its tunable solvent power, good transport properties and very low interfacial tensions. These applications involving SCFs include supercritical fluid fractionation, SCF chromatography, use as a replacement solvent for green chemistry, and anti-solvent applications [2]. Supercritical fluids more and more have been proved as environmentally benign media for chemical and related processes. Many new processes and products have been developed, using the inherent physical and chemical properties of SCFs. Moreover, these processes also promise economic effects. The prerequisites for this success however, are a sound knowledge of

physico-chemical properties of and phenomena in supercritical mixtures and the availability of other chemical engineering data.

Many applications and advantages for SCF have been presented in the literature:

- Yoon et al. [3] have studied the SCF extraction of specific materials such as ethanol, lactic acid, and pharmaceuticals from bioproducts of fermentation and it is the powerful recovery process, since it has the ability to break the azeotropic limit of the solutions containing target materials and does not damage fermentation bioproducts.

- Pereda et al. [4] shown that operation at supercritical conditions offers many interesting properties, such as: higher solubility of reactants and products in the supercritical phase; reduced deposition of reacting components on the catalyst pores; diffusion coefficients higher than liquids; independent control of the concentration of permanent gases like H_2 or O_2 or CO in the reaction mixture; higher thermal capacity and low interfacial tension among others.

- The commercialization of coffee decaffeination by supercritical fluid extraction (SFE) is one of the best known processes of interest. Other SFE processes related to the food industry include hops resin extraction, tea decaffeination, and the SFE of a wide variety of aromas and colors as well as fats and oils [5].

- Properties, such as liquid like density, low viscosity and high diffusivity, between others are increased the interest for SFE. Supercritical fluid technologies have been widely developed and applied in diverse fields, for example, extraction of metabolites [6-7], particle-forming techniques [8-10], pharmaceutical industries [11-13], food and biomaterials [14] and polymerization [15-16].

2.2.1. Supercritical Fluid Extraction (SFE)

In SFE, instead of a liquid solvent a SCF is used for extracting specific compounds from a solid or liquid matrix. A simple schematic of this process is shown in the Fig. 2.2. In the left-hand side of each of the figures, the pressurized SCF is introduced inside reactor. Its pressure and temperature are chosen as for dissolve most of the desired compound feasible. The pressure is quenched at the entrance to a vessel that receives the reaction product. The solvent expands and released the solute, which collects at the bottom of the receptable, while the gas is released from the top repressurized and recirculated.

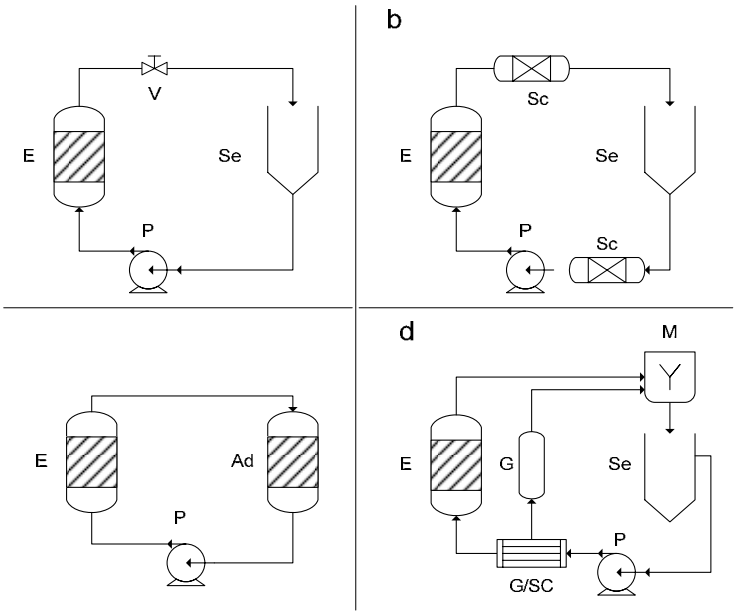

Fig. 2.2 Esquematic of supercritical extraction. P-Compressor, E- extraction vessel; Se- Separation vessel, V- expanssion valve; Sc- heat exchanger, G-antisolvent supply, G/SC- separator of antisolvent and SCF; M- mixing port [17].

Recently many applications for SFE have been presented in the literature, such as, production of controlled drug in delivery systems; powder processing, pollution prevention and remediation, methods for spraying paints and coatings, precipitation/crystallization processes, bio-separations, and food processing among others. Many other applications for SFE are discussed below:

- SFE has been used to extract antioxidants from natural matrices. However, due to the limited amount of experimental data currently available and the need for extensive data, to establish the solubility behavior in SCFs, is about great interest in thermodynamic models that are able to predict the phase behavior of such systems [18].

- Kim et al. [19] have made studies that have been concentrated on the extract quality and the influence of the operating parameters (pressure and temperature) on the yield of the extract, its quality, and its solubility in the solvent. This study used the general equations for the process of SFE similarly to mass transport operations involving solids and fluids such as leaching and adsorption/desorption processes.

- SFE has been demonstrated as a technically viable alternative, extraction and refining processes both. Their high selectivity leads to obtain, in single step or sequential extractions, commercial oil fractions with all quality parameters according to food normative [20-21]. In spite of the large variety of applications proposed in literature, pilot scale or industrial applications for vegetable oils extraction are limited. The only economically feasible SFE application to vegetable oils would involve the isolation of high valuable compounds or using high-scale continuous countercurrent operation.

- The purity and the quality of the obtained products using SFE overcome thoroughly the products obtained by conventional extractions using liquid-solvents. Their main disadvantage is the relatively high cost of the equipment required to carry out the process. Compared with liquid solvents, the SCF has a major capacity of dissolution, higher diffusion coefficients, viscosity and lower superficial tension that a liquid-solvent [22].

- Supercritical extraction processes of natural products usually require a cosolvent, a substance that serves to release the product of interest from the matrix of source materials such as limonene from lemon peels, astaxantine from micro algas, or caffeine from coffee grains, just to name some. Although water is the preferred cosolvent for the extraction of natural products, sometimes *n*-alkanols of low and high molecular weight are needed [23-25]. For example, the study of these mixtures is of special interest in the extraction of biomolecules with $SCCO_2$ [26-27], in the extraction of *n*-alkanols from aqueous solutions with carbon dioxide [28], and in the production of *n*-alkanols from syngas [29].

- Finally, many new processes and products that have been developed recently need of experimental data and the previous knowledge of the inherent physiochemical properties to the SCF. These aspects have allowed become the SCF in a more and more attractive option to carry out many chemical processes the suitable way (green chemistry).

2.2.2. Applications and advantages of supercritical carbon dioxide ($SCCO_2$)

Numerous researchers have investigated the fundamentals and process applications of SCFs. Supercritical fluids have advantages such as excellent mass transfer and control of solubility by temperature and pressure. Other processes also take advantage of the high diffusivities possible with SCFs. Carbon dioxide is the most widely used SCF. Carbon dioxide is nontoxic, non-flammable and is available at low cost with a high degree of purity non-reactive, does not leave any solvent residues in soil and is relatively inexpensive. Carbon dioxide has a technically convenient critical pressure (73.8 bar) and critical temperature (31°C) that allow supercritical operation of thermally labile compounds [30]. This let many applications and advantages of $SCCO_2$.

Other advantages of $SCCO_2$ are such as, environmentally friendly, readily available, easily removed, without evaporation or heating, and this will save electricity. $SCCO_2$ could be adjusted for selective separation and enhancement in separation rate, due to the low viscosity and high diffusivity. The carbon dioxide has been recognized as an environmentally benign solvent and has attracted much attention in many chemical processes, such as extraction and fractionation, chemical reactions, and material processing [23-24]. $SCCO_2$ has been utilized widely in biochemistry, material cleaning, food processing, material preparation, supercritical chromatography, and so forth. The advantages of $SCCO_2$ are such as, readily available, easily removed, without evaporation or heating, and this will save electricity. $SCCO_2$ could be adjusted for selective separation and enhancement in separation rate, due to the low viscosity and high diffusivity. For instance, the extraction of natural substances from solid matrices in packed beds forms is the basis of most present day commercial scale in SCF extraction. Therefore, many advantages and applications for $SCCO_2$ have been presented in the literature:

- Carbon dioxide is abundant and is commercially produced by recovery from flue gases, from fermentation gases in breweries and from ammonia and hydrogen plants. Pure $SCCO_2$ is a non-polar solvent. Close to the critical point it has a solubility parameter similar to liquid pentanes. The solubility parameter increases with pressure. Pure $SCCO_2$ is good solvent for hydrocarbons and non-polar solids. The solubility of a solute in $SCCO_2$ increases with the solute is vapor pressure. Short chain alcohols, for example, are quite soluble into $SCCO_2$ despite of their high polarity.

- Polar solids, such as carbohydrates and proteins are practically insoluble in $SCCO_2$. A very efficient way to enhance the solubility of polar, non-volatile solutes into $SCCO_2$ is to add small amounts of polar co-solvents, entrainers, in the bulk carbon dioxide. Water and short-chain alcohols are efficient and usually the most acceptable co-solvents in industrial practice. The non-polarity of $SCCO_2$ only the organic, non-polar or volatile pollutants are expected to be effectively extracted from soils by carbon dioxide extraction.

- The SCFs such as $SCCO_2$ have encouraged many studies of their uses as solvents in a wide range of materials applications. Though $SCCO_2$ is non-polar and hence not suitable for carbohydrates separation, yet previous studies have shown that using a polar organic cosolvent (or cosolvent) can increase considerably the solubility of carbohydrates in $SCCO_2$ [25].

- The use of SCF as solvents is of great interest because their liquid like solvency and gas like transport features; specific interest in carbon dioxide is magnified by its perceived green properties such as non flammability, relative non toxicity, and relative chemical inertness. The dipole of carbon dioxide is almost zero, rendering poor solvency for polar substances. So, usually modifiers or entrainers are used to improve its solvent character; the characteristics they impart include polarity, aromaticity, chirality, between others. Acetone, toluene, and monochlorobenzene are commonly used solvents in the chemical and polymer industry. They are also commonly used as cosolvents to modify carbon dioxide [26].

- Organic solvents expanded by $SCCO_2$ could become alternative media reaction. Many reports on the use of SCFs as media reaction several studies on enzymatic oxidation, hydrolysis, transesterification, esterification, interesterification, enantioselective synthesis have proven the feasibility of enzymatic reactions in SCFs [27-30]. Hammond et al. [31], Nakamura [32] have presented benefit of use SCFs along with enzymatic catalysis that it provides a medium for the recovery of products or reactants [33].

- Carbon dioxide has been used to replace toxic and more expensive solvents with the purpose of avoiding residual quantities of such solvents in the product, and to eliminate the disposition and waste treatment. Additionally, the use of $SCCO_2$ like a process fluid allows eliminating additional stages of sterilization. Indeed, with carbon dioxide has been proved is possible disable bacteria to moderate temperatures without corrupting organic components, reason why, this substance has been used for sterilize foods and drinks, otherwise as bloods and plasma. The $SCCO_2$, as well as other fluids in supercritical conditions, offer the possibility to reduce the reactor size and to increase the conversion with the purpose of accelerating the chemical process. In some specific cases the product purity compensates the costs that generate the high pressures use in the equipment [34-36].

- Xiaoting et al. [37] used $SCCO_2$ as a media reaction to synthesize a number of 1-methylimidazole-based ionic liquids. This is an important industrial material that is used as intermediate for pharmaceuticals, agrochemicals, dyes, textile auxiliaries, pigments and other organic chemicals, and as a catalyst for polyurethanes and epoxy resins.

- Sánchez et al. [7] take advantage of SFE to obtain oil from seeds of many materials with apricot, palm, and canola among others. They found that a carbon dioxide solvent property has been adequate for extraction of triglycerides. The addition of a small amount of a liquid modifier such as ethanol can enhance significantly the extraction of polar compound.

- Laitinen et al. [38] showed a review in environmental technology using $SCCO_2$ as solvent for non-polar solids and volatile compounds. $SCCO_2$ effectively were used to extract non-polar compounds from all soil types. For instance the $SCCO_2$ were used to dissolve hydrocarbons, polyaromatic hydrocarbons (PAH's), chlorinated hydrocarbons (such as PCB's and dioxins), phenols, chlorinated phenols and many pesticides and herbicides.

- Oliviera and Oliviera [39] recently have employed $SCCO_2$ as a solvent in enzyme-catalyzed reactions and it has had a matter of considerable research because its favorable transport properties can accelerate mass-transfer-limited enzymatic reactions.

- Zeljko and Habulin [40] studied the application of SCFs and liquid gases as an alternative reaction medium for enzyme-catalyzed reaction. This study shows that many researches should be oriented to novel materials for use of carbon dioxide as a solvent. These materials have important applications in the synthesis of polymers, pharmaceuticals and other commodity chemicals, in the formation of thin films and foams, in coatings and extractions and in the manufacturing of microelectronics circuits.

- Habulin et al. [41] have shown the SCF extraction importance of esters as the isoamyl acetate, ethyl caproate and ethyl laureate are widely used in the cosmetic, pharmacist and foods industry. The production of these compounds is generally carried out by chemical synthesis, but the use of toxics organic solvents for to obtain this products has being more and more restricted and consequently, the extraction with SCFs like the carbon dioxide is nowadays one the most interesting industrial alternatives for the production of them.

- Baiker [42] has employed $SCCO_2$ like attractive options for gas–liquid catalyzed reactions. These reactions are diffusion-controlled and the use of SCFs increases the reaction rate by eliminating the gas–liquid interface.

- Motonobu et al. [6] have employed carbon dioxide for the treatment of natural materials because its low critical temperature, absence of residual problems, odorless, colorless, nontoxic, nonflammable and inexpensive nature of the solvent. Besides SCFs extraction has been focused for the fractionation of citrus oil as a lower-temperature process.

- Hegel et al. [43] have studied the application of propane + carbon dioxide solvent mixture to the extraction of vegetable oils from ground seeds paying attention to the system phase behavior. These considerations suggest that propane + carbon dioxide mixtures could offer

special properties regarding solvent power, selectivity and safety (non-flammable mixtures) in vegetable oil extraction processes.

- Li et al. [44] presented the VLE data for the mixture tetrahydrofuran + carbon dioxide (THF/CO_2) and its correlation with a convenient equation of state. This study is important because the use of THF as a co-solvent may be useful to overcome solubility difficulties in many supercritical processes, such as the supercritical anti-solvent (SAS) process using carbon dioxide as the SCF.

- Houndonougbo et al. [45] have shown the carbon-dioxide expanded liquids (CXLs) as promising alternate media for performing catalytic reactions, such as homogeneous catalytic oxidations, hydroformylation and solid–acid catalyzed-reactions. The replacement of current solvents with more benign alternatives has become a necessity. This concern is because many common industrial solvents usage in chemical industries are high volatility and toxic nature.

- Knox [2] has found a wide variety of applications for solubilities in SCFs. These applications include: production of controlled drug delivery systems, powder processing, pollution prevention and remediation, methods for spraying paints and coatings, precipitation/crystallization processes, bio-separations, and food processing.

- Chen et al. [46] studied the experimental VLE data for carbon dioxide + isobutanol, carbon dioxide + 2-butanol, and carbon dioxide + tertbutanol systems. These studies greatly contribute to the developments of SCF technologies. Especially, short-chain alcohols extensively served as model substances to study the phase behavior of SCF + polar substance systems. For instance butyl alcohols can be solvents, entrainers, modifiers, and simulators for SCF extraction, SCF chromatography, biomaterials, and so forth.

- López et al. [47-48] have studied a wide quantity of mixtures that has great importance in the extraction with carbon dioxide in supercritical conditions. Some this mixtures containing carbon dioxide for example, the limonene and linalool are the main compounds that the citric oil made up. The linalool is one of the most important fractions of this oil and it is very common to remove the limonene to concentrate oxygenated compounds as the linalool. The study of mixtures as carbon dioxide + styrene has a great importance in the petrochemical industry. The styrene is usually produced by ethylbenzene dehydrogenation because the reaction is not complete, the separation of the mixture styrene + ethylbenzene using $SCCO_2$ like solvent it is a method more attractive. Additionally, some works have shown that polystyrene synthesis starting from the styrene polymerization in $SCCO_2$ has great importance [49-51].

- Robertson and Lester [52] have proved the SCFs intensively like a very good alternative in many chemical processes such as the extraction of herbicides like *s*-triazina and associate compounds using $SCCO_2$.

- Hauthal [1] exposed many applications for supercritical solutions process, e.g., allows the production of powders with a narrow distribution curve of the particle sizes, which is very important for the applications of those powders in several industrial branches.

- Tai and Brunner [53] studied the enzymatic synthesis of glucose palmitate in acetone, and simultaneously removing water using high-pressure carbon dioxide.

- Montañés et al. have evaluated the selectivity and yield obtained for the fractionation of binary carbohydrate mixtures such as lactose–lactulose, galactose–tagatose, and complex commercial carbohydrates mixtures. They have been studied and compared the solubility of four important pure carbohydrates tagatose, galactose, lactulose and lactose in $SCCO_2$ with the appropriate extraction conditions to fractionate prebiotic sugars from complex carbohydrate mixtures [54-57].

- Riha and Brunner [58] shown a study where vegetable oils are usually recovered from natural matrixes by pressing and/or solvent extraction procedures. Crude vegetable oils are submitted to refining processes for purification and to avoid degradation reactions.

Finally, different authors showed different reviews about advances and applications with SCFs that give summaries of applications using SCFs, some are: McHugh and Krukonis [59], Taylor [60], Gopalan et al. [61], Aymoniera et al. [62], Abraham and Sunol [63], and Johnston and Penninger [64], among others. Many texts in physical chemistry and thermodynamics address the physical basis and description of SCFs [65-67]. Methods for the experimental determination of solubilities in SCFs are reviewed by Aim and Fermeglia [68]. Methods for the calculation/estimation of solubilities are addressed by Prausnitz et al. [69]. Hauthal, [1] published a review of the recent advances with SCFs that included approximately 200 references. Meireles [70] has reviewed recent developments in SFE from solid substrates. Dehghani and Foster, [12] reviewed antisolvent processes for pharmaceutical formulation. Senorans et al. [71] reviewed the newest trends in food processing and prominently featured the use of SCF technology. Zougagh et al. [72] reviewed the use of SFE as an analytical tool. This sampling of recent review articles demonstrates the great interest that exists in applications of SCFs.

2.3 Fluid Phase behavior using supercritical carbon dioxide ($SCCO_2$)

Thermodynamic properties are necessary to describe the fluid phase behavior of carbon dioxide like the critical point CP (T_c=304.128±0.015) K, (P_c=73.773±0.003) bar, (V_c=2.1386±0.0006) cm^3/g where the two coexisting phases (liquid and vapor) become identical. When the pressure decrease appear the triple point *Tr* (216.58 K, 0.5185 MPa), where solid, liquid, and gaseous carbon dioxide are in equilibrium. In Figs. 2.3, 2.4 and 2.5 are shown the *P*-*T*, *P*-*V* and *T*-*V* diagrams for pure carbon dioxide.

The information about diagram of fluid phase equilibrium of carbon dioxide is important for propose ranges of temperatures and pressures, in which various separation methods (such as distillation, liquid extraction, gas cromatography (GC), supercritical fluid extraction (SFE), and cromatography) are normally performed. Chemical processes and separation operations that are conducted at high pressures, knowledge of the phase behavior is of special interest, mainly for SCF processes, where phase behavior can significantly influence the reaction rate, selectivity, mass transfer properties, among others [73-75].

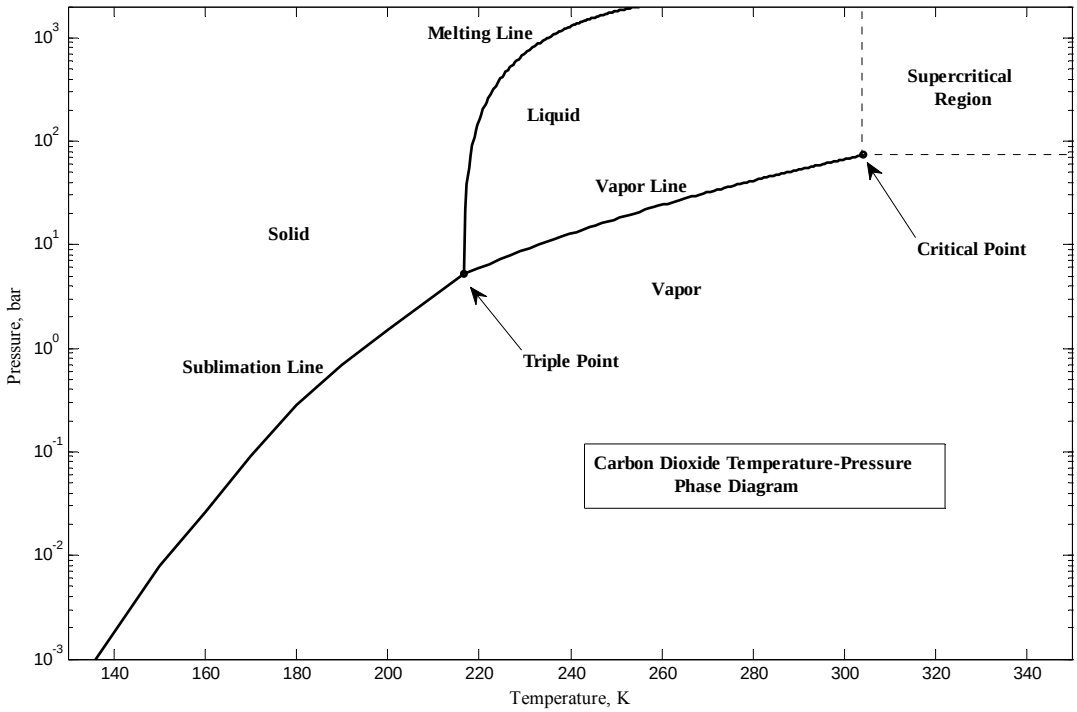

Fig. 2.3 Carbon dioxide temperature-pressure phase diagram showing the triple point and critical point of carbon dioxide. Experimental data taken from Span and Wagner [76] and Angus et al. [77].

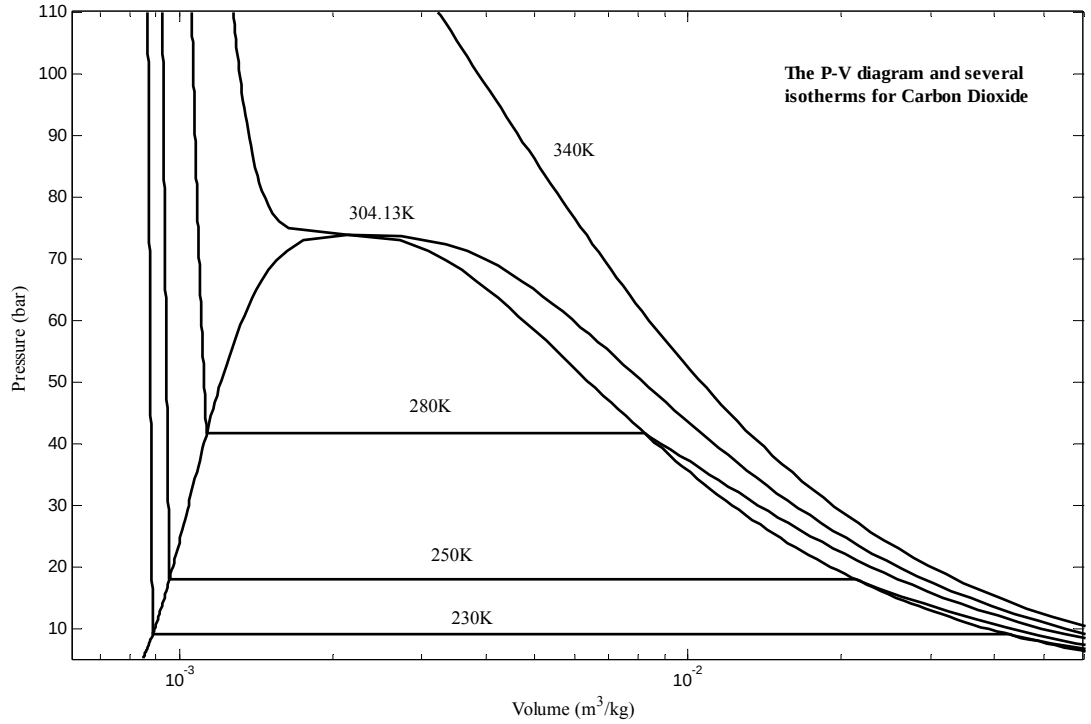

Fig. 2.4 The *P-V* diagram and isotherms of pure carbon dioxide. Experimental data taken from Span and Wagner [76].

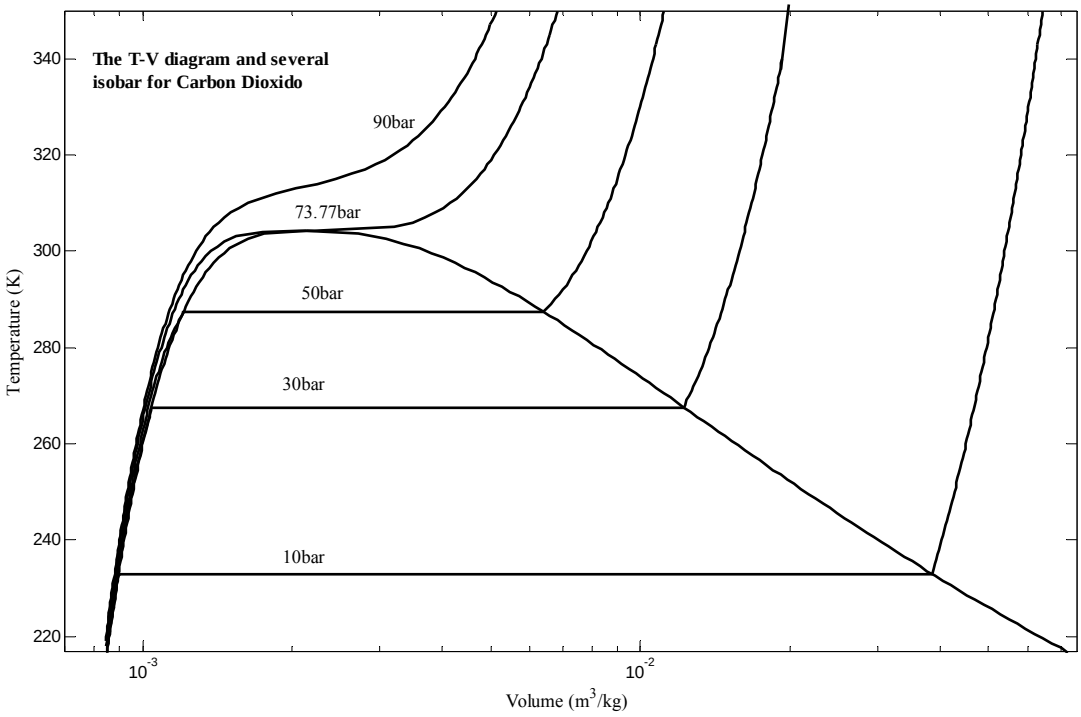

Fig. 2.5 The T-*V* diagram and isobars of pure carbon dioxide. Experimental data taken from Span and Wagner [76].

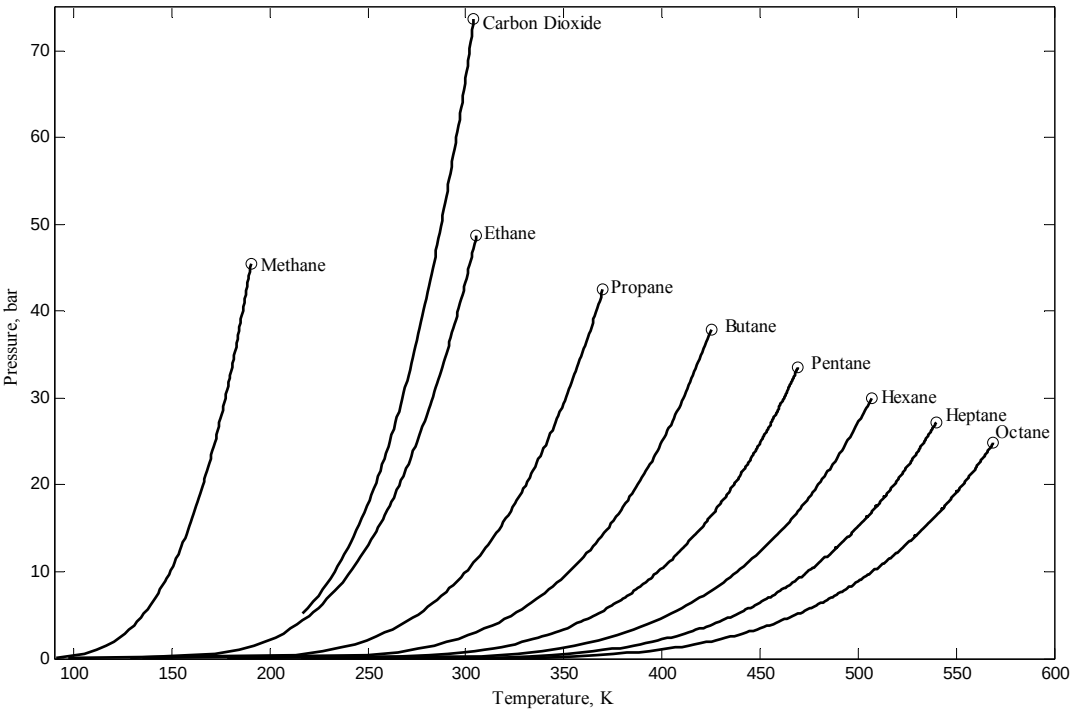

Fig. 2.6 The vapor pressure curves of pure carbon dioxide. Experimental data taken from Span and Wagner [76].

Phase diagrams for both pure components are the boundaries of a binary system and determine their phase behavior. Fig. 2.6 shows the vapor pressure curves of *n*-alkanes (from methane to *n*-octane) and the carbon dioxide. Heavier *n*-alkanes follow the tendency, becoming less volatile the increasing molecular weight or carbon number.

- Information about high-pressure phase equilibria is essential for many chemical processes and separation operations that are conducted at higher pressures. In particular, the interest in SFE processes has lead to an increase in the number of publications concerning high-pressure phase equilibrium data. Information about experimental equilibrium data is important, even when thermodynamic models are used to calculate the phase behavior of a mixture. Thermodynamic models can help to reduce the number of experimental data points needed for a special design problem. But often, at least some experimental data points are needed to adjust interaction parameters of the model. Of course, the expression ("high-pressure") is relative; we chose 1MPa as the lower limit: a paper was considered to contain high-pressure data if at least one data point was measured at a pressure of 1MPa or higher [78]. Many difficulties in the VLE calculations for SCFs are:

- The high complexity and asymmetry the mixtures compound + carbon dioxide are a great difficulty for supercritical processes evaluation [79]. Thus, VLE calculation requires of improved versions of the EOS. Among the many cubic EOS of van der Waals type currently available, the equation proposed by Peng and Robinson [80] is widely used due to its simplicity and flexibility [81]. Cubic equations of state incorporated with various mixing rules have been applied in high-pressure VLE calculations for estimating the phase equilibria. Several authors [82-85] have proposed various local composition mixing rules to use binary interaction parameters. Although these local composition mixing rules have been successfully applied to both the low- and high-pressure VLE systems, these models could not be correctly applied to the multicomponent systems containing very similar components and the systems at low-density limit conditions [86]. Different mixing rules using models EoS-G^{ex} have been developed for describe the VLE of asymmetric mixtures containing carbon dioxide. Models based in the zero-pressure model [87-88] and the infinite-pressure model [89]. Their capabilities and limitations for asymmetric systems have been discussed in some works [90-91]. VLE at high pressures can be calculated using the available values at low pressures of the activity model parameters. But sometimes, in the case of highly asymmetric mixtures as those containing carbon dioxide, these values are not available. In such case, it is more convenient to calculate the parameters of the activity coefficient models from VLE data using an adequate minimization algorithm and an appropriate objective function. This procedure should have a moderate computing time requirement and a well accuracy in the phase equilibrium prediction.

- Researchers have studied group contribution equations methods for predicting thermodynamic equilibrium in SCF processes, as a great variety of natural products can be represented with a limited number of functional groups.

2.3.1. Experimental data for mixtures at high pressure

- The computer aided design, simulation and optimization of chemical processes has had an impressive growth during the last decades. The analysis of SCF processes requires the support of simulation tools based on rigorous modeling of complex phase equilibrium behavior. There are many ways to obtain information about the phase behavior of fluid mixtures. The direct measurement of phase-equilibrium data remains an important source of information, though is difficult and expensive to take precise experimental data. Information about experimental equilibrium data is important, even when thermodynamic models are used to calculate the phase behavior of a mixture. Thermodynamic models can help to reduce the number of experimental data points needed for a special design problem. In the same way, due to the limited amount of experimental data currently available and the need for extensive data to establish the solubility behavior in SCFs, there is great interest in thermodynamic models that are able to predict the phase behavior of such systems.

- The development of thermodynamic models to describe the phase equilibrium in supercritical processes has been possible thanks to the wealth of experimental data that have been presented in the literature on high-pressure phase equilibria. A very extensive review of systems studied and the applied experimental techniques has been presented by Dohrn and Brunner [92]. Phase equilibria data are required for basic calculations in practical designs of a supercritical process. However, very few data have been published concerning the phase equilibria measurements of complex systems at high pressures. By means of drying in $SCCO_2$, fine particles with high porosity and large surface area can be obtained [93].

2.4. Conclusions

Properties, advantages, applications advantages and fluid phase equilibrium of SCFs were discussed. In the same way, different aspects related to solvent properties, environmental utilities, advantages, applications fluid phase diagrams and fluid phase using carbon dioxide were presented. Finally, were showed as SFE and SCF chromatography, SCFs mixtures have increasing interest for a variety of chemical industrial processes and other applications. At the same time the development of supercritical processes accompanied by improved models to describe the phase equilibrium of multicomponent mixtures at high pressures, and the prediction of physicochemical properties, viscosities, diffusivities and thermal conductivities in supercritical media were presented. The discussion of these methods together with rigorous mathematical modeling of different unit operations opens the way to the application of computer modeling and optimization of supercritical processes, which has great interest, considering the cost of high-pressure pilot plant facilities and industrial scale experimentation.

Acronyms

(SFE): Supercritical Fluid Extraction
($SCCO_2$): Supercritical Carbon Dioxide
(SCF): Supercritical Fluid
(CO_2): Carbon Dioxide

References

[1] Hauthal, W. H. Advances with supercritical Fluids (review) Chemosphere, 43 (2001) 123-135.
[2] Dana E. Knox, Solubilities in supercritical fluids. Pure Appl. Chem., 77 (2005) 513–530.
[3] Ji-Ho Yoon, Moon-Kyoon Chun, Won-Hi Hong, and Huen Lee. High-pressure Phase Equilibria for Carbon Dioxide-Methanol-Water System: Experimental Data and Critical Evaluation of Mixing Rules. Ind. Eng. Chem. Res. 32 (1993) 2881-2887.
[4] S. Pereda, E.A. Brignole, S.B. Bottini, Advances in phase equilibrium engineering of supercritical reactors. J. of Supercritical Fluids 47 (2009) 336–343.
[5] Carol A. Patterson. The commercialization of coffee decaffeination by supercritical fluid extraction (SFE). Technology watch, Pathfinders, 2 (2005) 1-5.
[6] Motonobu Goto, Masaki Sato, Akio Kodama, Tsutomu Hirose. Application of supercritical fluid technology to citrus oil processing. Physica 239 (1997) 167-170.
[7] Yolanda Sánchez-Vicente, Albertina Cabañas, Juan A.R. Renuncio, Concepción Pando, Supercritical fluid extraction of peach (Prunus persica) seed oil using carbon dioxide and ethanol. J. of Supercritical Fluids 49 (2009) 167–173.
[8] Matson, D. W.; Fulton, J. L.; Petersen, R. C.; Smith, R. D. Rapid Expansion of Supercritical Fluid Solutions: Solute Formation of Powders, Thin Films, and Fibers. Ind. Eng. Chem. Res. 26 (1987) 2298-2306.
[9] C. Wai, M.; H. Ohde, Synthesizing Nanoparticles in Supercritical Carbon Dioxide. J. Chin. Inst. Chem. Eng. 32 (2001) 253-261.
[10] Ji, M.; Chen, X.; Wai, C. M.; Fulton, J. L. Synthesizing and Dispersing Silver Nanoparticles in a Water-in-Supercritical Carbon Dioxide Microemulsion. J. Am. Chem. Soc. 1999, 121, 2631-2632.
[11] Subramaniam, B.; Rajewski, R. A.; Snavely, K. Pharmaceutical Processing with Supercritical Carbon Dioxide. J. Pharm. Sci. 86 (1997) 885-890.
[12] Charoenchaitrakool, M.; Dehghani, F.; Foster, N. R. Micronization by Rapid Expansion of Supercritical Solutions to Enhance the Dissolution Rates of Poorly Water-Soluble Pharmaceuticals. Ind. Eng. Chem. Res. 39 (2000) 4794-4802.
[13] Kim, J. H.; Paxton, T. E.; Tomasko, D. L. Microencapsulation of Naproxen Using Rapid Expansion of Supercritical Solutions. Biotechnol. Prog. 12 (1996) 650-661.
[14] Eissler, R. L.; Friedrich, J. P. Estimation of Supercritical Fluid- Liquid Solubility Parameter Differences for Vegetable Oils and Other Liquids From Data Taken with a Stirred Autoclave. J. Am. Oil Chem. Soc. 65 (1988) 764-767.
[15] Kendall, J. L.; Canelas, D. A.; Young, J. L.; DeSimone, J. M. Polymerizations in Supercritical Carbon Dioxide. Chem. Rev. 99 (1999) 543-563.
[16] Hénon, F. E.; Camaiti, M.; Burke, A. L. C.; Carbonell, R. G.; DeSimone, J. M.; Piacenti, F. Supercritical CO_2 as a Solvent for Polymeric Stone Protective Materials. J. Supercrit. Fluids 15 (1999) 173-179.
[17] Erdogan Kiran, Pablo G. Debenedetti and Cor J. Peters. Supercritical fluids, fundamentals and applications. Series E: Applied Sciencies vol 366, Published by Kluwer Academic Publishers 1994.
[18] Marleny D.A. Saldaña, Bruno Tomberli, Selma E. Guigard, Saul Goldmand, Chris G. Gray b, Feral Temelli. Determination of vapor pressure and solubility correlation of phenolic compounds in supercritical CO_2. J. of Supercritical Fluids 40 (2007) 7–19.
[19] Wan-Joo Kim, Jae-Duck Kim, Seong-Geun Oh. Supercritical Carbon Dioxide Extraction of Caffeine from Korean Green Tea. Separation Science and Technology, 42 (2007) 3229–3242.
[20] Lucas A. , Rincón J., I. Gracia, Influence of operation variables on yield and quality parameters of olive husk oil extracted with supercritical carbon dioxide, J. Am. Oil Chem. Soc. 79 (2002) 237.
[21] Lucas A. de, J. Rincón, I. Gracia, Influence of operation variables on quality parameters of olive husk oil extracted with CO_2: three-step sequential extraction, J. Am. Oil Chem. Soc. 80 (2003) 181-187.

[22] Lijun Wang, Curtis L. Weller, Vicki L. Schlegel, Timothy P. Carr and Susan L. Cuppett. Supercritical CO_2 extraction of lipids from grain sorghum dried distillers grains with solubles. Bioresource Technology, 99 (2008) 1373-1382.
[23] D.W. Jennings, R.J. Lee, A.S. Teja, Vapor–liquid equilibria in the CO_2-ethanol and CO_2-1-butanol systems, J. Chem. Eng. Data 36 (1991) 303–307.
[24] M. Artal, V. Pauchon, J. Muñoz, J. Jose, Solubilities of 1-nonanol, 1-undecanol, 1-tridecanol, and 1-pentadecanol in supercritical carbon dioxide at T = 323.15 K, J. Chem. Eng. Data 43 (1998) 983– 985.
[25] O. Elizalde - Solis, L.A. Galicia-Luna, S.I. Sandler, J.G. Sampayo- Hernandez, Vapor–liquid equilibria and critical points for the carbon dioxide + 1-hexanol and carbon dioxide + 1-heptanol systems, Fluid Phase Equil. 200 (2002) 161–172.
[26] S.T. Schaeffer, Zalkow L., A.S. Teja, Solubility of monocrotaline in supercritical carbon dioxide and carbon dioxide-ethanol mixtures, Fluid Phase Equil. 43 (1988) 45–56.
[27] J.M. Wong, Johnston K.P., Solubilization of biomolecules in carbon dioxide based supercritical fluids, Biotechnol. Prog. 2 (1986) 29–34.
[28] M. Ossa, E.V. Brandani, G. Del Re, G. Di Giacomo, E. Ferri, Binary and ternary phase behavior of the system water-ethanolcarbon dioxide, Fluid Phase Equil. 56 (1990) 325–361.
[29] K. Suzuki, H. Sue, M. Itou, R.L. Smith, H. Inomata, K. Arai, S. Saito, Isothermal vapor–liquid equilibrium data for binary systems at high pressures: CO_2-methanol, CO_2-ethanol, CO_2-1-propanol, methane-ethanol, methane-1-propanol, ethane-ethanol, and ethane-1- propanol systems, J. Chem. Data 35 (1990) 63–66.
[30] Reverchon E., Supercritical fluid extraction and fractionation of essential oils and related products, J. Supercrit. Fluids 10 (1997) 1–37.
[31] Hammond D.A., M. Karel, A.M. Klibanov, V.J. Krukonis, Enzymatic-reactions in supercritical gases, Appl. Biochem. Biotechnol. 11 (1985) 393-397.
[32] Nakamura K., Biochemical reactions in supercritical fluids, Trends Biotechnol. 8 (1990) 288-298.
[33] Gunnlaugsdottir H., Sivik B., Lipase-catalyzed alcoholysis of cod-liver oil in supercritical carbon-dioxide, J. Am. Oil Chem. Soc. 72 (1995) 399-403.
[34] Cardona C.A. and Gallego L.C. Supercritical fluids industrial applications I. Generalities and extraction processes, Ingeniería Química 411 (2004) 144–151 (in Spanish).
[35] Cardona C.A. and Gallego L.C. Supercritical fluids industrial applications II. Extraction models, Ingeniería Química 412 (2004) 185–188 (in Spanish).
[36] Cardona C.A. and Gallego L.C. Supercritical fluids industrial applications III. Supercritical conditions reactions, Ingeniería Química 413 (2004) 210–219 (in Spanish).
[37] Xiaoting Chena, Yucui Houb,WeizeWua, Shuhang Rena, Jianwei Zhanga, Jinlong Fan. High pressure phase behavior and density of the carbon dioxide + 1-methylimidazole binary system. J. of Supercritical Fluids 51 (2009) 104–108.
[38] Laitinen A., Michaux A. and Aaltonen O. Soil cleaning by carbon dioxide extraction: a review. Environmental Technology 15 (1994) 715-727.
[39] Oliviera J.V., D. Oliviera, Kinetics of the enzymatic alcoholysis of palm kernel oil in supercritical CO_2, Ind. Eng. Chem. Res. 39 (12) (2000) 4450.
[40] Zeljko Knez, Maja Habulin. Compressed gases as alternative enzymatic-reaction solvents: a short review. Journal of Supercritical Fluids 23 (2002) 29–42.
[41] Maja Habulin, Saša Šabeder, Željko Knez, Enzymatic synthesis of sugar fatty acid esters in organic solvent and in supercritical carbon dioxide and their antimicrobial activity. The Journal of Supercritical Fluids, 45 (2008) 338-345.
[42] Baiker A., Supercritical fluids in heterogeneous catalysis, Chem. Rev. 99 (1999) 453–474.
[43] Pablo E. Hegel, Marcelo S. Zabaloy, Guillermo D.B. Mabe, Selva Pereda, Esteban A. Brignole. Phase equilibrium engineering of the extraction of oils from seeds using carbon dioxide + propane solvent mixtures. J. of Supercritical Fluids 42 (2007) 318–324.

[44] Jun Li, Miguel Rodrigues, Alexandre Paiva, Henrique A. Matos, Edmundo Gomes de Azevedo. Vapor–liquid equilibria and volume expansion of the tetrahydrofuran/CO_2 system: Application to a SAS-atomization process. J. of Supercritical Fluids 41 (2007) 343–351.
[45] Houndonougbo Y., K. Kuczera, B. Subramanial and B. B. Laird. Prediction of phase equilibria and transport properties in carbon-dioxide expanded solvents by molecular simulation. Molecular Simulation, 33 (2007) 861–869.
[46] Huey-Ing Chen, Po-Hung Chen, and Hung-Yi Chang. High-Pressure Vapor−Liquid Equilibria for CO_2 + 2-Butanol, CO_2 + Isobutanol, and CO_2 + tert-Butanol Systems. J. Chem. Eng. Data, 48 (2003) 1407-1412.
[47] J.A. López, V.M. Trejos, C.A. Cardona, Objective functions analysis in the minimization of binary VLE data for asymmetric mixtures at high pressures, Fluid Phase Equilibria 248 (2006) 147–157.
[48] J.A. López, C.A. Cardona, Phase equilibrium calculations for carbon dioxide + n-alkanes binary mixtures with the Wong–Sandler mixing rules, Fluid Phase Equilibria 239 (2006) 206–212.
[49] Saraf V.P. and Kiran E., Free radical polymerization of styrene in supercritical fluids, J. Polymer, 31 (1990) 687–688.
[50] Shiho H. and DeSimone J.M., Preparation of micron-size polystyrene particles in supercritical carbon dioxide, J. Polym. Sci. 37 (1999) 2429–2437.
[51] Shiho H. and DeSimone J.M., Dispersion polymerizations of styrene in supercritical carbon dioxide utilizing random copolymers containing a fluorinated acrylate for preparing micron-size polystyrene particles, J. Polym. Sci. 38 (2000) 1146–1153.
[52] Zeljko Knez, Andreja Riz ner-Hras, Klementina Kokot and Davorin Bauman. Solubility of some solid triazine herbicides in supercritical carbon dioxide. 152 (1998) 95-108.
[53] Huan Phan Tai, Gerd Brunner. Sugar fatty acid ester synthesis in high-pressure acetone–CO_2 system. J. of Supercritical Fluids 48 (2009) 36–40.
[54] F. Montañés, T. Fornari, P.J. Martín-Álvarez, A. Montilla, N. Corzo, A. Olano, E. Ibáñez, Selective recovery of tagatose from mixtures galactose by direct extraction with supercritical CO_2 and different cosolvents, Journal of Agricultural and Food Chemistry 54 (2006) 8340–8345.
[55] F. Montañés, T. Fornari, P.J. Martín-Álvarez, A. Montilla, N. Corzo, A. Olano, E. Ibáñez, Selective fractionation of disaccharide mixtures by supercritical CO_2 with ethanol as co-solvent, Journal of Supercritical Fluids 41 (2007) 61–67.
[56] F. Montañés, N. Corzo, A. Olano, G. Reglero, E. Ibáñez, T. Fornari, Selective fractionation of carbohydrate complex mixtures by supercritical extraction with CO_2 with different co-solvents, Journal of Supercritical Fluids 45 (2008) 189–194.
[57] Montañés Fernando, Tiziana Fornarib, Roumiana P. Statevac, Agustín Olanoa, Elena Ibáñez. Solubility of carbohydrates in supercritical carbon dioxide with (ethanol +water) cosolvente. J. of Supercritical Fluids 49 (2009) 16–22.
[58] V. Riha, Brunner G., Separations of fish oil ethyl esters with supercritical carbon dioxide, J. Supercrit. Fluids 17 (2000) 55.
[59] M. A. McHugh and V. J. Krukonis. Supercritical Fluid Extraction Principles and Practice, 2nd ed., Butterworth-Heinemann, Boston (1993).
[60] L. T. Taylor. Supercritical Fluid Extraction, John Wiley, New York (1996).
[61] A. S. Gopalan, C. M. Wai, H. K. Jacobs. Supercritical Carbon Dioxide: Separations and Processes, ACS Symposium Series 860, American Chemical Society, Washington, DC (2003).
[62] Cyril Aymoniera, Anne Loppinet-Serania, Helen Reveróna, Yves Garrabosa and François Cansell. Review of supercritical fluids in inorganic materials science. Journal of Supercritical Fluids, 38 (2006) 242-251.
[63] M. A. Abraham and A. K. Sunol. Supercritical Fluids Extraction and Pollution Prevention, ACS Symposium Series 670, American Chemical Society, Washington, DC (1997).
[64] K. P. Johnston and J. M. L. Penninger. Supercritical Fluid Science and Technology, ACS Symposium Series 406, American Chemical Society, Washington, DC (1989).

[65] M. Poliakoff, N. Meehan. Chapter 9 Applications: 9.1 Chemical reactions in supercritical solvents (SCFs) Industrial Chemistry Library, 9 (2001) 473-485.
[66] P. H. Van Konynenburg and R. L. Scott. Philos. Trans. R. Soc. London, Series A 298 (1980) 495–540
[67] T. Clifford. Fundamentals of Supercritical Fluids, Oxford University Press, London (1999).
[68] K. Aim and M. Fermeglia. In The Experimental Determination of Solubilities, G. H. Hefter and R. P. T. Tomkins (Eds.), pp. 493–555, John Wiley, Chichester (2003).
[69] J. M. Prausnitz, R. N. Lichtenthaler, E. G. de Azevedo. Molecular Thermodynamics of Fluid-Phase Equilibria, 3rd ed., Prentice-Hall, Upper Saddle River, NJ (1999).
[70] M . A. A. Meireles, Supercritical extraction from solid: process design data (2001–2003), Current Opinion in Solid State and Materials Science 7 (2003) 321–330.
[71] F. J. Señoráns, Ruiz-Rodríguez, A, Ibáñez, E, Tabera, J, Reglero G. Optimization of countercurrent supercritical fluid extraction condiciones for brandy aroma isolation. Journal of Supercritical Fluids 26 (2003) 129-135
[72] M. Zougagh, M. Valcárcel, A. Ríos. Supercritical fluid extraction: a critical review of its analytical usefulness TrAC Trends in Analytical Chemistry. 23(2004) 399-405.
[73] J.F. Brennecke, J.E. Chateauneuf, Homogeneous organic reactions as mechanistic probes in supercritical fluids, Chem. Rev. 99 (1999) 433–452.
[74] D. Chouchi, D. Gourgouillon, M. Courel, J. Vital, M.Nunes da Ponte, The influence of phase behavior on reaction at supercritical conditions: the hydrogenation of -pinene, Ind. Eng. Chem. Res. 40 (2001) 2551–2554.
[75] S. Pereda, S.B. Bottini, E.A. Brignole, Supercritical fluids and phase behavior in heterogeneous gas–liquid catalytic reactions, Appl. Catal. A: Gen. 281 (2005) 129–137.
[76] Span, R. Wagner, W. A New Equation of State for Carbon Dioxide Covering the Fluid Region from the Triple-Point Temperature to 1100 K at Pressures up to 800 MPa, J. Phys. Chem. Ref. Data, 25 (1996) 1509-1596.
[77] Angus S., Armstrong B., de Reuck, K.M. Carbon Dioxide International Thermodynamic Tables of the Fluid State. IUPAC, Commission on thermodynamics and thermochemistry, Pergamon Press, 1976.
[78] Christov M., R. Dohrn. Review High-pressure fluid phase equilibria Experimental methods and systems investigated (1994–1999). Fluid Phase Equilibria 202 (2002) 153–218.
[79] Huanga Z., Chiew Y.C., Feng M., Miaoa H., Li J.H., Xua L., Modeling aspirin and naproxen ternary solubility in supercritical CO_2/alcohol with a new Peng–Robinson EOS plus association model, Journal of Supercritical Fluids 43 (2007) 259–266.
[80] Peng D.Y., Robinson D.B., A new two-constant equation of state, Industrial and Engineering Chemistry Fundamentals 15 (1976) 59–64.
[81] Valderrama J.O., The state of the cubic equations of state, Industrial and Engineering. Chemistry Research 42 (2003) 1603–1618.
[82] A.Z. Panagiotopoulos, R.C. Reid, New mixing rules for cubic equations of state for highly polar asymmetric mixtures, ACS Symp. Ser. 300 (1986) 571–582.
[83] Y. Adachi, H. Sugie, A new mixing rule–modified conventional mixing rule, Fluid Phase Equilib. 28 (1986) 103–118.
[84] J. Schwartzentruber, H. Renon, Development of a new cubic equation of state for phase equilibrium calculations, Fluid Phase Equilib. 52 (1989) 127–134.
[85] J. Schwartzentruber, H. Renon, Extension of UNIFAC to high pressures and temperatures by use of a cubic equation of state, Ind. Eng. Chem. Res. 28 (1989) 1049–1055.
[86] Michael L. Michelsen, Hans Kistenmacher, On composition-dependent interaction coefficeints, Fluid Phase Equilibria, 58 (1990) 229-230.
[87] Michelsen M.L., A modified Huron–Vidal mixing rule for cubic equation of state, Fluid Phase Equilibria 60 (1990) 213–219.

[88] Dahl S., M.L. Michelsen, High-pressure vapor–liquid equilibrium with a UNIFAC based equation of state, AIChE J. 68 (1990) 441-448.
[89] Wong D.S.H., Sandler S.I. Theoretically correct mixing rule for cubic equations of state, AIChE J. 38 (1992) 671–680.
[90] Coutsikos P., Kalospiros N.S., Tassios D.P., Capabilities and limitations of the Wong– Sandler mixing rules, Fluid Phase Equilibria 108 (1995) 59–78.
[91] Voros N.G., Tassios D.P., Vapor–liquid equilibria in nonpolar/weakly polar systems with different types of mixing rules, Fluid Phase Equilibria 91 (1993) 1-29.
[92] Ralf Dohrn and Gerd Brunner. High-pressure fluid phase equilibria: experimental methods and Systems investigated (1988-1993). Fluid Phase Equilibria 106 (1995) 213-282.
[93] Huey-Ing Chen, Hung-Yi Chang, and Po-Hung Chen. High-Pressure Phase Equilibria of Carbon Dioxide + 1-Butanol, and Carbon Dioxide + Water + 1-Butanol Systems. J. Chem. Eng. Data, 47 (2002) 776-780.

CHAPTER 3

OBJECTIVE FUNCTIONS ANALYSIS IN THE MINIMIZATION OF BINARY VLE DATA FOR MIXTURES CONTAINING CO_2

This chapter is intended to introduce the reader with the importance of the objective functions analysis in the minimization of binary vapor liquid equilibria (VLE) data for asymmetric mixtures containing carbon dioxide. In this chapter five different objective functions were studied with the purpose of analyzing their performance for parameters estimation of vapor–liquid equilibrium models for a series of 10 non-polar and 9 polar asymmetric binary mixtures containing carbon dioxide at high pressures. Peng–Robinson equation of state coupled with the Wong–Sandler mixing rules were used for modeling the VLE in all cases. The first two objective functions are based on the calculation of the distribution coefficients for each component in the mixture and the remaining objective functions involve additional calculations of other quantities such as the bubble point pressure. In general, the optimal parameters obtained from all objective functions showed a good prediction capacity of the behavior of the vapor phase. It is also demonstrated that a good prediction of the pressure depends on the form of the objective function. It was found that one objective function has slight advantages over the other analyzed objective functions: first, it does not involve additional iterative calculations as the bubble point or isothermal flash for each data point; second, the optimal second virial coefficient interaction parameter shows to be in concordance with the statistical thermodynamic postulates; and finally, VLE predictions using the optimal parameters obtained with the help of this objective function show very good representations of both the vapor phase and pressure.

3.1. Introduction

In chemical processes design, an accurate prediction of the phase equilibria of the involved mixtures is essential. Therefore, an appropriate thermodynamic model for representing phase behavior is required. The selection of a model requires the knowledge of at least the main characteristics of components in the mixture (polar and, non-polar molecules, light gases and heavy components) and system temperature and pressure. Usually, a γ–Φ approach is considered at low and moderated pressures. As both system pressure and asymmetry (which can be identified by a noticeable difference among the infinite dilution activity coefficients of each component) increase, a Φ–Φ approach is most appropriate. In this case, an equation of state (EOS) coupled with an appropriate mixing rule for the attractive-term and the covolume is strongly required for an accurate prediction of the vapor–liquid equilibrium (VLE).

The van der Waals (vdW) mixing rules can only represent mixtures of components with similar sizes. They are generally limited to non-polar and slightly polar mixtures. Moreover, its geometry is inadequate for composition variations and, although many works have been developed to improve the vdW mixing rules [1–9], they are, generally, unsuitable for describing complex systems. Since many mixtures involved in chemical processes are highly nonideal, mixing rules based on excess free energy takes great importance for representing the properties of nonideal mixtures. This kind of mixing rules has been originally developed by Huron and Vidal [10] who equated the excess Gibbs free energy at infinite pressure derived from a cubic EOS to that obtained from a liquid-activity coefficient model in order to calculate the attractive-term parameter, a_m. Additionally, they proposed a linear relationship for the covolume parameter, bm. Due to inconsistencies in this mixing rule [11,12], some researchers have made several efforts to relax the infinite-pressure limit imposed on the Huron–Vidal mixing rule [13–18], obtaining satisfactory VLE predictions for many complex mixtures. Other mixing rules based on zero reference pressure models have been developed by Twu and coworkers [19–21]. Such models reproduce the excess Gibbs free energy as well as the liquid activity coefficients of any activity model without requiring any additional binary interaction parameter.

Alternatively, the Wong–Sandler mixing rules [11], using the infinite pressure reference state and including the correct zero pressure limit for the composition dependence of the second virial coefficient, are currently one of the most popular mixing rules for cubic EOS. Several authors have shown the applicability of these mixing rules in phase equilibrium prediction [22–33] and others have demonstrated their limitations [19–21, 34].

Generally, VLE at high pressures can be calculated using activity coefficient model parameters from available values at low pressures. However, in the case of highly asymmetric mixtures, especially those containing light gases and heavy solutes, such parameters are not available. In such cases, it is possible to calculate the activity coefficient model parameters and the interaction parameter from VLE data by optimizing an appropriate objective function (OF). This approach has the advantage of achieving a moderate computing time and a good accuracy in the phase equilibrium prediction. These OF can be derived from the least squares principle or from the maximum likelihood principle [35]. In the least squares principle, the error is defined as the difference between the experimental point and the calculated value. Then, the OF to minimize is the quadratic error summation over the experimental data set:

$$f = \sum_{i=1}^{np} \sum_{j=1}^{nc} \left(u_{i,j}^{\exp} - u_{i,j}^{cal} \right)^2 \tag{1}$$

where *np* is the number of experimental data points, *nc* the number of components and u_{ij} are the dependent variables. The application of the maximum likelihood principle requires the knowledge of the measurement error for each experimental variable. In this case, the OF is similar to that of the least squares principle, but the statistical variance associated with the measured variables (σ_{ij}^2) should be taken into account:

$$f = \sum_{i=1}^{np} \sum_{j=1}^{nm} \frac{\left(w_{ij}^{\exp} - w_{ij}^{cal} \right)^2}{\sigma_{ij}^2} \tag{2}$$

where w_{ij} are the measured variables (liquid composition, x; vapor composition, y; temperature, T; and pressure, P), and nm is the number of measured variables. The optimal parameters which minimize the Eq. (2) are those that maximize the likelihood function of the parameters [36]. The maximum likelihood principle requires that the measurements are only subject to random errors. In addition, the model must be capable of representing the measurements within an order less than the order of the experimental uncertainties [37]. At the present time, the least squares principle (Eq. (1)) is the most popular for obtaining interaction parameters from VLE data. Additionally, several of these computational methods applicable to parameters optimization from VLE data have been strongly analyzed [36–44].

In the present work five different OF were analyzed in order to evaluate their accuracy to represent both the vapor phase and the pressure behavior in isothermal asymmetric binary mixtures at high pressures. The Peng–Robinson EOS [45] coupled with the Wong–Sandler mixing rules [11] have been used in the VLE estimation. The NRTL model [46] was utilized to predict the excess Helmholtz free energy. The second virial coefficient binary interaction parameter k_{12} and the NRTL model parameters τ_{12} and τ_{21} were calculated for 10 non-polar and 9 polar asymmetric mixtures containing carbon dioxide at high pressures by optimizing each one of the five analyzed OF. A Levenberg–Marquardt minimization algorithm was used in all cases.

3.2. Equation of state and mixing rules

The Peng-Robinson equation of state [45] has the following form:

$$P = \frac{RT}{v - b} - \frac{a}{v(v + b) + b(v - b)} \tag{3}$$

where P is the pressure, T the absolute temperature, R the ideal gas constant furthermore a and b are the energy and size parameters which are calculated from:

$$a = 0.457235 \frac{R^2 T_c^2}{P_c} \alpha(T_r) \tag{4}$$

$$b = 0.077796 \frac{RT_c}{P_c} \tag{5}$$

the subscripts c and r denotes critical and reduced conditions, respectively. The correlation for the α function is:

$$\alpha(T_r) = \left[1 + \kappa \left(1 - \sqrt{T_r} \right) \right]^2 \tag{6}$$

$$\kappa = 0.37464 + 1.54226\omega - 0.26992\omega^2 \tag{7}$$

where ω is the acentric factor. For introducing the PR EOS to mixtures the Wong-Sandler [11] mixing rules were used. The a_m and b_m parameters have the following form:

$$a_m = b_m \left[\sum_i z_i \frac{a_i}{b_i} + \frac{\underline{A}^E_\infty}{C} \right] \tag{8}$$

with

$$b_m = \frac{\sum_i \sum_j z_i z_j \left(b - \frac{a}{RT} \right)_{ij}}{1 - \sum_i z_i \frac{a_i}{b_i RT} - \frac{\underline{A}^E_\infty}{\sigma RT}} \tag{9}$$

$$C = \frac{1}{\sqrt{2}} \ln\left(\sqrt{2} - 1 \right) \tag{10}$$

and

$$\left(b - \frac{a}{RT} \right)_{ij} = \frac{\left(b - \frac{a}{RT} \right)_i + \left(b - \frac{a}{RT} \right)_j}{2} \left(1 - k_{ij} \right) \tag{11}$$

where k_{ij} is a second virial coefficient binary interaction parameter, z is the molar fraction and $\underline{A}^E_\infty$ is the excess Helmholtz free energy at infinite pressure which is calculated from an excess Gibbs free energy model. The thermodynamic relation between these excess free energies is:

$$\underline{G}^E \left(T, P, x \right) = \underline{A}^E \left(T, P, x \right) + P \underline{V}^E \left(T, P, x \right) \tag{12}$$

Since at low pressures, $\underline{V}^E$ is small, the difference between $\underline{G}^E$ and $\underline{A}^E$ is also small. Consequently, Wong and Sandler [11] established the following approximation:

$$\underline{G}^E \left(T, P = low, x \right) = \underline{A}^E \left(T, P = low, x \right) = \underline{A}^E \left(T, P = \infty, x \right) \tag{13}$$

Therefore, the excess Helmholtz free energy is much less pressure-dependent than the excess Gibbs free energy. In this work, the excess Helmholtz free energy at infinite pressure was calculated with the NRTL model [46]:

$$\frac{A_{\infty}^{E}}{RT} = \sum_{i} z_i \left(\frac{\sum_{j} z_j \tau_{ji} g_{ji}}{\sum_{k} z_k g_{ki}} \right) \tag{14}$$

$$g_{ij} = \exp\left(-\alpha_{ij} \tau_{ij}\right) \tag{15}$$

In the case of binary mixtures, α_{12} (=α_{21}), τ_{12} and τ_{21} are the three parameters of the NRTL model. As recommended by Renon and Prausnitz [46], a constant value of α_{12} (0.3) was used in this work. In this contribution, the adjustable parameters of the NRTL model: τ_{12} and τ_{21} and the second virial coefficient binary interaction parameter k_{12} have been determined using experimental phase equilibrium data at isothermal conditions for each of the 10 non-polar and the 9 polar asymmetric binary systems containing carbon dioxide by the minimization of five different OF.

3.3. Asymmetric binary mixtures

In the present work, 10 non-polar (CO_2 + non-polar solute) and 9 polar (CO_2 + polar solute) asymmetric binary mixtures containing carbon dioxide have been analyzed. The experimental conditions and the literature source of each data set are shown in Tables 1 and 2. Data for 27 isotherms with 349 experimental points were studied for CO_2 + non-polar mixtures and 25 isotherms with 219 experimental points were studied for CO_2 + polar mixtures.

Several mixtures containing carbon dioxide and other compounds (limonene, isoamyl acetate, ethyl caproate, ethyl laurate, 1- heptanol, linalool, decanal) have a great importance in the field of supercritical fluid extraction. For example, the limonene and the linalool are the principal compounds of citrus oil. Since the linalool is one of the most important flavor fractions of this oil, it is common to remove the limonene to concentrate the oxygenated compounds as the linalool. On the other hand, esters as isoamyl acetate, ethyl caproate and ethyl laurate are widely used in the food, cosmetic and pharmaceutical industries. The production of these compounds is generally carried out by chemical synthesis, but the use of toxic organic solvents for food and health products is being progressively restricted. Therefore, the supercritical fluid extraction with carbon dioxide is one of the industrial alternatives to produce these and other esters [47].

The VLE study of carbon dioxide + styrene mixtures has a great importance in petrochemical industries. Styrene is commonly produced by dehydrogenation of ethylbenzene. As the reaction is not completed, separation of styrene + ethylbenzene mixtures using supercritical carbon dioxide as a solvent may be an attractive method [48]. Additionally, some works have shown that the synthesis of polystyrene from the polymerization of styrene in supercritical carbon dioxide has an increasing importance as production process [49–52].

Table 3.1 Experimental conditions for non-polar asymmetric binary mixtures.

Carbon Dioxide +	np	*T*(K)	Pressure range (bar)	Reference
	20	230.00	8.920–69.91	[53]
Methane	20	250.00	17.83–80.53	[53]
	13	270.00	32.09–83.81	[53]
Propane	25	230.00	8.9-71.1	[54]
	17	270.00	32.0-79.5	[54]
	12	310.15	5.6–73.1	[55]
n-Pentane	13	333.15	5.9–87.5	[55]
	16	363.15	9.4–96.7	[55]
n-Hexane	10	298.15	4.432–52.05	[56]
	10	313.15	6.319–76.57	[56]
	23	310.65	1.861–75.63	[57]
n-Heptane	17	352.59	4.240–116.1	[57]
	17	394.26	11.30–133.1	[57]
	6	313.15	15.00–75.00	[58]
n-Octane	6	328.15	20.00–95.00	[58]
	8	348.15	20.00–113.5	[58]
n-Decane	22	344.30	63.8–127.4	[59]
	26	377.60	103.4–164.8	[59]
Benzene	8	298.15	8.9–57.7	[56]
	9	313.15	14.8–77.5	[56]
	9	333.15	60.3-112.0	[60]
Styrene	9	338.15	62.40-119.0	[60]
	10	343.15	60.0–131.0	[60]
	8	348.15	62.9–134.2	[60]
Limonene	5	313.20	39.4-78.7	[61]
	5	323.20	39.4- 92.7	[61]
	5	333.20	49.9- 102.6	[61]

Table 3.2 Experimental conditions for polar asymmetric binary mixtures.

Carbon Dioxide +	np	*T*(K)	Pressure range (bar)	Reference
	7	293.15	6.30-54.60	[62]
n-Butanol	14	303.15	5.20-67.4	[62]
	8	314.80	46.33-79.84	[63]
	9	325.30	52.26-98.73	[63]
	4	431.82	83.63-135.55	[64]
n-Hexanol	7	432.45	22.68-201.28	[64]
	8	374.63	40.38-145.72	[64]
n-Heptanol	6	431.54	68.3-168.06	[64]
	15	328.18	28.6-156	[65]
n-Nonanol	10	318.13	25.2-104.4	[65]
	9	308.14	22.3-79.1	[65]
	7	308.15	10.3–69.3	[66]
Isoamyl acetate	8	318.15	10.0–80.3	[66]
	9	328.15	10.3–90.7	[66]
	8	308.20	17.0-64.6	[67]
Ethyl caproate	10	318.20	17.0-78.2	[67]
	12	328.20	17.3-92.2	[67]
	10	288.20	19.3-48.1	[68]
Decanal	11	303.20	21.7-67.6	[68]
	12	313.20	82.2-16.8	[68]
	8	308.15	14.8–70.0	[69]
Ethyl laurate	8	318.15	14.8–83.1	[69]
	9	328.15	14.8–100.1	[69]
	5	313.20	40.0-79.9	[70]
Linalool	5	323.20	40.0-97.8	[70]

3.4. Objective functions

In order to determine the optimal parameters for the VLE model, two OF that take into account the coefficient distribution calculation and three OF that require bubble point pressure calculation from an additional iterative process have been analyzed. The first two OF are implicit models which are based on the calculation of the distribution coefficients for each component:

$$f_1 = \sum_{i=1}^{np}\sum_{j=1}^{nc}\left[\ln K_{i,j}^{cal} - \ln K_{i,j}^{\exp}\right]^2 \tag{16}$$

$$f_2 = \sum_{i=1}^{np}\sum_{j=1}^{nc}\left[y_{i,j}^{\exp} - K_{i,j}^{cal}\cdot x_{i,j}^{\exp}\right]^2 \tag{17}$$

where *np* is the number of experimental data points, *nc* is the number of components in the mixture and *K* is the distribution coefficient in both phases. The remaining objective functions OF involve additional iterative procedures for calculating their optimal values and are explicit models because the adjusted variables are calculated from a bubble point pressure calculation algorithm. Therefore, the implementation of these OF has larger computing time requirements in comparison with the implicit functions. The studied explicit OF are:

$$f_3 = \sum_{i=1}^{np}\left[\frac{P_i^{\exp} - P_i^{cal}}{P_i^{\exp}}\right]^2 \tag{18}$$

$$f_4 = \sum_{i=1}^{np}\sum_{j=1}^{nc}\left[\frac{y_{i,j}^{\exp} - y_{i,j}^{cal}}{y_{i,j}^{\exp}}\right]^2 \tag{19}$$

$$f_5 = \sum_{i=1}^{np}\left[\frac{P_i^{\exp} - P_i^{cal}}{P_i^{\exp}}\right]^2 + \sum_{i=1}^{np}\sum_{j=1}^{nc}\left[\frac{y_{i,j}^{\exp} - y_{i,j}^{cal}}{y_{i,j}^{\exp}}\right]^2 \tag{20}$$

where *P* is the bubble point pressure and y represents the molar fraction in vapor phase. As it has seen shown, OF f_5 is a complement of functions f_3 and f_4. However, this does not assure that the binary parameters obtained by these three functions will be identical. Although these OF have very similar computing times, the vapor–liquid equilibrium calculations using their optimal parameters will give a major precision represented in the pressure or the vapor phase composition (or both), but this depends of the objective function form.

In the literature, some authors have used OF f_1 for the parameters optimization of VLE data in asymmetric mixtures of light gases + hydrocarbons and alcohols [71] and carbon dioxide + *n*-alkanes [72], obtaining good predictions for pressure and not very good predictions for vapor composition. OF f_2 and f_4 are the less used to estimate binary interaction parameters in both symmetric and asymmetric systems at high pressures. On the other hand, OF f_3 and f_5 are the most popular for estimating both the binary interaction parameter and the activity coefficient models parameters from VLE data at high pressures and temperatures. Therefore, it is necessary to develop a detailed study which involves explicit and implicit models and to find an adequate OF that guarantees small computing times and suitable exactitude for representing the VLE with respect to the correlated data.

3.5. Results and discussion

The parameters estimation was performed using the Levenberg-Marquardt minimization algorithm for each mixture with OF f_1–f_5. Therefore, 349 minimizations in CO_2 + non-polar binary mixtures and 219 minimizations in CO_2 + polar binary mixtures were carried out. The optimal NRTL model parameters (τ_{12} and τ_{21}) and the second virial coefficient interaction parameter (k_{12}) are reported for the non-polar asymmetric binary mixtures and for the polar asymmetric binary mixtures containing carbon dioxide in the Appendix A.

The deviations between experimental data and calculated values with PR EOS and the Wong–Sandler mixing rules were established through the relative percentage deviations in the bubble point pressure:

$$\Delta P = \sum_{i=1}^{np} \frac{\left| P_{\exp} - P_{cal} \right|}{P_{\exp}} \left(\frac{100}{np} \right) \tag{21}$$

The absolute mean deviation in the molar fraction in the vapor phase is a follows:

$$\Delta y = \sum_{i=1}^{np} \left| y_{\exp} - y_{cal} \right| \frac{1}{np} \tag{22}$$

They are also reported in the Appendix A. The optimal parameters shown in Tables 3.1 and 3.2 in the Appendix A were used to predict the phase equilibrium of the considered mixtures. The agreement with the experimental data is generally satisfactory as shown in Figs. 1–9. Experimental and predicted phase equilibrium for the carbon dioxide + limonene binary system is shown in Fig. 3.1. Predictions with the optimal parameters obtained from OF f_3 and f_5 are compared. It can be appreciated that predictions corresponding to f_5 are slightly better than those corresponding to f_3.

Figs. 2–4 show experimental and predicted VLE for carbon dioxide + propane, carbon dioxide + pentane and carbon dioxide + octane binary mixtures, respectively. In these three figures, the OF that do not involve additional iterative calculations as the bubble point pressure (f_1 and f_2) are compared with those that involve this kind of calculations (f_3–f_5). It is important to note that the advantage of using implicit methods over explicit ones is the great reduction in the computing time. As it was mentioned in a previous work [72], explicit methods require on the average nine times more CPU time per iteration related to the implicit methods. A good agreement with the experimental data can be seen in these figures. Moreover, in carbon dioxide + pentane binary mixture (see Fig. 3.3) the predictions obtained from implicit methods does not present very well the VLE near the critical point. Experimental and predicted phase equilibrium for the carbon dioxide + propane binary system is shown in Fig. 3.2. Predictions with the optimal parameters obtained from OF f_2 and f_4 were compared. In the case of carbon dioxide + octane binary mixture (see Appendix A), the predictions with the optimal parameters obtained from OF f_2 and f_5 are almost identical.

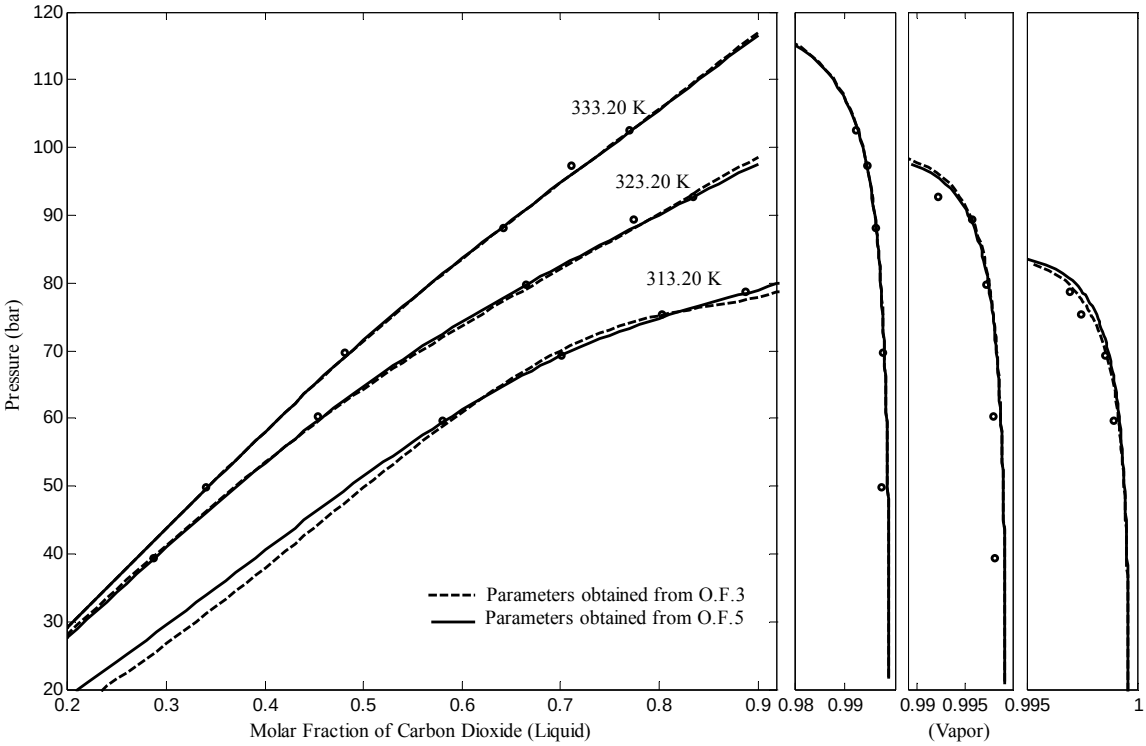

Fig. 3.1 Experimental and predicted VLE for CO_2 + limonene binary system. Comparison of accuracy of two objective functions. Experimental data taken from Iwai et al. [61].

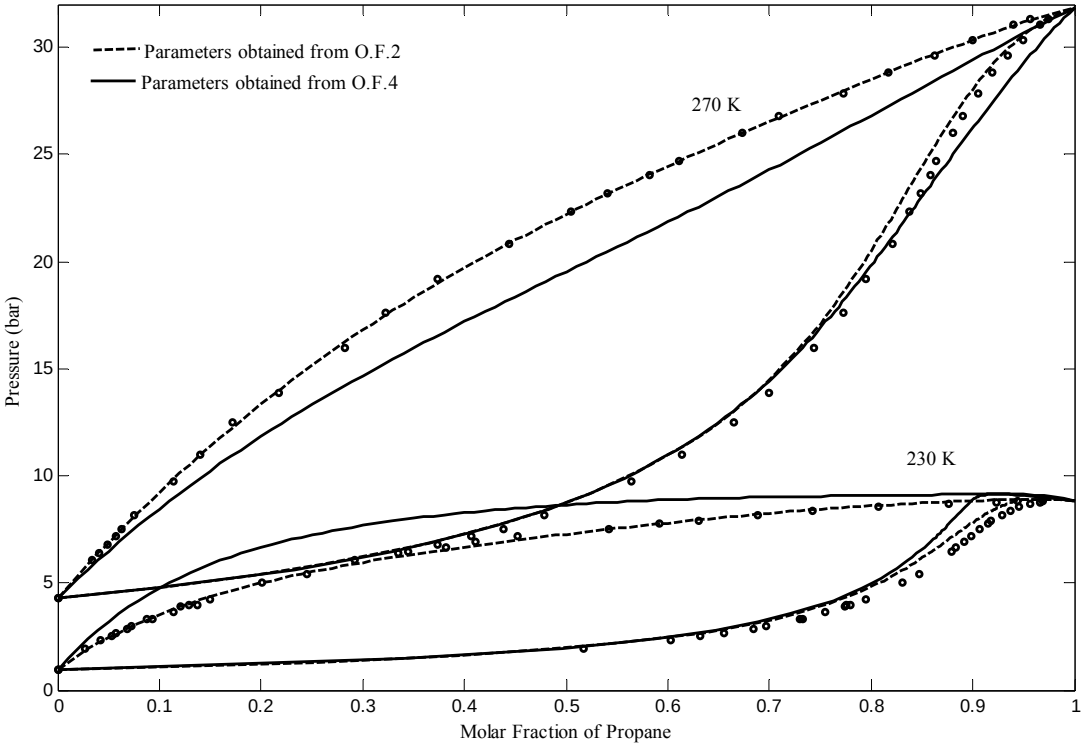

Fig. 3.2 Experimental and predicted VLE for CO_2 + propane binary system. Comparison of accuracy of two objective functions. Experimental data taken from Webster and Kidnay [54].

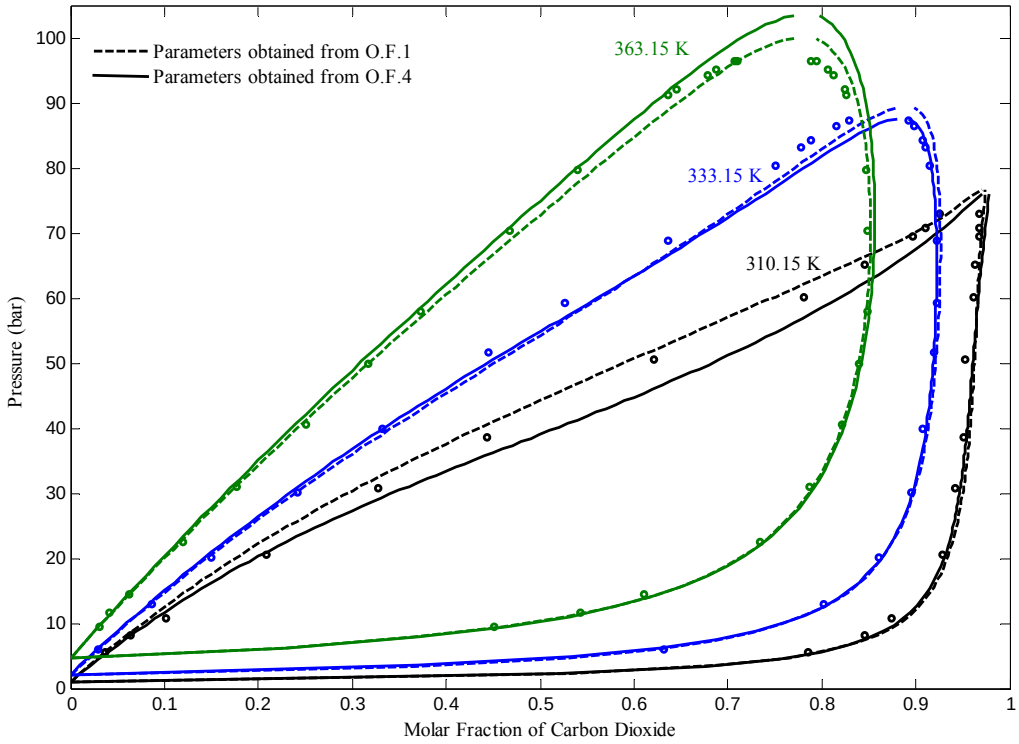

Fig. 3.3 Experimental and predicted VLE for CO_2 + pentane binary system. Comparison of accuracy of two objective functions. Experimental data taken from Tochigi et al. [55].

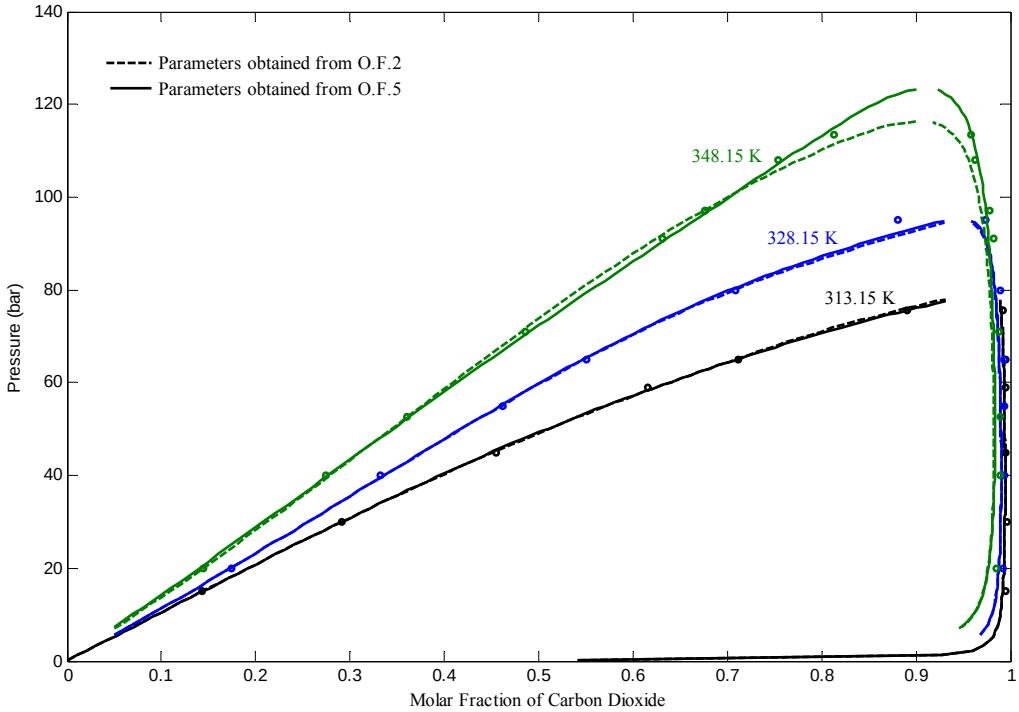

Fig. 3.4 Experimental and predicted VLE for CO_2 + octane binary system. Comparison of accuracy of two objective functions (OF 2 and OF 5, identical predictions). Experimental data taken from Weng and Lee [58]. Prediction with PR EOS coupled with the WS mixing rules.

Fig. 3.5 shows the experimental and predicted VLE for the highly asymmetric carbon dioxide + ethyl caproate binary system. Here, OF f_2 and f_4 are compared. In both cases, the vapor phase representations are very accurate taking into account the range of experimental data. It can be observed that OF f_4 gave poor predictions for pressure, while OF f_2 gave excellent predictions.

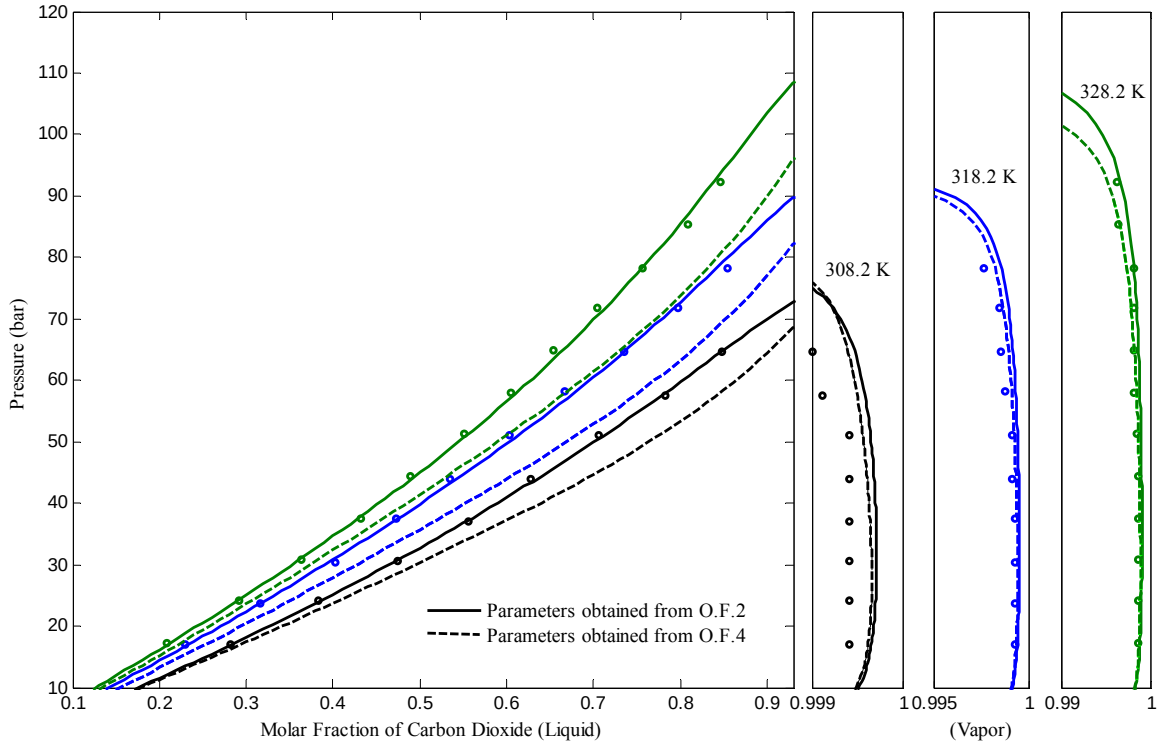

Fig. 3.5 Experimental and predicted VLE for CO_2 + ethyl caproate binary system. Comparison of accuracy of two objective functions. Experimental data taken from Hwu et al. [67].

The VLE for carbon dioxide + ethyl laurate asymmetric binary system is shown in Fig. 3.6. Experimental data are compared with the calculations with optimal parameters obtained from OF f_2. At the three considered temperatures, all the predictions were accurate in both pressure and vapor phase composition.

The capability of OF f_3 is analyzed in Fig. 3.7. This figure shows the experimental and predicted phase equilibrium for carbon dioxide + 1-heptanol binary system. The predictions with the optimal parameters obtained using this OF are very accurate related to the experimental data. Moreover, for the two considered temperatures, the deviations corresponding to OF f_3 and f_5 are similar (see Apendix A).

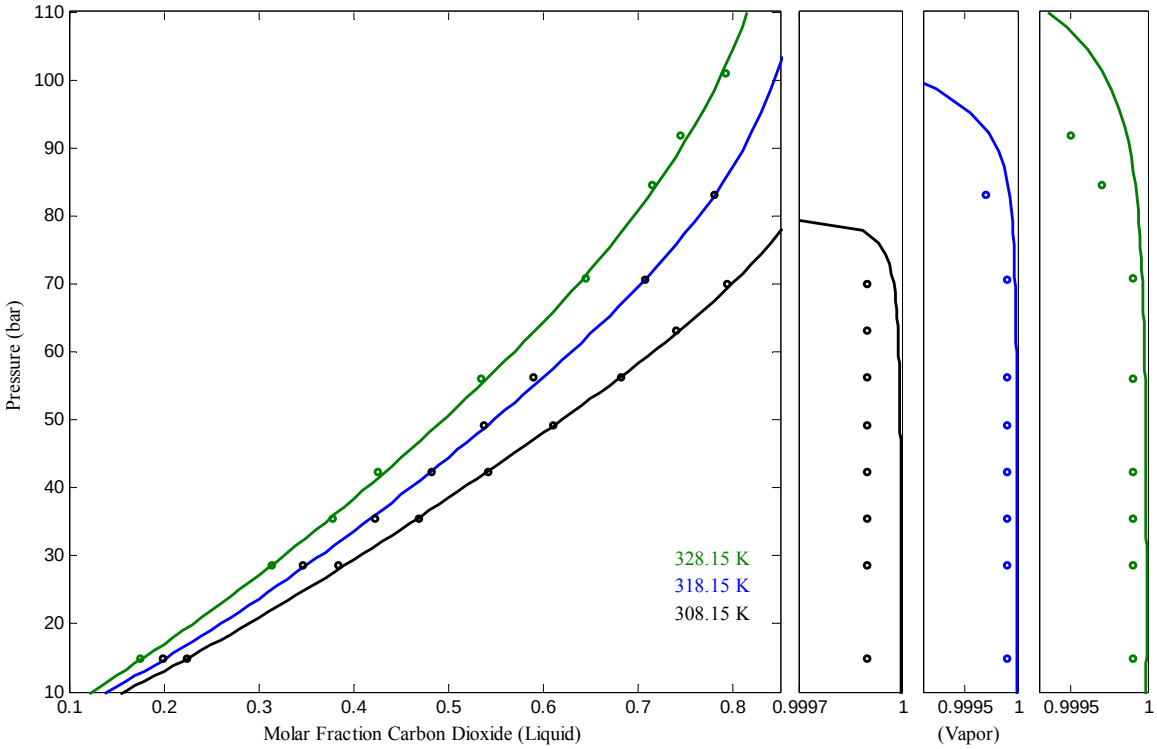

Fig. 3.6 Experimental and predicted VLE for CO_2 + ethyl laurate binary system. Experimental data taken from Cheng et al. [69]. Parameters obtained from OF 2.

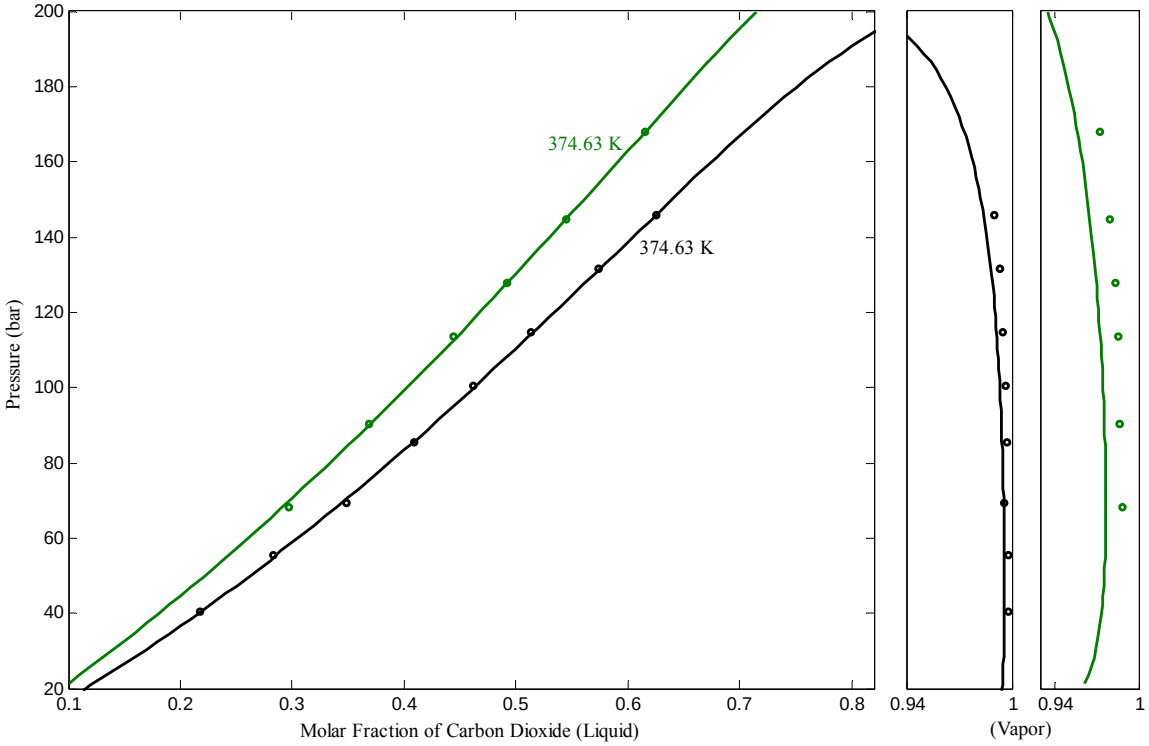

Fig. 3.7 Experimental and predicted VLE for carbon dioxide + 1-heptanol binary system. Experimental data taken from Elizalde-Solis et al. [64]. Parameters obtained from OF 3.

Two important systems for the analysis of supercritical fluid extraction with carbon dioxide are shown in Fig. 3.8 (carbon dioxide + linalool) and Fig. 3.9 (carbon dioxide + decanal). Again, implicit and explicit models are compared. Although all predictions are very similar for both asymmetric mixtures, calculations developed with OF f_2 present light deviations near the critical point of both mixtures.

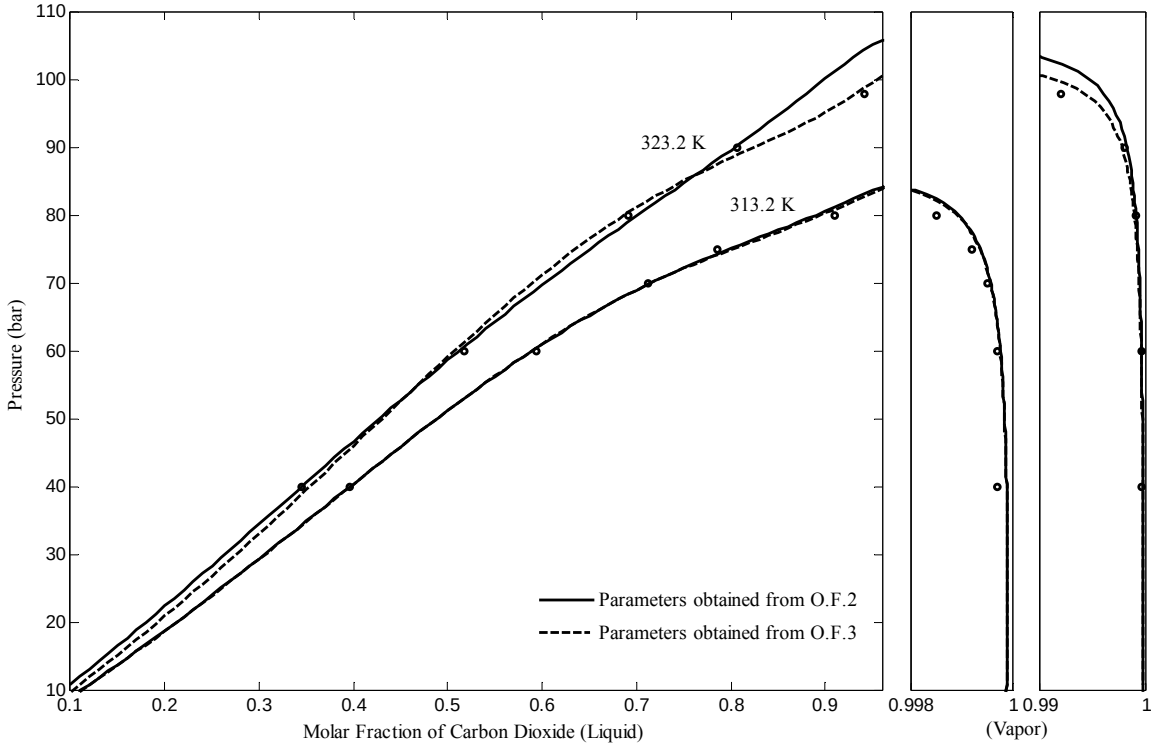

Fig. 3.8 Experimental and predicted VLE for CO_2 + linalool binary system. Comparison of accuracy of two objective functions. Experimental data taken from Iwai et al. [70].

In terms of numerical capacity, OF f_1 shows a bigger numerical instability than the other analyzed OF. First, for several binary mixtures (carbon dioxide + methane at 230K, 250K, 270K, carbon dioxide + *n*-butanol at 293.15K, 303.15K, carbon dioxide + *n*-nonanol at 308.14K, 318.13K, 328.18K and carbon dioxide + decanal at 288.20K, 303.20K), the optimal second virial coefficient interaction parameter violates the quadratic composition dependence of the second virial coefficient; since it takes unrealistic values (see Appendix A). In addition, in very few cases (carbon dioxide + propane at 270K, carbon dioxide + decanal at 303.20K, 313.20K), the other OF also generated unrealistic values for this parameter. An explanation to this fact is that the second virial coefficient interaction parameter is used with the purpose of compensating the initial difference between the excess Helmholtz free energy at infinite pressure calculated using an EOS and the excess Gibbs free energy at low pressure calculated from activity coefficient model. Additionally, in highly asymmetric systems, its value is strongly dependent on the composition. This dependence becomes larger as the asymmetry increases. Therefore, a constant value of k_{ij} over the entire composition range will not be enough to reproduce the G^E activity model from an equation of state. These illogical values lead to the violation of the quadratic composition dependence of the second virial coefficient [34]. Therefore, for highly nonideal mixtures, it is necessary to find the virial coefficient binary interaction parameter as a function of

the composition. On the other hand, in some cases (carbon dioxide + methane at 230K, 250K, 270K, carbon dioxide + *n*-butanol at 293.15K, 303.15K, carbon dioxide + *n*-nonanol at 308.14K, 318.13K, 328.18K and carbon dioxide + decanal at 288.20 K), the OF f_1 did not show convergence in a real range of initial values. Additionally, in some systems (carbon dioxide + decanal at 303.20K, 313.20K, carbon dioxide + ethyl laurate at 308.15K, 318.15K, carbon dioxide + linalool at 323.20 K), the minimization using this objective function presented satisfactory convergence, but when the deviations were calculated with the corresponding optimal parameters, illogical values were obtained, which were not reported here. This is because, OF f_1 does not involve procedures for bubble point pressure calculation, which are necessary to calculate those deviations. When OF f_1 fails, the other OFs satisfactory converge (see Tables 1 and 2 in the Apendix A). This error is directly due to the OF geometric form and not to the application of the Peng–Robinson equation of state coupled with the Wong–Sandler mixing rules.

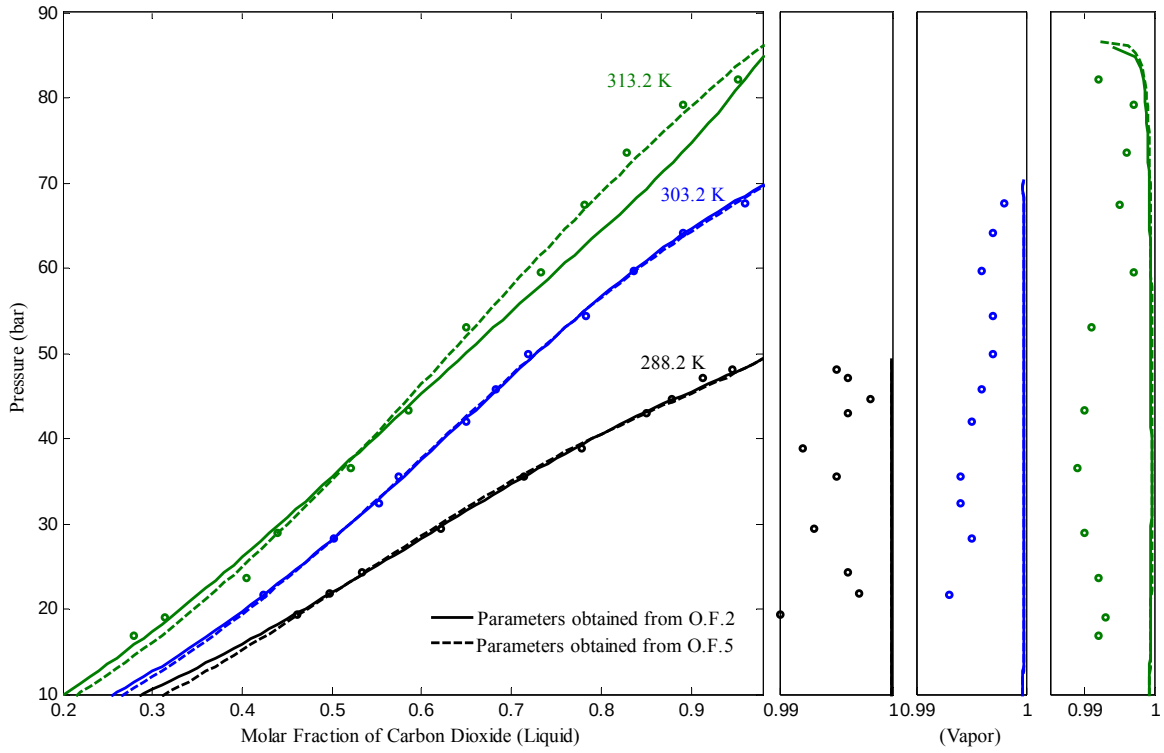

Fig. 3.9. Experimental and predicted VLE for CO_2 + decanal binary system. Comparison of accuracy of two objective functions. Experimental data taken fromVázquez da Silva et al. [68].

With the purpose of comparing the accuracy of each OF for predicting the phase equilibrium of both CO_2 + non-polar solute and CO_2 + polar solute asymmetric binary mixtures at high pressures, Table 3.3 shows the average deviations of these predictions obtained from each OF. Also, for two of the studied asymmetric systems, the residuals were calculated with the purpose of making more informative the quality of the obtained parameters.

Table 3.3 Average deviations in the VLE prediction of the parameters obtained from each objective functions for both non-polar and polar binary systems.

	Polar systems		Non-polar systems	
Objective Function	ΔP	Δy	ΔP	Δy
f_1	8.3756	0.0106	9.6874	0.0061
f_2	1.3415	0.0082	1.2098	0.0054
f_3	1.6342	0.0944	1.1812	0.0039
f_4	6.0870	0.0080	9.7399	0.0035
f_5	1.8292	0.0067	1.6780	0.0037

These residuals are the difference between the experimental point and the calculated value. Their statistical analysis can indicate how well the thermodynamic model represents the data and how precise the data are [38]. The residuals plot for carbon dioxide + *n*-pentane at 363.15K is shown in Fig. 3.10. In general terms, the optimal parameters obtained from the different explicit models (OFs f_3–f_5) are similar, but not identical.

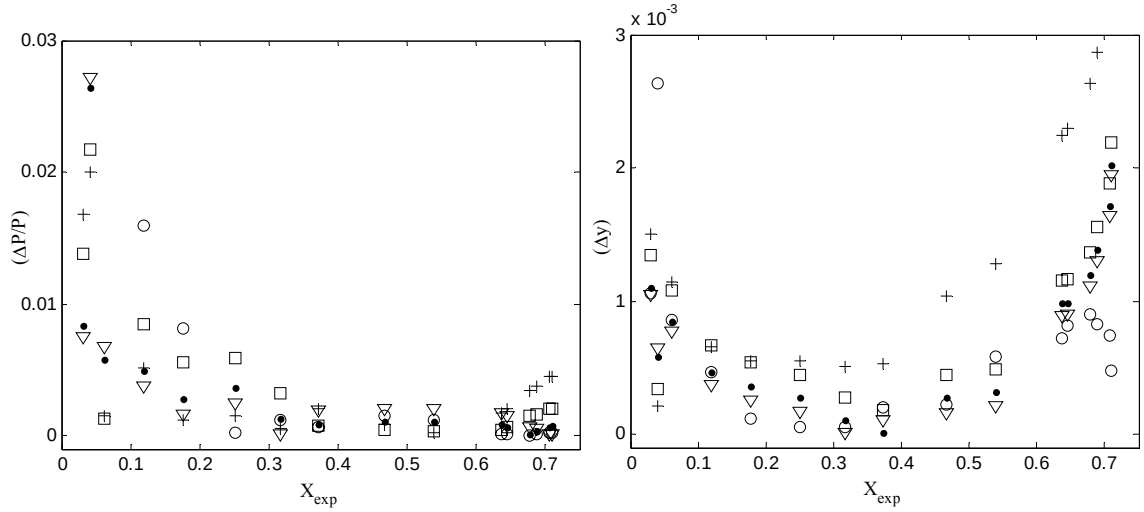

Fig. 3.10 Deviations between experimental points and calculated values of y and P for CO_2 + *n*-pentane at 363.15 K. Parameters obtained from: ▽, OF 1; +, OF 2; ●, OF 3; □, OF 4; ○, OF 5.

On the other hand, the optimal parameters obtained using implicit models (OFs f_1 and f_2) are very different. In terms of accuracy for representing the phase equilibria, all the OF gave good predictions for the vapor phase composition, but OF f_4 showed best results than the others in both CO_2 + non-polar and CO_2 + polar binary systems. The OF represented the bubble point pressure in a best way were f_2, f_3 and f_5.

3.6. Conclusions

In this work, five different OF were analyzed regarding its capability to represent the phase equilibrium in highly asymmetric binary mixtures containing carbon dioxide at elevated temperatures and pressures. Additionally, the ability of Peng–Robinson EOS coupled with the Wong–Sandler mixing rules and the NRTL model for representing fluid phase equilibrium of these non-ideal mixtures was demonstrated. All the OF gave good predictions for the vapor

phase behavior. Only OF f_2 (based on coefficient distribution calculations), f_3 (based on bubble point pressure calculations) and f_5 (based on bubble point pressure and vapor phase composition calculations) represented the bubble point pressure satisfactory.

Furthermore, it was found that OF f_2 has some advantages over the other analyzed OFs. Firstly, this OF does not involve additional iterative calculations as the bubble point or isothermal flash for each data point, resulting in a great reduction in the computing time requirements. Secondly, the optimal second virial coefficient interaction parameter showed to be concordant with the statistical thermodynamic postulates, since its value does not violate the quadratic composition dependence of the second virial coefficient. Finally, VLE predictions with the optimal parameters obtained using this OF showed very good predictions for both vapor phase and pressure. Therefore, objective function f_2 presents attractive features for parameter estimation of EOS and activity coefficient models from experimental data for appropriately representing the VLE.

List of symbols

a, b	equation of state parameters
$\underline{A}^E$	excess Helmholtz free energy
$(b\text{-}a/RT)_{ij}$	cross second virial coefficient
C	constant defined by Eq. (10)
f	objective function (Eqs. (1) and (2))
f_1 - f_5	objective functions denoted by Eqs. ((16)-(20)), respectively
gij	parameter defined by Eq. (15)
$\underline{G}^E$	excess Gibbs free energy
K_{ij}	distribution coefficient
k_{ij}	second virial coefficient interaction parameter
nc	number of components
np	number of experimental data points
P	pressure
R	gas constant
T	temperature
V	volume in molar units
x	liquid molar fraction
y	vapor molar fraction
z	molar fraction
V^E	excess volume
u_{ij}	dependent variables in Eq. (1)
w_{ij}	measured variables in Eq. (2)

Greek Letters

Δ	Deviation
$\alpha(Tr)$	temperature-dependent alpha function
α_{ij}	NRTL model parameter
k	Peng-Robinson alpha function parameter

τ_{12}, τ_{21}	NRTL model binary interaction parameter.
σ	statistical variance in Eq. (2)
ϕ	fugacity coefficient
ω	acentric factor

Subscripts

c	critical point
m	mixture
r	reduced conditions
∞	infinite condition

Superscripts

E	excess property
Exp	experimental
Cal	calculated

Acronyms

EOS	equation of state
NRTL	non Random Two Liquid
OF	objective function
PR	Peng-Robinson
VLE	vapor-liquid equilibrium

References

[1] A.Z. Panagiotopoulos, R.C. Reid, New mixing rules for cubic equations of state for highly polar asymmetric mixtures, ACS Symp. Ser. 300 (1986) 571–582.
[2] Y. Adachi, H. Sugie, A new mixing rule–modified conventional mixing rule, Fluid Phase Equilib. 28 (1986) 103–118.
[3] R. Sandoval, G. Wilczek-Vera, J.H. Vera, Prediction of the ternary vapor–liquid equilibria with the PRSV equation of state, Fluid Phase Equilib. 52 (1989) 119–126.
[4] J. Schwartzentruber, H. Renon, Development of a new cubic equation of state for phase equilibrium calculations, Fluid Phase Equilib. 52 (1989) 127–134.
[5] J. Schwartzentruber, H. Renon, Extension of UNIFAC to high pressures and temperatures by use of a cubic equation of state, Ind. Eng. Chem. Res. 28 (1989) 1049–1055.
[6] S.K. Shibata, S.I. Sandler, Critical evaluation of equation of state mixing rules for the prediction of high-pressure phase equilibria, Ind. Eng. Chem. Res. 28 (1989) 1893–1898.
[7] G.A. Melhem, R. Saini, B.M. Goodwin, A modified Peng–Robinson equation of state, Fluid Phase Equilib. 47 (1989) 189–237.
[8] R. Stryjek, J.H. Vera, PRSV—an improved Peng–Robinson equation of state with new mixing rules for strongly nonideal mixtures, Can. J. Chem. Eng. 64 (1986) 334–340.
[9] P.M. Mathias, H.C. Klotz, J.M. Prausnitz, Equation-of-state mixing rules for multicomponent mixtures: the problem of invariance, Fluid Phase Equilib. 67 (1991) 31–44.
[10] M.J. Huron, J. Vidal, New mixing rules in simple equations of state for representing vapour–liquid equilibria of strongly non-ideal mixtures, Fluid Phase Equilib. 3 (1979) 255–271.
[11] D.S.H. Wong, S.I. Sandler, Theoretically correct mixing rule for cubic equations of state, AIChE J. 38 (1992) 671–680.

[12] S.I. Sandler, Models for Thermodynamic and Phase Equilibria Calculations, Marcel Dekker, New York, 1994.
[13] J. Mollerup, A note on the derivation of mixing rules from excess Gibbs energy models, Fluid Phase Equilib. 25 (1986) 323–327.
[14] M.L. Michelsen, A method for incorporating excess Gibbs energy models in equations of state, Fluid Phase Equilib. 60 (1990) 47–58.
[15] M.L. Michelsen, A modified Huron–Vidal mixing rule for cubic equation of state, Fluid Phase Equilib. 60 (1990) 213–219.
[16] S. Dahl, M.L. Michelsen, A high-pressure vapor–liquid equilibrium with a UNIFAC based equation of state, AIChE J. 36 (1990) 1829–1836.
[17] P.A. Gupte, P. Rasmussen, A. Fredenslund,Anewgroup contribution equation of state for vapor–liquid equilibria, Ind. Eng. Chem. Fund. 25 (1986) 636–645.
[18] G. Soave, A New Expression of $q(\alpha)$ for the modified Huron–Vidal methods, Fluid Phase Equilib. 72 (1992) 325–328.
[19] C.H. Twu, J.E. Coon, CEOS/AE mixing rules constrained by vdW mixing rule and second virial coefficient, AIChE J. 42 (1996) 3212–3222.
[20] C.H. Twu, J.E. Coon, D. Bluck, A zero-pressure cubic equation of state mixing rule for predicting high pressure phase equilibria using infinite dilution activity coefficients at low temperatures, Fluid Phase Equilib. 150–151 (1998) 181–189.
[21] C.H. Twu, J.E. Coon, D. Bluck, Comparison of the Peng–Robinson and Soave–Redlich–Kwong equations of state using a new zero-pressure-basedmixing rule for the prediction of high-pressure and high-temperature phase equilibria, Ind. Eng. Chem. Res. 37 (1998) 1580–1585.
[22] D.S.H. Wong, H. Orbey, S.I. Sandler, Equation of state mixing rule for nonideal mixtures using available activity coefficient model parameters and that allows extrapolation over large ranges of temperature and pressure, Ind. Eng. Chem. Res. 31 (1992) 2033–2039.
[23] K.A. Pividal, C. Sterner, S.I. Sandler, H. Orbey, Vapor–liquid equilibrium from infinite dilution activity coefficients: measurement and prediction of oxygenated fuel additives with alkanes, Fluid Phase Equilib. 72 (1992) 227–250.
[24] H. Orbey, S.I. Sandler, D.S.H.Wong, Accurate equation of state predictions at high temperatures and pressures using the existing UNIFACmodel, Fluid Phase Equilib. 85 (1993) 41–54
[25] H. Huang, S.I. Sandler, Prediction of vapor–liquid equilibria at high pressures using activity coefficient parameter obtained from low-pressure data: a comparison of two equations of state mixing rules, Ind. Eng. Chem. Res. 32 (1993) 1498–1503.
[26] H. Huang, S.I. Sandler, H. Orbey, Vapor–liquid equilibria of some hydrogen + hydrocarbon systems with the Wong–Sandler mixing rule, Fluid Phase Equilib. 96 (1994) 143–153.
[27] H. Orbey, S.I. Sandler, Reformulation of Wong–Sandler mixing rule for cubic equations of state, AIChE J. 41 (1995) 683–690.
[28] P.T. Eubank, G.-S. Shyu, N.S.M. Hanif, New procedures for application of theWong–Sandler mixing rules to the prediction of vapor–liquid equilibria, Ind. Eng. Chem. Res. 34 (1995) 314–325.
[29] P. Ghosh, T. Taraphdar, Prediction of vapor–liquid equilibria of binary systems using PRSV equation of state and Wong–Sandler mixing rules, Chem. Eng. J. 70 (1998) 15–24.
[30] G.N. Escobedo-Alvarado, S.I. Sandler, Study of EOS-Gex mixing rules for liquid-liquid equilibria, AIChE J. 44 (1998) 1178–1187.
[31] H. Orbey, C. Balci, G.A. Gürüz, Phase equilibrium of asymmetric systems by predictive equations of state models, Ind. Eng. Chem. Res. 41 (2002) 963–967.
[32] M.B. Shiflett, S.I. Sandler, modeling flourocarbon vapor–liquid equilibria using the Wong–Sandler model, Fluid Phase Equilib. 147 (1998) 145– 162.
[33] T. Yang, G.-J. Chen, W. Yan, T.-M. Guo, Extension of the Wong–Sandler mixing rule to the three parameter Patel–Teja equation of state: application up to the near-critical region, Chem. Eng. J. 67 (1997) 26–36.

[34] P. Coutsikos, N.S. Kalospiros, D.P. Tassios, Capabilities and limitations of the Wong–Sandler mixing rules, Fluid Phase Equilib. 108 (1995) 59–78.
[35] Y. Bard, Nonlinear Parameters Estimation, Academic Press, 1974.
[36] T.L. Sutton, J.F. MacGregor, The analysis and design of binary vapour–liquid equilibrium experiments. I. Parameter estimation and consistency test, Can. J. Chem. Eng. 55 (1977) 602–608.
[37] V.G. Niesen, V.F. Yesavage, Application of a maximum likelihood method using implicit constraints to determine equation of state parameters from binary phase behaviour data, Fluid Phase Equilib. 50 (1989) 249–266.
[38] T.F. Anderson, D.S. Abrams, E.A. Grens II, Evaluation of parameters for nonlinear thermodynamic models, AIChE J. 24 (1978) 20–29.
[39] R. Paunovic, S. Jovanovic, A. Mihajlov, Rapid computation of binary interaction coefficients of an equation of state for vapor–liquid equilibrium calculations: application to the Redlich–Kwong–Soave equation of state, Fluid Phase Equilib. 6 (1981) 141–148.
[40] D. Salazar-Sotelo, A. Boiveaut-Boudehen, H. Renon, Computer calculation of the optimal parameters of a model for the simultaneous representation of experimental binary and ternary vapor–liquid and liquid–liquid equilibrium data, Fluid Phase Equilib. 27 (1986) 383–403.
[41] P. Englezos, N. Kalogerakis, P.R. Bishnoi, Estimation of binary interaction parameters for equations of state subject to liquid phase stability requirements, Fluid Phase Equilib. 53 (1989) 81–88.
[42] P. Englezos, N. Kalogerakis, M.A. Trebble, P.R. Bishnoi, Estimation of multiple binary interaction parameters in equations of state usingVLEdata: application to the Trebble–Bishnoi equation of state, Fluid Phase Equilib. 58 (1990) 117–132.
[43] P. Englezos, N. Kalogerakis, P.R. Bishnoi, A systematic approach for the efficient estimation of interaction parameters in equations of state using binary VLE data, Can. J. Chem. Eng. 71 (1993) 322–326.
[44] J.R. Nunhez, C.B.B. Costa, R. Guirardello, A new spline approach for data fitting, Fluid Phase Equilib. 220 (2004) 171–180.
[45] D.Y. Peng, D.B. Robinson, A new two constant equation of state, Ind. Eng. Chem. Fundam. 15 (1976) 59–64.
[46] H. Renon, J.M. Prausnitz, Local compositions in thermodynamic excess functions for liquid mixtures, AIChE J. 14 (1967) 135–144.
[47] Z. Knez, M. Habulin, Compressed gases as alternative enzymatic reaction solvent. A short review, J. Supercrit. Fluids 23 (2002) 29–42.
[48] H.J. Dai, J.M. Simonson, H.D. Cochran, Density measurements of styrene solutions in supercritical CO2, J. Chem. Eng. Data 46 (2001) 1571– 1573.
[49] V.P. Saraf, E. Kiran, Free radical polymerization of styrene in supercritical fluids, Polymer 31 (1990) 687–688.
[50] H. Shiho, J.M. DeSimone, Preparation of micron-size polystyrene particles in supercritical carbon dioxide, J. Polym. Sci. 37 (1999) 2429–2437.
[51] H. Shiho, J.M. DeSimone, Dispersion polymerizations of styrene in supercritical carbon dioxide utilizing random copolymers containing a fluorinated acrylate for preparing micron-size polystyrene particles, J. Polym.
Sci. 38 (2000) 1146–1153.
[52] D.A. Canelas, J.M. DeSimone, Dispersion polymerizations of styrene in carbon dioxide stabilized with poly(styrene-*b*-dimethylsiloxane), Macromolecules 30 (1997) 5673–5682.
[53] M.S. W. Wei, T.S. Brown, A.J. Kidnay, E.D. Sloan, Vapor + liquid equilibria for the ternary system methane + ethane + carbon dioxide at 230K and its constituent binaries at temperatures from 207 to 270 K, J. Chem. Eng. Data 40 (1995) 726–731.
[54] L.A. Webster, A.J. Kidnay, Vapor–liquid equilibria for the methane–propane–carbon dioxide systems at 230 and 270 K, J. Chem. Eng. Data46 (2001) 759–764.
[55] K. Tochigi, K. Hasegawa, N. Asano, K. Kojima, Vapor–liquid equilibria for the carbon dioxide + pentane and carbon dioxide + toluene systems, J. Chem. Eng. Data 43 (1998) 954–956.

[56] K. Ohgaki, T. Katayama, Isothermal vapor–liquid equilibrium data for binary systems containing carbon dioxide at high pressures: methanol–carbon dioxide, n-hexane–carbon dioxide, and benzene–carbon dioxide systems, J. Chem. Eng. Data 21 (1976) 53–55.
[57] Kalra H., Kubota H., D.B. Robinson, H.-J. Ng, Equilibrium phase properties of the carbon dioxide–n-heptane system, J. Chem. Eng. Data 23 (1978) 317–321.
[58] W. L. Weng, M. J. Lee, Vapor–liquid equilibrium of the octane/carbon dioxide, octane/ethane, and octane/ethylene systems, J. Chem. Eng. Data 37 (1992) 213–215.
[59] N. Nagarajan, R.L. Robinson, Equilibrium phase compositions, phase densities, and interfacial tensions for CO_2 + hydrocarbon systems. CO_2 + *n*-decane, J. Chem. Eng. Data 31 (1986) 168–171.
[60] M. Akgün, D. Emel, N. Baran, N. A. Akgûn, Deniz S., Dincer S., Styrene–carbon dioxide phase equilibria at high pressures, J. Supercrit. Fluids 31 (2004) 27–32.
[61] Y. Iwai, Tatsuo Morotomi, Kenji Sakamoto, Yoshio Koga, and Yasuhiko Arai, High-Pressure Vapor-Liquid Equilibria for Carbon Dioxide + Limonene. J. Chem. Eng. Data 1996, 41, 951-952.
[62] C. Secuianu, V. Feroiu and D. Geana, High-Pressure Vapor-Liquid Equilibria in the System Carbon Dioxide + 1-Butanol at Temperatures from (293.15 to 324.15) K. Journal of chemical and Engineering Data, 49 (2004) 1635-1638.
[63] D. W. Jennings, , Lee, R. and Teja A. S. Vapor-Liquid Equilibria in the Carbon Dioxide + Ethanol and Carbon Dioxide + l-Butanol Systems. Journal of Chemical and Engineering Data, 36 (1991) 303-307.
[64] O. E. Solis, L.A. G. Luna, S.I. Sandler, J.G. S. Hernández, Vapor–liquid equilibria and critical points of the CO_2 + 1-hexanol and CO_2 + 1-heptanol systems. Fluid Phase Equilibria 210 (2003) 215–227.
[65] C. J. Chiehming, , C. K. Lunga, D. C. Yih, A new apparatus for the determination of P–x–y diagrams and Henry's constants in high pressure alcohols with critical carbon dioxide. Journal of Supercritical Fluids 12 (1998) 223–237.
[66] Li C. Feng, K.-W. Cheng, M. Tang, Y.-P. Chen, Vapor–liquid equilibria of carbon dioxide with ethyl benzoate, diethyl succinate and isoamyl acetate binary mixtures at elevated pressures, J. Supercrit. Fluids 21 (2001) 111–121.
[67] W.-H. Hwu, J.-S. Cheng, K.-W. Cheng, Y.-P. Chen, Vapor–liquid equilibrium of carbon dioxide with ethyl caproate, ethyl caprylate and ethyl caprate at elevated pressures, J. Supercrit. Fluids 28 (2004) 1–9.
[68] M. Vázquez da Silva, D. Barbosa, P.O. Ferreira, High pressure vapor–liquid equilibrium data for the system carbon dioxide + decanal at 288.2, 303.2, and 313 2K, J. Chem. Eng. Data 47 (2002) 1171–1172.
[69] K.-W. Cheng, M. Tang, Y.-P. Chen, Vapor–liquid equilibria of carbon dioxide with diethyl oxalate, ethyl laurate, and dibutyl phthalate binary mixtures at elevated pressures, Fluid Phase Equilib. 181 (2001) 1–16.
[70] Y. Iwai, N. Hosotani, T. Morotomi, Y. Koga, Y. Arai, High-pressure vapor–liquid equilibria for carbon dioxide + linalool, J. Chem. Eng. Data 39 (1994) 900–902.
[71] I. Ashour, G. Aly, Effect of computation techniques for equation of state binary interaction parameters on the prediction of binary VLE data, Comput. Chem. Eng. 20 (1996) 79–91.
[72] J.A. López, C.A. Cardona, Phase equilibrium calculations for carbon dioxide + n-alkanes binary mixtures with theWong–Sandler mixing rules, Fluid Phase Equilib. 239 (2006) 206–212.

CHAPTER 4

MIXING RULES COMBINING AN EQUATION OF STATE WITH FREE ENERGY MODELS (EOS-G^{ex}) FOR ASYMMETRIC MIXTURES CONTAINING CO_2

In this chapter is presented the summary for a collection of mixing rules that combine activity coefficient (or excess free energy of mixing) models with equations of state. The original Huron-Vidal (HVO), the modified Michelsen-Huron-Vidal first-order (MHV1), the modified Michelsen-Huron-Vidal second-order (MHV2), the Wong-Sandler (WS), and the modified Orbey-Sandler (HVOS) mixing rules were used for phase equilibrium calculation of asymmetric mixtures containing carbon dioxide. Their correlative and predictive capabilities were compared for asymmetric binary mixtures containing carbon dioxide at high pressures. Peng–Robinson (PR) equation of state (EOS) coupled with the HVO, MHV1, MHV2, WS and HVOS mixing rules were used for modeling the vapor liquid equilibrium (VLE) in all cases. It was found that the correlation capacity of the WS mixing rule is better than the HVOS mixing rule. The prediction capacities of the WS and HVOS mixing rules, based on the extrapolation of model parameters obtained at the lowest available temperature and pressure to higher values, were found to be acceptable. Each of the mixing rules reviewed here is successful for at least some range of temperatures, though some of their shortcomings are discussed.

4.1. Introduction

Equations of state (EOS) are widely used for modeling the phase equilibrium and *PVT* properties of mixtures of non-polar and slightly polar substances with the proper choice of a mixing rule. Although EOS coupled with the classical van der Waals (VDW) one-fluid mixing rule is probably the most extensively used modeling tool for the VLE of relatively simple mixtures, it cannot accurately represent complex mixtures. The inability of classical quadratic mixing rules to represent the phase behavior of nonideal mixtures such as hydrocarbons with industrial gases and organic solvents has been treated using empirical composition-dependent combining rules [1-3]. When fitting VLE data with the VDW model, the referred binary interaction parameters is approximately zero for simple mixtures, however for highly nonideal mixtures accurate correlation of VLE is not possible by this method.

In recent years equations of state mixing rules have been developed that combine excess free-energy models with a cubic EOS [4]. This referred group of mixing rules is based on

equating the excess free energy from a liquid-phase activity coefficient model with the corresponding term from an EOS [5]. Huron and Vidal [6] proposed the first successful combination of an EOS and activity coefficient models by requiring that the mixture EOS at liquid densities should behave like an activity coefficient model. This mixing rule will be referred as the HVO model. For nonideal mixtures the HVO model shows good correlation capabilities but is not satisfactory for extrapolation over a range of temperatures. The problem with the HVO model resulting from the pressure dependence of the excess Gibbs free energy of mixing led to propose EOS mixing rules based on the idea of combining activity coefficient models and equations of state at low pressures (or zero). The modified Huron-Vidal mixing rule of Michelsen (MHV1) [7,8] and that of Dahl and Michelsen (MHV2) [9] are the most used ones of the low pressure class. An assumption inherent in both models is that the ratio of the zero pressure liquid molar volume to close packing parameter b is the same for the mixture and each of its pure components. Although MHV1 and MHV2 do not satisfy the second virial coefficient boundary condition and include approximate linear and quadratic extrapolation procedure respectively, good results have been obtained by the predictions of experimental data for highly nonideal systems. In the same way the Wong-Sandler (WS) have developed a mixing rule [10] that combines an EOS with an excess Helmholtz free energy at infinite pressure, providing a number of advantages, and has the correct low-density composition dependence. This mixing rule has been successful in several applications [11-14]. The reformulation introduced by Orbey and Sandler [15] for the HVOS mixing rule is based on the assumption of k_{ij} could also be obtained from excess free energy model parameters and therefore does not contain any additional information. Furthermore, the authors proposed the assumption of a universal linear algebraic function, u, which relates the liquid molar volumes and their hard core volume. The parameters in the reformulated mixing rule can be obtained from correlation of vapor liquid equilibrium data or from the two infinite dilution activity coefficients for each binary pair in the mixture.

In the present chapter the VLE of asymmetric binary mixtures containing carbon dioxide was studied with the PR equation of state [16] coupled with HVO, MHV1, MHV2, WS and HVOS mixing rules. The correlative and predictive capabilities of these mixing rules were compared for asymmetric binary mixtures containing carbon dioxide at high pressures. The NRTL model [17] was utilized to predict the Gibbs and Helmholtz free energy. A Levenberg-Marquartdt minimization algorithm was used in all cases.

4.2. Phase equilibrium using EOS approach

Many equations of state are available in the literature and some recent and complete reviews are available [18-19]. For the purposes of illustration, here we use the Peng-Robinson equation of state [16] this EOS has the following form:

$$P = \frac{RT}{\underline{V} - b} - \frac{a(T)}{\underline{V}(\underline{V} + b) + b(\underline{V} - b)} \tag{1}$$

where P is the pressure, T the absolute temperature, R the ideal gas constant furthermore a and b are the energy and size parameters which are calculated from:

$$a(T) = 0.457235 \frac{R^2 T_c^2}{P_c} \alpha(T_r) \tag{2}$$

$$b = 0.077796 \frac{RT_c}{P_c} \tag{3}$$

the subscripts c and r denotes critical and reduced conditions, respectively. The correlation for the α function is:

$$\alpha(T_r) = \left[1 + \kappa\left(1 - \sqrt{T_r}\right)\right]^2 \tag{4}$$

$$\kappa = 0.37464 + 1.54226\omega - 0.26992\omega^2 \tag{5}$$

where ω is the acentric factor and T_r is the temperature reduce.

4.3. Combined equation of state and excess Gibbs energy model

The first successful mixing rule for mixtures was the one-fluid model proposed by van der Waals. This model is applicable at all densities and temperatures, but only to relatively simple mixtures. Describe the VLE of mixtures in which one component is above its critical temperature has been complicated. The absence of an accurate gas phase model for polar organic compounds has resulted in difficulties in describing the vapor liquid equilibrium of polar mixtures at high pressures and supercritical fluid extraction processes. On the other hand, methods that combine an equation of state with an excess Gibbs energy or activity coefficient models have been developed to describe accurately highly nonideal mixtures over large ranges of temperatures and pressures. The idea of these models is to recognize that EOS, such as PR, PSRV and PSRK equations, have two constants, a and b, used to satisfy two boundary conditions. The first condition is that at low-density and high-

density limits the composition dependence of the second virial coefficient obtained from an equation of state should be agree with the statistical thermodynamic postulates:

$$B_{mix}(T,x) = \sum_i \sum_j x_i x_j B_{ij}(T) \tag{6}$$

According with the eq. (6) the second virial coefficient from a cubic equation of state is:

$$B(T) = b - \frac{a(T)}{RT} \tag{7}$$

Finally the first boundary condition can be written as:

$$b - \frac{a}{RT} = \sum_i \sum_j x_i x_j \left(b_{ij} - \frac{a_{ij}}{RT} \right) \tag{8}$$

This condition conclude that is necessary to use another equation to find the parameters *a* and *b* separately. A second equation comes from requiring that the excess Gibbs free energy at infinite pressure (i.e., at liquid-like densities) calculated from an equation of state be equivalent to that from excess Gibbs free energy (activity coefficient) model for liquids.

4.3.1. The original Huron-Vidal (HVO) model

Huron and Vidal proposed the first successful combination of an EOS and activity coefficient models. The relation between excess Gibbs free energy at infinite pressure calculated from an equation of state and the excess Gibbs free energy calculated from an activity coefficient model can be written as:

$$\underline{G}^{ex}_{\gamma}(T, P=\infty, x) = \underline{G}^{ex}_{EOS}(T, P=\infty, x) \tag{9}$$

Where the subscripts EOS and γ indicate $\underline{G}^{ex}$ as computed from an equation of state and an activity coefficient model, respectively. The relation between an activity coefficient and EOS is:

$$\gamma_i = \overline{\phi}_i(T,P,x_i) / \phi_i(T,P) \tag{10}$$

where $\overline{\phi}_i(T,P,x_i)$ is the fugacity coefficient of species *i* in a mixture, $\phi_i(T,P)$ is the pure component fugacity coefficient, both obtained from the EOS at the temperature and pressure of the mixture. Thus the molar excess Gibbs free energy is defined by the eq. (11):

$$\frac{\underline{G}^{ex}}{RT} = \sum_i x_i \ln(\gamma_i) \tag{11}$$

By replacing Eqs. (10) into (11):

$$\frac{\underline{G}^{ex}_{EOS}\left(T,P,x_i\right)}{RT}=\ln\left(\bar{\phi}\left(T,P,x_i\right)\right)-\sum_i x_i\ln\left(\phi_i\left(T,P\right)\right) \tag{12}$$

According with the definition for fugacity coefficient the eq. (12) can be expressed as:

$$\frac{\underline{G}^{ex}_{EOS}}{RT}=\left[Z-\sum_i x_i Z_i\right]-\left[\ln\left(Z\right)-\sum_i x_i\ln\left(Z_i\right)\right]-\left[\int_\infty^{\underline{V}}\frac{\left(Z-1\right)}{\underline{V}}d\underline{V}-\sum_i x_i\int_\infty^{\underline{V}}\frac{\left(Z-1\right)}{\underline{V}}d\underline{V}\right] \tag{13}$$

For the PR equation the eqn. (13) become:

$$\begin{aligned}\frac{\underline{G}^{ex}_{EOS}}{RT}=Z-\sum_i x_i Z_i-\sum_i x_i\ln\left(\frac{Z}{Z_i}\right)-\sum_i x_i\ln\left(\frac{1-b/\underline{V}}{1-b_i/\underline{V}_i}\right)+\frac{a}{2\sqrt{2}bRT}\ln\left(\frac{\underline{V}+\left(1-\sqrt{2}\right)b}{\underline{V}+\left(1+\sqrt{2}\right)b}\right)\\ -\sum_i x_i\left(\frac{a_i}{b_i RT}\right)\frac{1}{2\sqrt{2}}\ln\left(\frac{\underline{V}_i+\left(1-\sqrt{2}\right)b_i}{\underline{V}_i+\left(1+\sqrt{2}\right)b_i}\right)\end{aligned} \tag{14}$$

The expression (14) is the starting point for solve the EOS parameters *a* and *b* in terms of the mole fraction. Since, from an EOS in the limit of infinite pressure, as $P\to\infty$, $\underline{V}_i\to b_i$ and $\underline{V}\to b$, replacing into eqn. (14), giving:

$$\left[\ln\left(Z\right)-\sum_i x_i\ln\left(Z_i\right)\right]+\sum_i x_i\ln\left(\frac{1-b/\underline{V}}{1-b_i/\underline{V}_i}\right)=0 \tag{15}$$

$$\frac{\underline{G}^{ex}_{EOS}\left(T,P\to\infty,x_i\right)}{RT}=\frac{C^*}{RT}\left[\frac{a}{b}-\sum_i x_i\frac{a_i}{b_i}\right]+\frac{P}{RT}\sum_i x_i\left(b-b_i\right) \tag{16}$$

The equation (16) is a rigorous combination of an EOS and an activity coefficient model when the left hand side of this equation is expressed using an activity coefficient activity such as NRTL. The excess Gibbs free energy of mixing computed from an EOS is a function of pressure, whereas activity coefficient models are independent of pressure or density. The thermodynamic relation between Gibbs free energy and Helmholtz free energy is defined by:

$$\underline{G}^{ex}\left(T,P,x\right)=\underline{A}^{ex}\left(T,P,x\right)+P\underline{V}^{ex}\left(T,P,x\right) \tag{17}$$

According with the eqn. (17) the $\underline{A}^{ex}(T,P,x)$ in the liquid state being almost independent of pressure, to use eqn. (16) it is necessary that:

$$\underline{V}^{ex} = \underline{V} - \sum_i x_i \underline{V}_i = b - \sum_i x_i b_i = 0 \tag{18}$$

Since at infinite pressure from an equation of state $\underline{V}_i = b_i$. The eqn. (18) can be replaced in eq. (16) providing the two equations necessary to determine the two EOS constants. The resulting mixing rule for the *a* parameters is:

$$a = b\left[\sum_i x_i \left(\frac{a_i}{b_i}\right) + \frac{\underline{G}^{ex}}{C^*}\right] \tag{19}$$

The EOS constant *b* is expressed as follows:

$$b = \sum_i x_i b_i \tag{20}$$

The eqs. (19) and (20) constitute the original Huron-Vidal mixing rule, referred as the HVO in this chapter.

4.3.2. The Michelsen-Huron-Vidal (MHV1) model

The modified Huron Vidal mixing rule of Michelsen (MHV1) fixes the problem with the HVO model resulting from the pressure dependence of the excess Gibbs free energy of mixing. The idea behind this mixing rule is to use the eqn. (14) at *P*=0 to obtain:

$$\frac{\underline{G}^{ex}_{EOS}(P=0)}{RT} = -\sum_i x_i \ln\left(\frac{\underline{V}^o/b - 1}{\underline{V}^o_i/b_i - 1}\right) - \sum_i x_i \ln\left(\frac{b}{b_i}\right) + \left(\frac{a}{bRT}\right)\frac{1}{2\sqrt{2}}\ln\left(\frac{\underline{V}^o + \left(1-\sqrt{2}\right)b}{\underline{V}^o + \left(1+\sqrt{2}\right)b}\right) - \sum_i x_i \left(\frac{a_i}{b_i RT}\right)\frac{1}{2\sqrt{2}}\ln\left(\frac{\underline{V}^o_i + \left(1-\sqrt{2}\right)b_i}{\underline{V}^o_i + \left(1+\sqrt{2}\right)b_i}\right) \tag{21}$$

where the superscript 0 denotes the value of the volume at *P*=0. Michelsen (1990b) rewrite the eqn. (21) in terms of *q* to obtain:

$$q(\alpha) = \sum_i x_i q(\alpha_i) + \frac{\underline{G}^{ex}_{\gamma}(T, P=0, x_i)}{RT} + \sum_i x_i \ln\left(\frac{b}{b_i}\right) \tag{22}$$

where $\alpha = a/bRT$ and here the function $q(\alpha)$ is given by:

$$q(\alpha) = -\ln\left(\underline{V}^o/b - 1\right) + \left(\frac{a}{bRT}\right)\frac{1}{2\sqrt{2}}\ln\left(\frac{\underline{V}^o + \left(1-\sqrt{2}\right)b}{\underline{V}^o + \left(1+\sqrt{2}\right)b}\right) \tag{23}$$

The equation used to define the mixing rule completely is eqn. (20). However, it is not necessary to impose the eqn. (20) because the term of the Gibbs free energy using a reference pressure zero is not longer. Other choices, such as the last equality of eqn. (8), could be used as well. A variety of approximations were suggested in the cases in which temperatures at which there is no liquid root of the EOS to use in the right hand side of eqn. (23), Michelsen (1990b) proposed a linear relation:

$$q(\alpha) \approx q_0 + q_1\alpha \tag{24}$$

Substitution of this expression into eqn. (22) results in the explicit mixing rule:

$$\frac{a}{bRT} = \sum_i x_i\left(\frac{a_i}{b_iRT}\right) + \frac{1}{q_1}\left[\frac{\underline{G}_\gamma^{ex}}{RT} + \sum_i x_i \ln\left(\frac{b}{b_i}\right)\right] \tag{25}$$

The recommended value of q_1 being -0.593. The eqn. (25) combined with the eqn. (20) is similar to the original Huron-Vidal mixing rule and is to known as the modified Huron-Vidal first order (MHV1).

4.3.3. The Michelsen-Huron-Vidal (MHV2) model

The modified Huron-Vidal first order (MHV1) provides a fair reproduction of the free Gibbs energy model, but for better accuracy, a quadratic extrapolation was proposed for $q(\alpha)$:

$$q(\alpha) \approx q_0 + q_1\alpha + q_2\alpha^2 \tag{26}$$

The relation between the excess Gibbs free energy from an EOS and from an activity coefficient models takes the following quadratic form in this approach:

$$q_1\left(\frac{a}{bRT} - \sum_i x_i\frac{a_i}{b_iRT}\right) - q_2\left(\left(\frac{a}{bRT}\right)^2 - \sum_i x_i\left(\frac{a_i}{b_iRT}\right)^2\right) = \frac{\underline{G}_\gamma^{ex}}{RT} + \sum_i x_i \ln\left(\frac{b}{b_i}\right) \tag{27}$$

The eqn. (27) combined with the eqn. (20) is to known as the modified Huron-Vidal second order (MHV2) mixing rule. The recommended values of q_1 and q_2 are -0.478 and -0.0047, respectively. The derivation of fugacity coefficients from the MHV2 mixing rule is described in the Appendix B.

4.3.4. Orbey-Sandler modification of the Huron-Vidal mixing rules (HVOS)

The model introduce by Orbey and Sandler (1995c) assumed that there is a universal linear algebraic function that relates the liquid molar volumes to their hard core volumes, such as $\underline{V} = ub$, where u is a positive constant larger than unity. This assumption is similar to the concept of constant packing fraction. Using the Helmholtz free energy and assuming that at infinite pressure, both for mixtures and for pure components, u approaches a unique value, one obtains:

$$\frac{\underline{A}^{ex}_{EOS}}{RT} = -\sum_i x_i \ln\left(\frac{ub}{ub_i}\right) - \sum_i x_i \ln\left(\frac{1-u}{1-u_i}\right) + \frac{a}{2\sqrt{2}bRT}\ln\left(\frac{u+\left(1-\sqrt{2}\right)}{u+\left(1+\sqrt{2}\right)}\right) - \sum_i x_i \left(\frac{a_i}{b_i RT}\right)\frac{1}{2\sqrt{2}}\ln\left(\frac{u_i+\left(1-\sqrt{2}\right)}{u_i+\left(1+\sqrt{2}\right)}\right) \tag{28}$$

The equation (28) can be rewritten as:

$$\frac{\underline{A}^{ex}_{EO}}{RT} = -\sum_i x_i \ln\left(\frac{b}{b_i}\right) - \frac{a}{2\sqrt{2}bRT}\ln\left(\frac{u+\left(1-\sqrt{2}\right)}{u+\left(1+\sqrt{2}\right)}\right) - \sum_i x_i \left(\frac{a_i}{b_i RT}\right)\frac{1}{2\sqrt{2}}\ln\left(\frac{u_i+\left(1-\sqrt{2}\right)}{u_i+\left(1+\sqrt{2}\right)}\right) \tag{29}$$

Further, since u approaches unity at both infinite pressure and at very low temperatures, for simplicity, as an approximation, one can take u=1 at all conditions and obtain:

$$\frac{\underline{A}^{ex}_{EOS}}{RT} = \frac{\underline{G}^{ex}_{\gamma}}{RT} = -\sum_i x_i \ln\left(\frac{b}{b_i}\right) + C\left(\frac{a}{bRT} - \sum_i x_i \left(\frac{a_i}{b_i RT}\right)\right) \tag{30}$$

$$a = bRT\left[\sum_i x_i \frac{a_i}{RTb_i} + \frac{1}{C}\left[\sum_i x_i \ln\left(\frac{b}{b_i}\right) + \frac{\underline{G}^{ex}_{\gamma}}{RT}\right]\right] \tag{31}$$

In the eqn. (30) the parameter C is defined by the PR EOS. In this model, eqns. (31) and (20) are used to obtain the EOS parameters a and b. It is an approximate model but is agreement with the spirit of the van der Waals hard core concept, and it is algebraically very similar to several of the commonly used zero pressure models mentioned in this chapter. The derivation of fugacity coefficients from the HVOS mixing rule is described in the Appendix B.

4.3.5. The Wong-Sandler (WS) model

Wong and Sandler (1992) have developed a new mixing rule for cubic EOS equates the excess Helmholtz free energy at infinite pressure from an EOS to that from an activity coefficient model. Hence, use of the Helmholtz free energy insures that the second virial

coefficient calculated from an EOS has a quadratic dependence as required by statistical mechanics. The WS mixing rule satisfy the first boundary condition in agree with the statistical thermodynamic postulates

$$B_{mix}\left(T,x\right)=\sum_i\sum_j x_i x_j B_{ij}\left(T\right)=\sum_i\sum_j x_i x_j\left(b_{ij}-\frac{a_{ij}}{RT}\right)=b-\frac{a}{RT} \tag{32}$$

The eqn. (32) is a restriction on the parameters together with the combining rule:

$$\left(b-\frac{a}{RT}\right)_{ij}=\frac{\left(b-\frac{a}{RT}\right)_i+\left(b-\frac{a}{RT}\right)_j}{2}\left(1-k_{ij}\right) \tag{33}$$

where k_{ij} is the second virial coefficient binary interaction parameter. Note that eqn. (33) does not provide relations for the parameters a and b separately and thus an additional equation is necessary. A second equation comes from requiring that the excess Gibbs energy predicted from an EOS at liquid like densities be equivalent to that from excess Gibbs energy or activity coefficient models. The thermodynamic relation between excess Gibbs energy and Helmholtz free energy were described by the eqn. (17). Since at low pressures, $\underline{V}^E$ is small, the difference between $\underline{G}^E$ and $\underline{A}^E$ is also small. Consequently, Wong and Sandler established the following approximation:

$$\underline{G}^{ex}\left(T,P=1bar,x\right)=\underline{A}^{ex}\left(T,P=1bar,x\right)=\underline{A}^{ex}\left(T,P=\infty,x\right) \tag{34}$$

The pressure independence of $\underline{A}^{ex}$ at liquid densities provides the second equation for the a and b parameters comes from eqn. (34) expressed as:

$$\underline{A}^{ex}_{EOS}\left(T,P=\infty,x\right)=\underline{A}^{ex}_{\gamma}\left(T,P=\infty,x\right)=\underline{A}^{ex}_{\gamma}\left(T,P=1bar,x\right)=\underline{G}^{ex}_{\gamma}\left(T,P=1bar,x\right) \tag{35}$$

To proceed further, we note that as $P\to\infty$ (and $\underline{V}_i\to b_i$ and $\underline{V}\to b$) can be obtain:

$$a=b\left[\sum_i x_i\frac{a_i}{b_i}+\frac{\underline{A}^{ex}_{\gamma}}{C}\right] \tag{36}$$

$$b=\frac{\sum_i\sum_j x_i x_j\left(b-\frac{a}{RT}\right)_{ij}}{1-\sum_i x_i\frac{a_i}{b_i RT}-\frac{\underline{A}^{ex}_{\gamma}}{CRT}} \tag{37}$$

with

$$C = \frac{1}{\sqrt{2}} \ln\left(\sqrt{2} - 1\right) \tag{38}$$

where x is the liquid molar fraction, and $\underline{A}_{\gamma}^{ex}$ is the excess Helmholtz free energy at infinite pressure which is calculated from an excess Gibbs free energy model. The derivation of fugacity coefficients from the WS mixing rule is described in the Appendix B.

In this work, the excess Helmholtz free energy at infinite pressure was calculated with the NRTL model [17]:

$$\frac{\underline{A}_{\infty}^{E}}{RT} = \sum_{i} z_i \left(\frac{\sum_{j} z_j \tau_{ji} g_{ji}}{\sum_{k} z_k g_{ki}} \right) \tag{39}$$

$$g_{ij} = \exp\left(-\alpha_{ij} \tau_{ij}\right) \tag{40}$$

In the case of binary mixtures, α_{12} (=α_{21}), τ_{12} and τ_{21} are the three parameters of the NRTL model. As recommended by Renon and Prausnitz [17], a constant value of α_{12} (0.3) was used in this work. In this contribution, the adjustable parameters of the NRTL model: τ_{12} and τ_{21} and the second virial coefficient binary interaction parameter k_{12} have been determined using experimental phase equilibrium data at isothermal conditions for each asymmetric mixture containing carbon dioxide by the OF minimization. Furthermore, the VLE parameters were obtained from sets of experimental data using the following objective function [12]:

$$f_{ob} = \sum_{i=1}^{np} \sum_{j=1}^{nc} \left[y_{i,j}^{\exp} - x_{i,j}^{\exp} K_{i,j}^{cal} \right]^2 \tag{41}$$

where K is the distribution coefficient between vapor and liquid phases, the superscripts np and nc denote the numbers of experimental data points and components, and y and x are the molar fraction in the vapor and liquid phases, respectively. This objective function has shown very acceptable performances for VLE of asymmetric binary mixtures at high pressures [11-14]. The summary of EOS-G^{ex} matching conditions is presented in Table 4.1.

The binaries studied in order to investigate the correlation and prediction capabilities of HVO, MHV1, MHV2, WS and HVOS mixing rules, the range of temperatures investigated and the experimental conditions are shown in Table 4.2. The systems studied are asymmetric and are widely used in industrial applications. The phase behavior of CO_2 mixtures is of technological interest because of the occurrence of CO_2 in natural gas, crude oil, and numerous chemical processes.

Table 4.1. Combination of equation of state with excess free energy models, (EOS-G^{ex}), matching conditions

Mixing rules	P, match	G^E, match	b_m
HVO (Original Huron-Vidal, 1979)	∞	$\frac{\underline{G}^{ex}_{EOS}}{RT} = \frac{C}{RT}\left[\frac{a}{b} - \sum_i z_i \frac{a_i}{b_i}\right] + \frac{P}{RT}\sum_i z_i (b - b_i)$	$\sum_i z_i b_{ii}$
MHV1 (Michelsen, 1990)	0	$\frac{\underline{G}^{ex}_{\gamma}}{RT} = q_1\left[\frac{a}{bRT} - \sum_i z_i \left(\frac{a_i}{b_i RT}\right)\right] - \sum_i z_i \ln\left(\frac{b}{b_i}\right),\ q_1 = -0.593$	$\sum_i z_i b_{ii}$
MHV2 (Dahl and Michelsen, 1990)	0	$q_1\left(\frac{a}{bRT} - \sum_i z_i \frac{a_i}{b_i RT}\right) - q_2\left(\left(\frac{a}{bRT}\right)^2 - \sum_i z_i \left(\frac{a_i}{b_i RT}\right)^2\right) = \frac{\underline{G}^{ex}_{\gamma}}{RT} + \sum_i z_i \ln\left(\frac{b}{b_i}\right)$ $q_1 = -0.478\ \ q_2 = -0.0047$	$\sum_i z_i b_{ii}$
WS (Wong and Sandler, 1992)	∞	$\frac{\underline{A}^{ex}_{\gamma}}{RT} = C\left[\frac{a}{bRT} - \sum_i z_i \frac{a_i}{b_i RT}\right]$	${}^{*}b_m$
HVOS (Orbey and Sandler, 1995)	∞	$\frac{\underline{A}^{ex}_{EOS}}{RT} = -\sum_i z_i \ln\left(\frac{b}{b_i}\right) + C\left(\frac{a}{bRT} - \sum_i z_i \left(\frac{a_i}{b_i RT}\right)\right)$	$\sum_i z_i b_{ii}$

${}^{*}b_m = \sum_i \sum_j z_i z_j \left(b - \frac{a}{RT}\right)^{1}_{ij} \Bigg/ \left[1 - \sum_i z_i \frac{a_i}{b_i RT} - \frac{\underline{A}^{E}_{\infty}}{C(1)RT}\right] \qquad {}^{1}\left(b - \frac{a}{RT}\right)_{ij} = \frac{1}{2}\left[\left(b - \frac{a}{RT}\right)_i + \left(b - \frac{a}{RT}\right)_j\right](1 - k_{ij})$

Where k_{ij} is a second virial coefficient binary interaction parameter, z is the molar fraction, $\underline{A}^{ex}$ is the excess Helmholtz free energy which is calculated from an excess Gibbs free energy model and $\underline{G}^{ex}$ is the excess Gibbs free energy model.

4.4 Results and discussion

The deviations between experimental data and calculated values with PR EOS and the Wong–Sandler mixing rules were established through the relative percentage deviations in the bubble point pressure:

$$\Delta P = \sum_{i=1}^{np} \frac{\left| P_{\exp} - P_{cal} \right|}{P_{\exp}} \left(\frac{100}{np} \right) \tag{42}$$

The absolute mean deviation in the molar fraction in the vapor phase is a follows:

$$\Delta y = \sum_{i=1}^{np} \left| y_{\exp} - y_{cal} \right| \frac{1}{np} \tag{43}$$

The optimal parameters shown in Table 4.3 were used to predict the phase equilibrium of the considered mixtures. The agreement with the experimental data is generally satisfactory as shown in Figs. 4.1–4.4.

Table 4.2 Experimental conditions for asymmetric binary mixtures containing CO_2.

Carbon Dioxide +	np	T(K)	Pressure range (bar)	Reference
Methane	20	230.00	8.920–69.91	[20]
	20	250.00	17.83–80.53	[20]
	13	270.00	32.09–83.81	[20]
Ethane	10	207.00	2.920-4.710	[20]
	17	210.00	3.350-5.380	[20]
	15	213.00	3.760-5.640	[20]
Propane	25	230.00	8.9-71.1	[21]
	17	270.00	32.0-79.5	[21]
Methanol	8	298.15	7.89-59.52	[22]
	11	291.15	5.6-43.3	[23]
	16	308.15	13.2-77.2	[23]

Table 4.3 Optimal parameters and deviations values for asymmetric mixtures using EOS-G^{ex} mixing rules

	Carbon dioxide + propane, T=230 K					Carbon dioxide + propane, T=270 K				
	HVO	MHV1	MHV2	WS	HVOS	HVO	MHV1	MHV2	WS	HVOS
τ_{12}	2.2338	2.0158	1.5709	4.5317	1.9126	1.1005	1.2162	1.3014	4.3880	1.1921
τ_{21}	0.7053	0.3891	0.5718	1.3974	0.5363	0.6007	0.1265	0.0523	0.6800	0.2031
ΔP	2.4042	2.8807	2.7976	1.6090	2.5996	3.6021	1.7878	1.1003	1.4843	1.9921
Δy	0.0174	0.0183	0.0178	0.0116	0.0177	0.0106	0.0078	0.0065	0.0022	0.0082
	Carbon dioxide + methane, T=230 K					Carbon dioxide + methane, T= 250 K				
τ_{12}	0.8646	0.8861	1.0149	0.8901	0.9589	0.9004	0.9959	1.0809	0.7882	1.0714
τ_{21}	0.6077	0.5211	0.4091	1.5526	0.5280	0.4003	0.2332	0.1404	1.4623	0.2269
ΔP	1.5046	1.1529	1.1497	2.5008	0.9238	0.8131	0.4056	0.4127	1.5361	0.4311
Δy	0.0051	0.0039	0.0038	0.0246	0.0036	0.0066	0.0068	0.0069	0.0167	0.0070
	Carbon dioxide + methane, T=270 K					Carbon dioxide + methanol, T=291.15 K				
τ_{12}	1.0982	1.0457	1.0080	0.2308	1.0074	1.1189	1.1075	1.2105	2.9947	0.2352
τ_{21}	0.0374	0.0273	0.0149	4.1994	0.1045	-0.2619	-0.3641	0.1104	-0.3473	0.3171
ΔP	0.9403	0.9079	0.7891	1.0604	0.8305	1.2727	1.3376	3.0814	2.1548	3.1172
Δy	0.0063	0.0061	0.0056	0.0269	0.0057	0.0038	0.0038	0.0037	0.0025	0.0038
	Carbon dioxide + methanol , T=298.16 K					Carbon dioxide + methanol , T=308.15 K				
τ_{12}	1.1181	0.8589	1.8532	6.4430	1.0149	1.2115	1.2083	1.9033	5.6889	1.1119
τ_{21}	0.0187	0.0617	0.0078	0.1953	-0.0025	0.07317	-0.0677	-0.0357	0.1204	0.0449
ΔP	5.3478	6.1531	1.6385	0.9526	5.5711	5.4876	4.9996	3.0275	2.9878	5.7292
Δy	0.0041	0.0041	0.0041	0.0027	0.0041	0.00321	0.00318	0.0026	0.0049	0.00323

(Continued)

	Carbon dioxide + ethano, T= 207 K					Carbon dioxide + ethano, T=210 K				
	HVO	MHV1	MHV2	WS	HVOS	HVO	MHV1	MHV2	WS	HVOS
τ_{12}	2.0193	2.1111	2.2251	2.2590	2.2204	2.3023	2.3948	2.3033	2.2015	2.3067
τ_{21}	0.7445	0.4829	0.3693	1.3164	0.5537	0.5254	0.2628	0.2282	1.3188	0.4174
ΔP	0.5171	0.7894	0.9604	0.2416	0.7828	1.1914	1.6216	1.5655	0.2492	1.3123
Δy	0.0067	0.0114	0.0143	0.0066	0.0113	0.0119	0.0187	0.0175	0.0045	0.0137

	Carbon dioxide + ethano, T= 213 K				
τ_{12}	2.1982	2.2283	2.2353	2.0655	2.2533
τ_{21}	0.5134	0.2782	0.1945	1.2500	0.3787
ΔP	1.5331	1.9560	2.0971	0.5655	1.8050
Δy	0.0125	0.0162	0.0176	0.0084	0.0148

The correlation capacities of the mixing rules used and the results for CO_2 systems are presented here. The parameters estimation was performed using the Levenberg-Marquardt minimization algorithm for each mixture with eqn. (41). The optimal NRTL model parameters (τ_{12} and τ_{21}) are presented for asymmetric binary mixtures containing carbon dioxide in Table 4.3.

Experimental and predicted phase equilibrium for the carbon dioxide + propane binary system is shown in Fig. 4.1. Predictions with the optimal parameters obtained from HVO and MHV1 mixing rules are compared. It can be appreciated that predictions corresponding to MHV1 are slightly better than those corresponding to HVO.

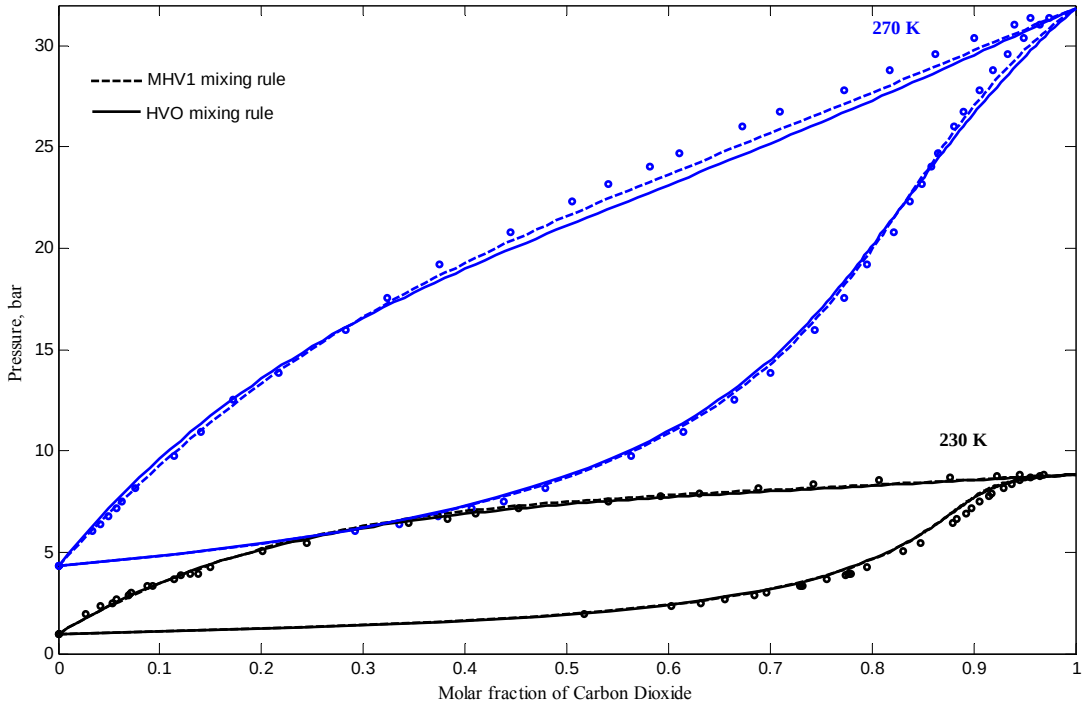

Fig. 4.1 VLE correlation of the CO_2 + propane system by MHV1 and HVO mixing rules. Experimental data were taken from Webster and Kidnay [21].

VLE for carbon dioxide + methane asymmetric binary system is shown in Fig. 4.2. Experimental data are compared with the calculations with optimal parameters obtained from the objective function (eqn. (41)). At the three considered temperatures (230, 250 and 270 K), all the predictions were accurate in both pressure and vapor phase composition by MHV2 mixing rule. In this particular case the predictions obtained by WS mixing rule were not completely satisfactory.

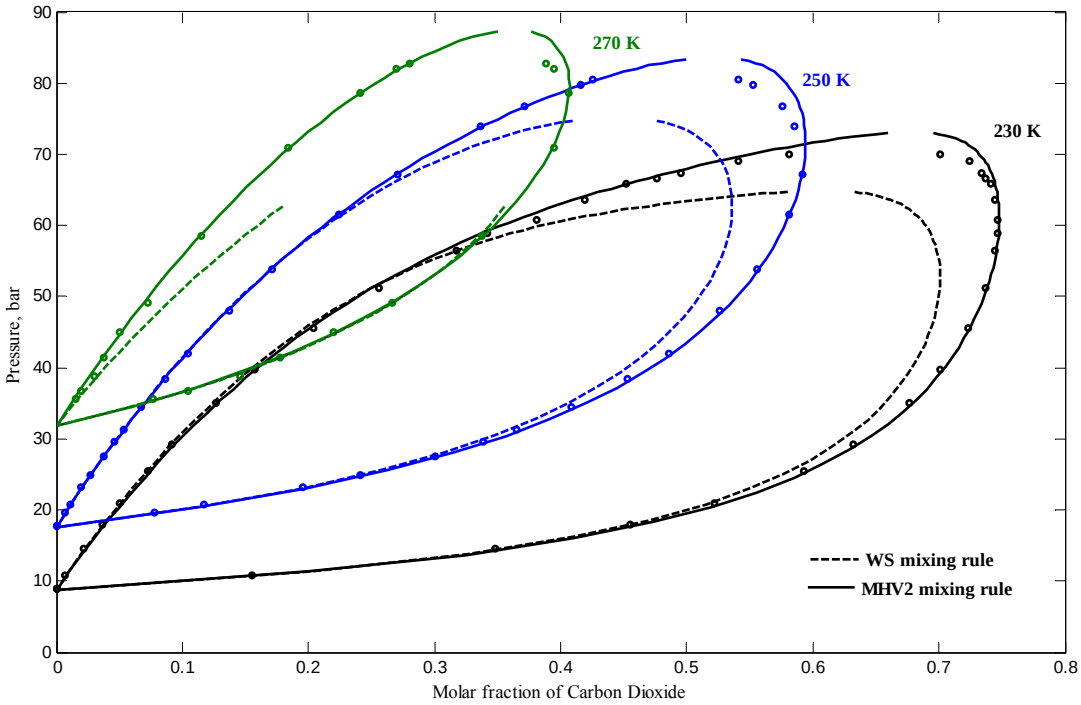

Fig. 4.2 VLE correlation of the CO_2 + methane system by WS and MHV2 mixing rules. Experimental data were taken from Wei *et al*. [20].

The results for the correlation of carbon dioxide + methanol system are shown in Fig. 4.3. The WS mixing rule captures the phase equilibrium behavior very well. For the case of the HVOS mixing rule, the general phase behavior is captured; however, pressures are found to be slightly lower than the experimental measurements. Fig. 4.3 at 291.15 and 298.16 K, the CO_2 is subcritical while at other temperature it is supercritical. In general good matches were obtained with the WS mixing rule.

Fig. 4.4 shows the experimental and predicted VLE for the asymmetric carbon dioxide + ethane binary system. Here, WS, MHV1 and MHV2 mixing rules are compared. In both cases, for the two temperatures WS mixing rule showed the vapor phase representations are very accurate taking into account the range of experimental data. It can be observed that MHV1 and MHV2 gave poor predictions for pressure and vapor phase.

In general, as the asymmetry of the system increases, the MHV2 mixing rule has some shortcomings around the critical region, but as the non randomness of the binaries decreases, its results are comparable to those obtained by WS mixing rule. The results are similar to that obtained by the WS mixing rule although the latter was more accurate at the critical region.

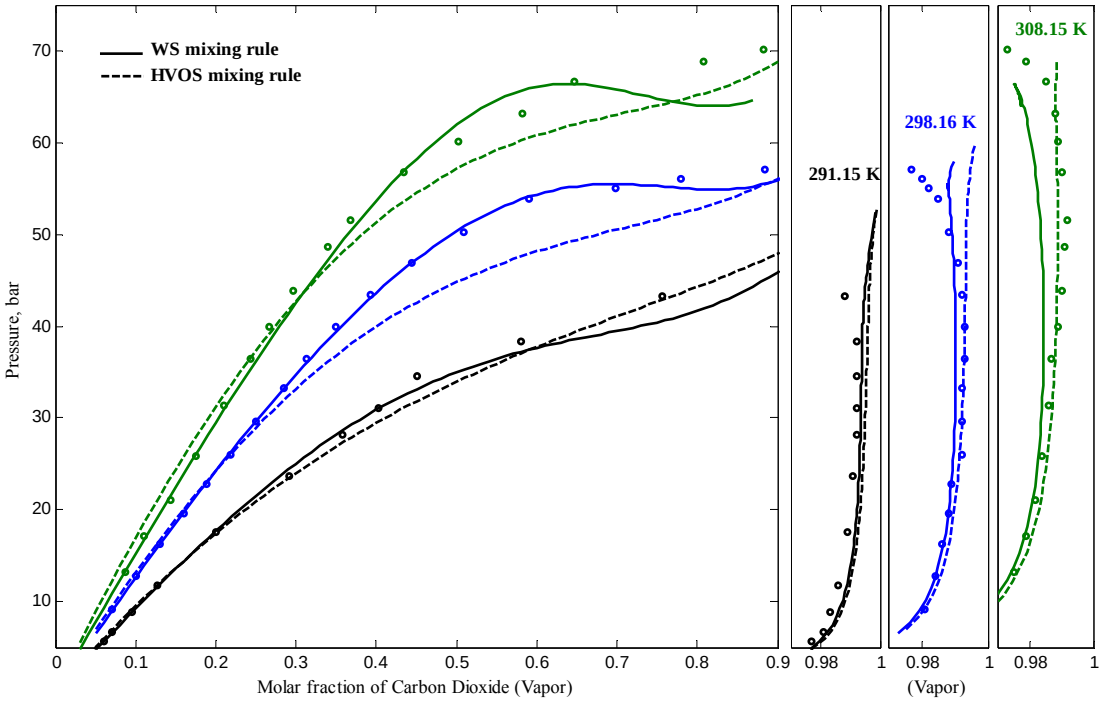

Fig. 4.3 VLE correlation of the CO_2 + methanol system by WS and HVOS mixing rules. Experimental data were taken from Ohgaki and Katayama [22] and Chiehming *et al*. [23].

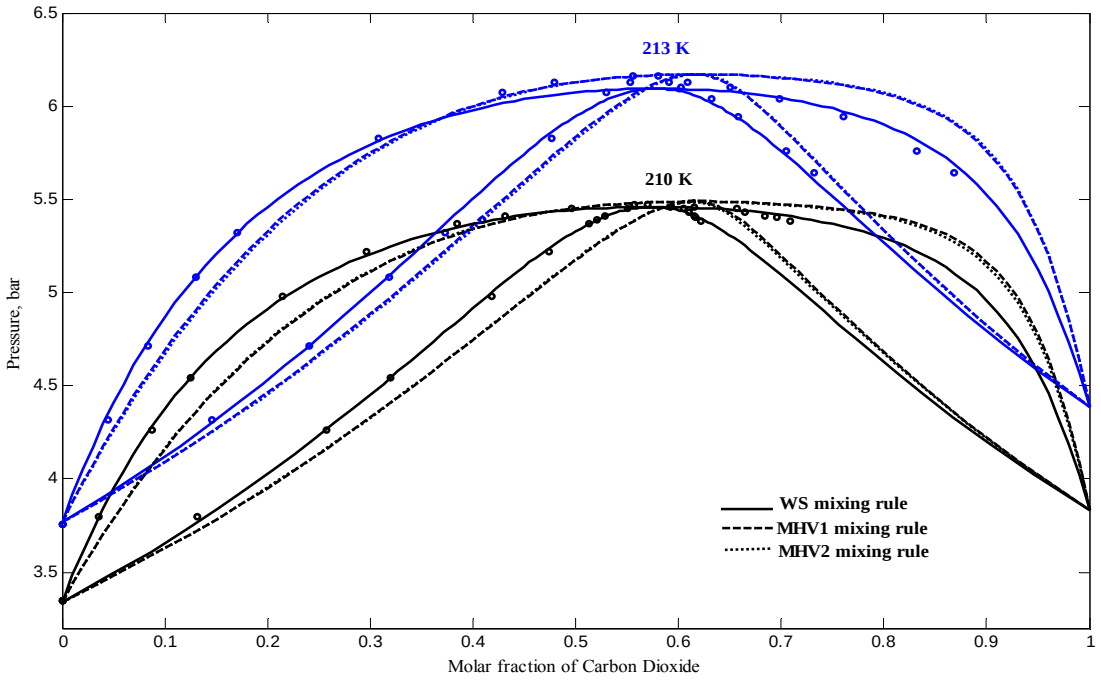

Fig. 4 .4 VLE correlation of the CO_2 + ethane system by WS MHV1 and MHV2 mixing rules. Experimental data were taken from Wei *et al*. [20].

With the purpose of comparing the accuracy of each mixing rules for predicting the phase equilibrium for asymmetric binary mixtures containing carbon dioxide at high pressures, Table 4.4 shows the average deviations of these predictions obtained from each mixing rule.

Table 4.4 Average deviations in the VLE prediction of the parameters obtained from each mixing rules for asymmetric systems.

	Asymmetric systems	
Mixing Rules	***ΔP***	***Δy***
HVO	24.6140	0.0882
MHV1	23.9922	0.1003
MHV2	18.6198	0.1004
WS	15.3421	0.1116
HVOS	25.0947	0.0931

Also, for one of the studied asymmetric systems, the residuals deviations were calculated with the purpose of making more informative the quality of the obtained parameters from the mixing rules analyzed. These residuals deviations are the difference between the experimental point and the calculated value. The residual plot for carbon dioxide + methanol at 298.16 K and is shown in Fig 4.5.

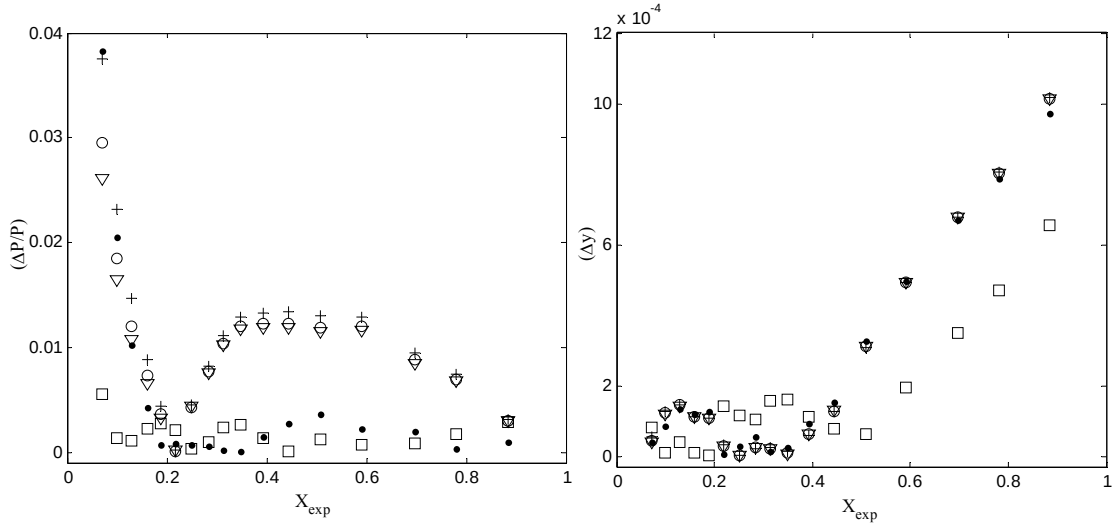

Fig. 4.5 Deviations between experimental points and calculated values of *y* and *P* for CO_2 + methanol at 298.16K. Parameters obtained from: ▽, HVO; +, MHV1; ●, MHV2; □, WS; ○, HVOS

In general terms, the optimal parameters obtained from the different mixing rules (HVO, MHV1, and MHV2) are similar, but not identical. On the other hand, the optimal parameters obtained using the other mixing rules (WS, HVOS) are very different. In terms of accuracy for representing the phase equilibria, according to the Table 4.4 all the mixing rules gave good predictions for the vapor phase composition, but HVO mixing rule showed

mildly better results than the others mixing rules for the binary systems analyzed. The WS mixing rule represented the bubble point pressure better than other mixing rules.

4.5 Conclusions

It is difficult to accurately predict, or even correlate, the isothermal vapor-liquid equilibrium of carbon dioxide systems owing to the asymmetric nature. In this study, the correlation capability of WS mixing rule were shown to be successful and comparable to other mixtures rules, except that near the critical region the former was superior. The MHV2 mixing rule failed for asymmetric systems, in the critical region. Prediction capacities of WS and HVOS mixing rules were tested by using the model parameters found at the lowest available temperature, and it was found that the WS mixing rule was better than the HVOS mixing rule.

References

[1] Orbey, H.; Sandler, S. I. On the Combination of Equations of State and Excess Free Energy Models. Fluid Phase Equilib. 111 (1995) 53-70.
[2] Panagiotopoulos, A. Z.; Reid, R. C. New Mixing Rules for Cubic Equations of State for Highly Polar Asymmetric Mixtures. ACS Symp. Ser. 300 (1986) 571-582.
[3] Schwartzentruber, J.; Renon, H. Extension of UNIFAC to High Pressures and Temperature by the Use of a Cubic Equation of State. Ind. Eng. Chem. Res. 28 (1989) 1049-1055.
[4] Orbey, H.; Sandler, S. I. Modeling Vapor Liquid Equilibrium; Cambridge University Press: Cambridge, England, 1998.
[5] Schwartzentruber, J.; Ponce-Ramirez, L.; Renon, H. Prediction of Binary Parameters of a Cubic Equation of State from a Group Contribution Method. Ind. Eng. Chem. Process Des. Dev. 25 (1986) 804-809.
[6] Huron, M.; Vidal, J. New Mixing Rules in Simple Equations of State for Representing Vapor-liquid Equilibria of Strongly Nonideal Mixtures. Fluid Phase Equilib. 3 (1979) 255-271.
[7] Michelsen, M. L. A Method for Incorporating Excess Gibbs Energy Models in Equations of State. Fluid Phase Equilib. 60 (1990) 47.
[8] Michelsen, M. L. A Modified Huron-Vidal Mixing Rule for Cubic Equations of State. Fluid Phase Equilib. 60 (1990) 213-219.
[9] Dahl, S.; Michelsen, M. L. High-Pressure Vapor-liquid Equilibrium with a UNIFAC Based Equation of State. AIChE J. 36 (1990) 1829-1836.
[10] Wong, D. S. H.; Sandler, S. I. A Theoretically Correct Mixing Rule for Cubic Equations of State. AIChE J. 38 (1992) 671-680.
[11] J.A. López, C.A. Cardona, Phase equilibrium calculations for carbon dioxide + *n*-alkanes binary mixtures with the Wong–Sandler mixing rules, Fluid Phase Equilib. 239 (2006) 206–212.
[12] J.A. López, V.M. Trejos, C.A. Cardona, Objective functions analysis in the minimization of binary VLE data for asymmetric mixtures at high pressures, Fluid Phase Equilibria 248 (2006) 147–157.
[13] J.A. López, V.M. Trejos, C.A. Cardona, Parameters Estimation and VLE Calculation in Asymmetric Binary Mixtures Containing Carbon Dioxide + *n*-Alkanols, Fluid Phase Equilibria 275 (2008) 1-7.
[14] V.M. Trejos, J.A. López, C.A. Cardona, Thermodynamic consistency of experimental VLE data for asymmetric binary mixtures at high pressures. Fluid phase equilibria, 230 (2010) 1-10.

[15] Orbey, H.; Sandler, S. I. Reformulation of Wong-Sandler Mixing Rule for Cubic Equations of State. AIChE J. 41 (1995) 683-690.
[16] D.Y. Peng, D.B. Robinson, A new two-constant equation of state, Industrial and Engineering Chemistry Fundamentals 15 (1976) 59–64.
[17] H. Renon, J.M. Prausnitz, Local compositions in thermodynamic excess functions 1for liquid mixtures, American Institute of Chemical Engineering Journal 14 (1967) 135–144.
[18] Malanowski, Stanislaw., Modelling phase equilibria: Termodynamic background and practical tools, J. Wiley & Sons. New York, 1992.
[19] Sandler, Stanley I., Models for thermodynamic and phase equilibria calculations New York Marcel Dekker 1994
[20] M.S.W. Wei, T.S. Brown, A.J. Kidnay, E.D. Sloan, Vapor + liquid equilibria for the ternary system methane + ethane + carbon dioxide at 230K and its constituent binaries at temperatures from 207 to 270 K, J. Chem. Eng. Data 40 (1995) 726–731.
[21] L.A. Webster, A.J. Kidnay, Vapor–liquid equilibria for methane– propane–carbon dioxide systems at 230K and 270 K, J. Chem. Eng. Data 46 (2001) 759–764.
[22] K. Ohgaki, T. Katayama, Isothermal vapor–liquid equilibrium data for binary systems containing carbon dioxide at high pressures: methanol-carbon dioxide, *n*-hexane-carbon dioxide, and benzene-carbon dioxide systems, Journal of chemical and Engineering Data 21 (1976) 53–55.
[23] C.J. Chiehming, C.K. Lung, D.C. Yih, A new apparatus for the determination of *P–x–y* diagrams and Henry's constants in high pressure alcohols with critical carbon dioxide, Journal of Supercritical Fluids 12 (1998) 223–237.

CHAPTER 5

PARAMETERS ESTIMATION AND VLE CALCULATION IN BINARY MIXTURES CONTAINING CARBON DIOXIDE + *n*-ALKANES AND *n*-ALKANOLS

In the present chapter, the estimation of the parameters for asymmetric binary mixtures of carbon dioxide + n-alkanes and n-alkanols has been developed. The binary interaction parameter k_{12} of the second virial coefficient and non-random two liquid model parameters were obtained using Peng–Robinson equation of state coupled with the Wong–Sandler mixing rules. In all cases, Levenberg–Marquardt minimization algorithm was used for the parameters optimization employing an objective function based on the calculation of the distribution coefficients for each component. Vapor–liquid equilibrium for binary mixtures (CO_2 + n-alkane, from methane to 1-decane and CO_2 + n-alkanol, from methanol to 1-decanol) was calculated using the obtained values of the mentioned parameters. The agreement between calculated and experimental values was satisfactory.

5.1 Introduction

In the last decade, supercritical fluids (SCF) have intensively been proved as environmentally benign media for chemical and related processes. Many processes and products have been developed applying the inherent physical and chemical properties of SCF [1]. The use of SCF represents an attractive option to implement diverse chemical processes in a sustainable manner. The CO_2 is commonly used in processes involving SCF since it is not toxic, not explosive, chemically inert, economic, not corrosive, easily recyclable and available in a high purity. The main disadvantage of the SCF processes is the relatively high cost of the required equipment. However, the quality of the products widely overcomes that of the products obtained by conventional extraction using solvents. This fact may offset the investment in high-pressure equipment [2–4].

Supercritical carbon dioxide, as other supercritical fluids, offers the possibility of reducing the reactor size in a great extent, as well as the acceleration of many chemical processes [1]. The SCF have features of both gases and liquids. Compared to liquid solvents, SCF have a major dissolving capability, higher diffusion coefficient, and lower viscosity and surface tension than a liquid solvent leading to more favorable mass transfer [5].

The information on the high-pressure behavior of fluids under supercritical conditions has been valuable during the design of new separation processes in various fields like food,

pharmaceutical and fine chemical industries [6]. The information of high-pressure phase equilibrium of mixtures containing CO_2 and alcohols is particularly relevant and has been actively studied for various purposes. For instance, the phase equilibrium behavior of low molecular weight alcohols, such as methanol and ethanol, in CO_2 is essential for the effective evaluation of cosolvents for CO_2-based supercritical processes [7]. Additionally, high-pressure VLE measurements of CO_2 + alkanols systems are of great interest due to their role during the supercritical extraction of thermally labile compounds, dehydration of alcohols, and extraction of natural products using near critical solvents [8]. Finally, CO_2 + alcohol systems have a high potential as supercritical fluid/cosolvent pairs for separation of different metabolites. Therefore, the knowledge of vapor–liquid equilibrium in these systems is needed in order to evaluate the employed models for describing the extraction of biomaterials with supercritical fluid/cosolvent pairs [9].

The evaluation of supercritical extraction processes has its major difficulty in the modeling of VLE. This is related to the high complexity and asymmetry of the mixtures treated [10]. Thus, VLE calculation requires of improved versions of the EOS. Among the many cubic EOS of van der Waals type currently available, the equation proposed by Peng and Robinson [11] is widely used due to its simplicity and flexibility [12]. The application of this cubic EOS to systems containing highly non-ideal components requires an appropriate mixing rule for the attractive-term and covolume, which generally are based on excess Gibbs free energy [13,14]. Other models have also been successful as the zero-pressure model [15,16] and the infinite-pressure model [17]. Their capabilities and limitations for asymmetric systems have been discussed in some works [18,19].

VLE at high pressures can be calculated using the available values at low pressures of the activity model parameters. But sometimes, in the case of highly asymmetric mixtures as those containing CO_2, these values are not available. In such case, it is more convenient to calculate the parameters of the activity coefficient models from VLE data using an adequate minimization algorithm and an appropriate objective function. This procedure should have a moderate computing time requirement and a well accuracy in the phase equilibrium prediction [13].

In this work, an objective function based on the calculation of the distribution coefficient has been used to represent both the phase vapor and the pressure behavior in the case of isothermal binary mixtures containing carbon dioxide, *n*-alkanes and *n*-alkanols at high pressures (CO_2 + *n*-alkanols, from methanol to 1-decanol and CO_2 + *n*-alkane, from methane to 1-decane). The experimental data were correctly correlated with the Peng–Robinson EOS using the Wong–Sandler mixing rules. The binary interaction parameter k_{12} of the second virial coefficient and the non-random two liquid (NRTL) model parameters τ_{12} and τ_{21} were calculated for the VLE of binary asymmetric mixtures at high pressures. For this, a Levenberg–Marquardt minimization algorithm was used.

5.2 Equation of state and mixing rules

The Peng–Robinson EOS [11] has the following form:

$$P = \frac{RT}{v-b} - \frac{a}{v(v+b)+b(v-b)} \tag{1}$$

where P is the absolute pressure, T the absolute temperature, R is the ideal gas constant, a and b are the energy and size parameters respectively. These parameters are calculated from following correlations:

$$a = 0.457235 \frac{R^2 T_c^2}{P_c} \alpha(T_r) \tag{2}$$

$$b = 0.077796 \frac{RT_c}{P_c} \tag{3}$$

where subscripts c and r denote critical and reduced conditions, respectively. The α function is calculated from:

$$\alpha(T_r) = \left[1 + \kappa\left(1 - \sqrt{T_r}\right)\right]^2 \tag{4}$$

$$\kappa = 0.37464 + 1.54226\omega - 0.26992\omega^2 \tag{5}$$

where ω is the acentric factor. For extending Peng-Robinson EOS to mixtures the Wong-Sandler [17] mixing rules were used. The a_m and b_m parameters are calculated from:

$$a_m = b_m \left[\sum_i z_i \frac{a_i}{b_i} + \frac{\underline{A}_\infty^E}{\sigma} \right] \tag{6}$$

with

$$b_m = \frac{\sum_i \sum_j z_i z_j \left(b - \frac{a}{RT}\right)_{ij}}{1 - \sum_i z_i \frac{a_i}{b_i RT} - \frac{\underline{A}_\infty^E}{\sigma RT}} \tag{7}$$

$$\sigma = \frac{1}{\sqrt{2}} \ln\left(\sqrt{2} - 1\right) \tag{8}$$

and

$$\left(b-\frac{a}{RT}\right)_{ij}=\frac{\left(b-\frac{a}{RT}\right)_i+\left(b-\frac{a}{RT}\right)_j}{2}\left(1-k_{ij}\right) \tag{9}$$

where k_{ij} is a binary interaction parameter of the second virial coefficient, z is the molar fraction and $\underline{A}_{\infty}^{E}$ is the excess Helmholtz free energy at infinite pressure which is calculated from NRTL model for binary mixtures [20]:

$$\frac{\underline{A}_{\infty}^{E}}{RT}=\sum_i z_i\left(\frac{\sum_j z_j\tau_{ji}g_{ji}}{\sum_k z_k g_{ki}}\right) \tag{10}$$

$$g_{ij}=\exp\left(-\alpha_{ij}\tau_{ij}\right) \tag{11}$$

where α_{12} (=α_{21}), τ_{12} and τ_{21} are the three parameters of the NRTL model. A constant value for τ_{21} of 0.3 was used in this work. The adjustable parameters of NRTL model, τ_{12} and τ_{21}, and binary interaction parameter k_{12} of the second virial coefficient have been determined using experimental phase equilibrium data at isothermal conditions for 20 binary mixtures.

5.2.1 Parameters optimization

Binary interaction parameters for Peng–Robinson EOS and NRTL model have been determined by using Levenberg–Marquardt minimization algorithm. The objective function used for all cases is as follows:

$$OF=\sum_{i=1}^{np}\sum_{j=1}^{nc}\left[y_{i,j}^{\exp}-K_{i,j}^{cal}\cdot x_{i,j}^{\exp}\right]^2 \tag{12}$$

where np is the number of experimental data points, nc the number of components, y and x are the molar fraction in the vapor and liquid phases, respectively. K is the distribution coefficient between vapor and liquid phases. The superscripts exp and cal correspond to the experimental and calculated values, respectively. In a previous work [13], it has been found that the objective function represented by Eq. (12) has three principal advantages over the commonly used objective functions based on bubble point pressure and vapor phase composition calculation. Mentioned advantages are: (1) minimum computing time requirement considering that this objective function does not involve additional iterative calculations as the bubble point or isothermal flash for each experimental data point. (2) The optimal second virial coefficient interaction parameter is concordant with the statistical thermodynamic postulates since its value does not violate the quadratic composition dependence of the second virial coefficient. (3) Phase equilibrium calculations using the optimal parameters obtained with this objective function show very good predictions for both vapor phase and pressure. Therefore, all these features make the objective function

(eqn. (12)) adequate for parameters optimization from experimental VLE data in highly asymmetric binary mixtures. For this reason, it is used in the present work. Twenty binary mixtures containing carbon dioxide, *n*-alkanes and *n*-alkanols have been studied. The critical properties, acentric factors and the literature source of the components involved in this study are shown in Table 5.1.

Table 5.1 Properties of pure substances for *n*-akanols and *n*-alkanes

Compound	T_c, *K*	P_c, bar	*w*	Ref.
Carbon dioxide	304.21	73.83	0.22500	[21]
Methane	190.55	45.99	0.01045	[22]
Ethane	305.43	48.72	0.09781	[22]
Propane	369.82	42.48	0.15416	[22]
n-Butane	425.16	37.96	0.20096	[22]
n-Pentane	469.70	33.70	0.25143	[22]
n-Hexane	507.30	30.25	0.30075	[22]
n-Heptane	540.10	27.40	0.35022	[22]
n-Octane	568.76	24.90	0.39822	[22]
n-Nonane	594.56	22.90	0.44517	[22]
n-Decane	617.50	21.10	0.49052	[22]
Methanol	512.64	80.97	0.56500	[22]
Ethanol	513.92	61.40	0.64356	[22]
Propanol	536.80	51.69	0.62043	[22]
1-Butanol	563.10	44.14	0.58946	[22]
1-Pentanol	588.10	38.97	0.57314	[22]
1-Hexanol	610.30	34.17	0.57636	[22]
1-Heptanol	631.90	31.50	0.58800	[22]
1-Octanol	652.50	28.60	0.58291	[22]
1-Nonanol	671.00	26.30	0.59969	[22]
1-Decanol	687.30	23.15	0.62192	[22]

The deviation between the experimental data and the calculated values with PR coupled with the Wong–Sandler mixing rules was established through the relative percentage deviations in the bubble point pressure:

$$\Delta P = \sum_{i=1}^{np} \frac{\left|P_{\exp} - P_{cal}\right|}{P_{\exp}} \left(\frac{100}{np}\right) \tag{13}$$

and the absolute mean deviation in the molar fraction in the vapor phase was calculated as follows:

$$\Delta y = \sum_{i=1}^{np} \left|y_{\exp} - y_{cal}\right| \frac{1}{np} \tag{14}$$

5.3 Results and discussion

A total of 28 isotherms with 470 experimental data points for *n*-alkanes and 38 isotherms with 371 experimental data points for *n*-alkanols and have been analyzed. Then, 198 optimal parameters have been obtained for the 20 mixtures involved in the study. These NRTL model parameters (τ_{12} and τ_{21}) and the binary interaction parameter k_{12} of the second virial coefficient of the Peng–Robinson EOS for non-polar and polar mixtures and the deviations between experimental data and calculated values are reported in Tables 5.2 and 5.3.

The optimal parameters showed in Tables 5.2 and 5.3 gave very good predictions for the molar fractions in the vapor phase but poor predictions for bubble point pressure. However, we consider that the results are acceptable since the Levenberg–Marquardt minimization algorithm has the disadvantage of that can guarantee a local minimum and not a global one (Palosaari et al. [23]).

For the 10 mixtures of carbon dioxide with *n*-alkanes the agreement with the experimental data is generally satisfactory as shown in Table 5.2 and graphically in Figs. 5.1–5.3. Fig.5.1 shows the results for the lightly asymmetric binary system carbon dioxide + methane. At the three evaluated temperatures, methane is in supercritical conditions. Also, we can see that as the temperature of equilibrium increases, the prediction in the vapor phase is lightly superior. The carbon dioxide + ethane binary system is shown in Fig. 5.2. Since the chemical affinities between the two molecules, this system exhibits a maximum pressure azeotrope, which is perfectly predicted with the PR EOS and Wong–Sandler mixing rules. Also, at low temperatures the phase equilibrium is correctly represented until the one it limits in which the solidification of carbon dioxide occurs.

Fig. 5.3 shows the VLE prediction for carbon dioxide + *n*-heptane asymmetric binary systems, respectively. In this case, the temperature of carbon dioxide is over its critical temperature and excellent predictions for both mixtures are obtained. We can notice that the highest deviation in the carbon dioxide + *n*-heptane binary system is found for that case in which the *n*-alkane concentration in the vapor phase is low.

Table 5.2 Optimal parameters obtained from optimization and deviations between calculated and experimental values for *n*-alkanes.

CO_2+	np	T, *K*	NRTL parameters		k_{12}	Deviations		Ref.
			τ_{12}	τ_{21}		ΔP	Δy	
C_1	20	230.00	0.9231	0.7099	0.1563	1.1070	0.0029	[24]
	19	250.00	1.0580	0.4165	0.1428	0.6750	0.0046	[24]
	13	270.00	0.9374	0.0846	0.2039	0.7432	0.0092	[24]
C_2	10	207.00	1.6375	1.1054	0.1277	0.2483	0.0043	[24]
	17	210.00	1.6925	1.0796	0.1237	0.1893	0.0064	[24]
	15	213.00	1.8180	1.0630	0.0795	0.4780	0.0084	[24]
	16	230.00	1.8426	0.7901	0.0907	0.3615	0.0032	[24]
	20	250.00	1.7215	0.7743	0.0466	0.3347	0.0068	[24]
	6	270.00	1.6871	0.5308	0.0505	0.4281	0.0114	[24]
C_3	29	230.00	4.3311	1.3291	0.0169	1.5120	0.0213	[25]
	27	270.00	2.4946	0.2091	0.1908	0.4002	0.0112	[25]
C_4	47	311.09	2.7235	-0.4951	0.3309	1.8418	0.0373	[26]
	37	344.43	5.4368	-0.8042	0.3277	4.1466	0.0658	[26]
C_5	12	310.15	0.2957	0.9251	0.5603	2.9072	0.0110	[27]
	13	333.15	1.0449	0.2109	0.5287	1.2980	0.0137	[27]
	16	363.15	0.3094	0.6142	0.5597	2.7394	0.0250	[27]
C_6	10	298.15	1.5917	0.0557	0.5676	2.5149	0.0053	[28]
	10	313.15	1.4805	-0.0728	0.5449	1.8079	0.0044	[28]
C_7	23	310.65	3.8381	-0.3973	0.5774	2.0079	0.0095	[29]
	17	352.59	2.8376	-0.6426	0.6095	1.0223	0.0103	[29]
	17	394.26	4.9407	-0.8718	0.5613	2.4930	0.0414	[29]
	7	477.20	0.7192	-0.3115	0.6906	1.6567	0.0381	[29]
C_8	6	313.15	3.1397	-0.1264	0.6726	0.4398	0.0019	[30]
	6	328.15	3.8866	-0.2908	0.6512	1.0694	0.0047	[30]
	8	348.15	3.5901	-0.3804	0.6641	1.0491	0.0078	[30]
C_9	6	343.25	3.5353	-0.5094	0.7021	0.1985	0.0072	[31]
C_{10}	20	344.30	4.3681	-0.4012	0.7321	0.3955	0.0105	[32]
	23	377.60	3.7302	-0.7114	0.7521	0.5231	0.0064	[32]

Table 5.3 Optimal parameters obtained from optimization and deviations between calculated and experimental values for *n*-alkanols.

CO_2+	np	T, *K*	NRTL parameters		k_{12}	Deviations		Ref.
			τ_{12}	τ_{21}		ΔP	Δy	
C_1	8	298.15	0.5013	0.1187	0.3972	1.1723	0.0016	[33]
	11	291.15	1.3345	-0.3352	0.2205	1.1878	0.0037	[34]
	16	303.18	3.2387	-0.4343	0.1771	2.3629	0.0022	[34]
	16	308.15	2.7720	-0.4156	0.2144	2.2206	0.0028	[34]
	17	313.14	1.5843	-0.1363	0.2992	0.9024	0.0025	[34]
C_2	8	298.17	1.3143	-0.6677	0.4298	1.5124	0.0069	[34]
	11	303.12	0.1705	0.4247	0.4504	1.6339	0.0064	[34]
	6	314.50	1.9314	-0.0701	0.3772	1.7598	0.0010	[9]
	9	325.20	1.1963	0.2243	0.4084	0.1633	0.0023	[9]
	8	337.20	1.0835	0.2871	0.4071	0.3257	0.0031	[9]
C_3	8	315.00	2.2793	-0.0110	0.4065	0.2879	0.0021	[35]
	10	326.60	0.7280	0.5953	0.5048	0.7484	0.0011	[35]
	10	337.20	1.6067	0.0402	0.4537	1.7443	0.0020	[35]
	10	313.40	2.5113	-0.4762	0.4422	1.3856	0.0016	[36]
	9	333.40	1.8870	-0.1471	0.4388	0.9273	0.0051	[36]
C_4	14	303.15	1.0752	0.4405	0.5812	3.2506	0.0042	[37]
	8	314.80	1.9332	-0.0061	0.5273	0.0866	0.0008	[37]
	9	325.30	1.8663	-0.0445	0.5244	0.1412	0.0012	[9]
	11	337.20	1.8003	-0.0833	0.5221	0.0952	0.0018	[9]
C_5	7	333.08	2.3425	-0.3235	0.5633	1.0132	0.0086	[38]
	4	343.69	2.3645	-0.3975	0.5612	0.1887	0.0089	[38]
	4	374.93	1.5248	-0.0477	0.5790	0.3246	0.0121	[38]
	12	426.86	2.0271	-0.7586	0.5460	1.4383	0.0033	[38]
C_6	4	431.82	1.4259	-0.7219	0.6310	0.1367	0.0058	[39]
	7	432.45	-0.5979	1.8222	0.6773	2.6389	0.0332	[39]
C_7	8	374.63	2.3674	-0.8955	0.6597	0.6572	0.0029	[39]
	6	431.54	3.9066	-1.0822	0.5106	2.0066	0.0459	[39]
	8	298.15	2.6575	-0.1594	0.6808	0.6078	0.0062	[40]
	10	316.15	2.5770	-0.3556	0.6772	4.0665	0.0075	[40]
C_8	12	308.15	2.5807	-0.1218	0.7377	0.6292	0.0015	[34]
	9	318.19	1.7590	0.0606	0.7579	0.5795	0.0015	[34]
	16	328.15	2.3629	-0.2511	0.7325	0.9807	0.0079	[34]

C_9	9	308.14	2.9503	-0.1062	0.7564	0.4157	0.0017	[34]
	10	318.13	1.9111	-0.0169	0.7926	0.7922	0.0040	[34]
	15	328.18	2.4344	-0.2631	0.7704	0.8844	0.0055	[34]
C_{10}	9	308.14	3.0836	-0.0749	0.7904	0.5919	0.0005	[34]
	9	318.14	2.2640	-0.1460	0.8130	1.0967	0.0019	[34]
	13	328.16	2.0742	-0.1706	0.8218	1.2016	0.0039	[34]

Graphical results of phase equilibrium calculations using the optimal parameters reported in the Table 5.3 are shown in Figs. 5.4–5.8 for carbon dioxide + *n*-alkanols mixtures. Experimental and predicted VLE for binary mixture carbon dioxide + methanol is shown in Fig. 5.4. In mentioned figure, parameters optimization has been developed. For all cases, the agreement between experimental data and calculated values was satisfactory.

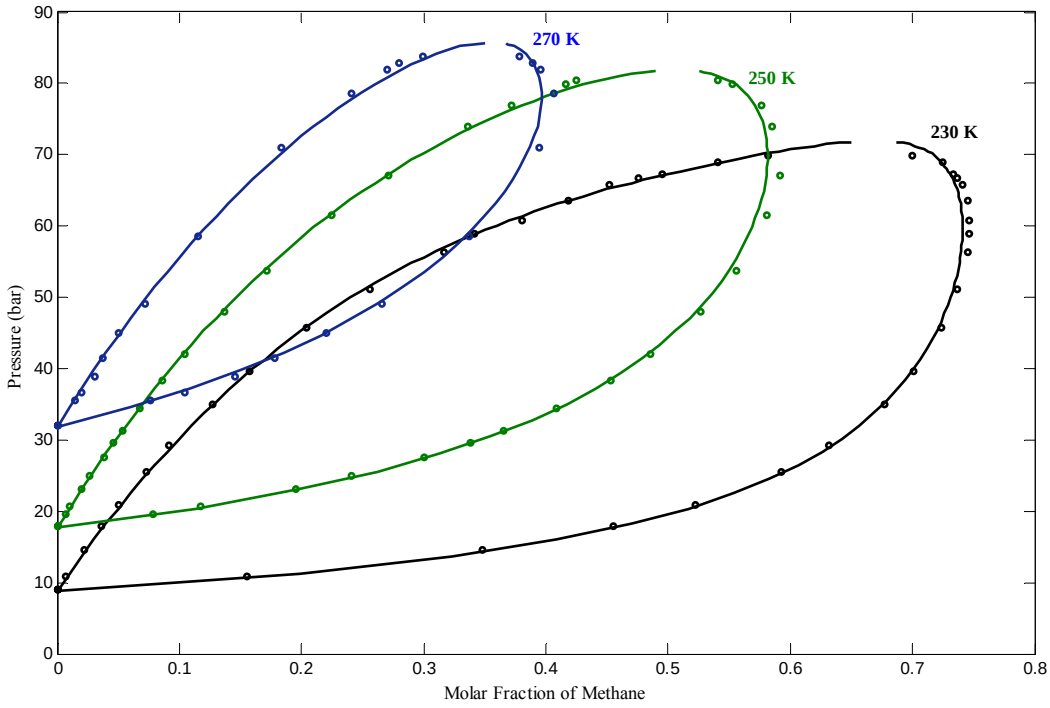

Fig. 5.1 Experimental and predicted VLE for carbon dioxide + methane binary system. Experimental data were taken from Wei *et al*. [24].

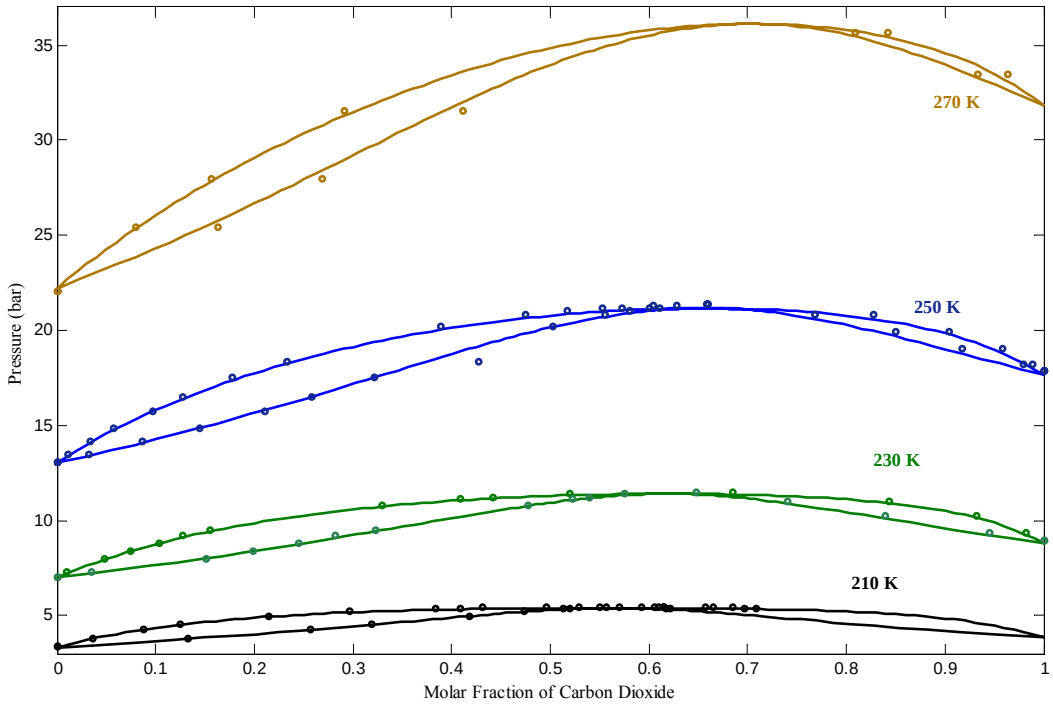

Fig. 5.2 Experimental and predicted VLE for carbon dioxide + ethane binary system. Experimental data were taken from Wei *et al*. [24].

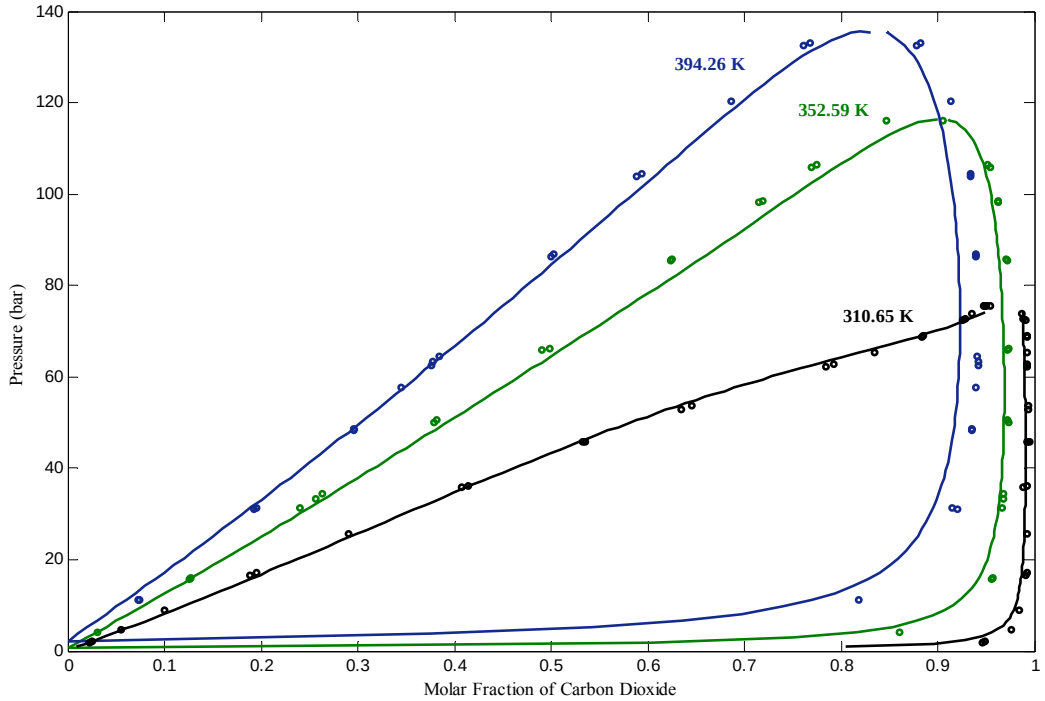

Fig. 5.3 Experimental and predicted VLE for carbon dioxide + heptane binary system. Experimental data were taken from Kaira *et al*. [29].

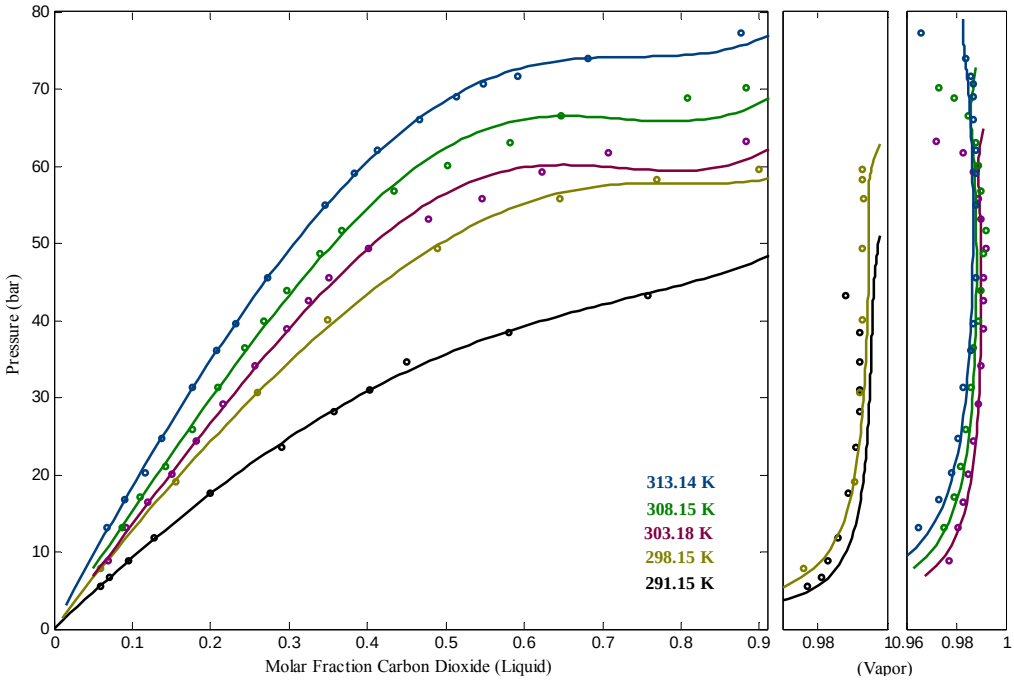

Fig. 5.4 Experimental and predicted VLE for carbon dioxide + methanol binary system. Experimental data were taken from Ohgaki and Katayama [33] and Chiehming *et al*. [34].

Isothermal VLE for carbon dioxide + 1-butanol binary system is shown in Fig. 5.5. Both liquid and vapor phase predictions were correct for the pressure range analyzed. However, in the mentioned figure, it can be noted that calculations present light deviations near the critical point of the mixture at the five temperatures evaluated. This has been observed for the other treated cases as well. This behavior can be explained by the fact that the experimental data points, in almost all cases, do not include data near the critical point.

Therefore the minimizations were developed over the available points. Fig. 5.6 shows the experimental and predicted phase equilibrium for the highly asymmetric carbon dioxide + 1–hexanol binary mixture. For the two temperatures analyzed, the vapor phase and liquid phase representations are very accurate related to the experimental points, as can be noted from the deviations reported in Table 5.4. Two highly asymmetric binary mixtures are shown in Fig. 5.7 (carbon dioxide + 1-octanol) and Fig. 5.8 (carbon dioxide + 1-decanol). For these two systems all predictions are correct in the total range of pressure analyzed. However, small deviations in the vapor phase were observed.

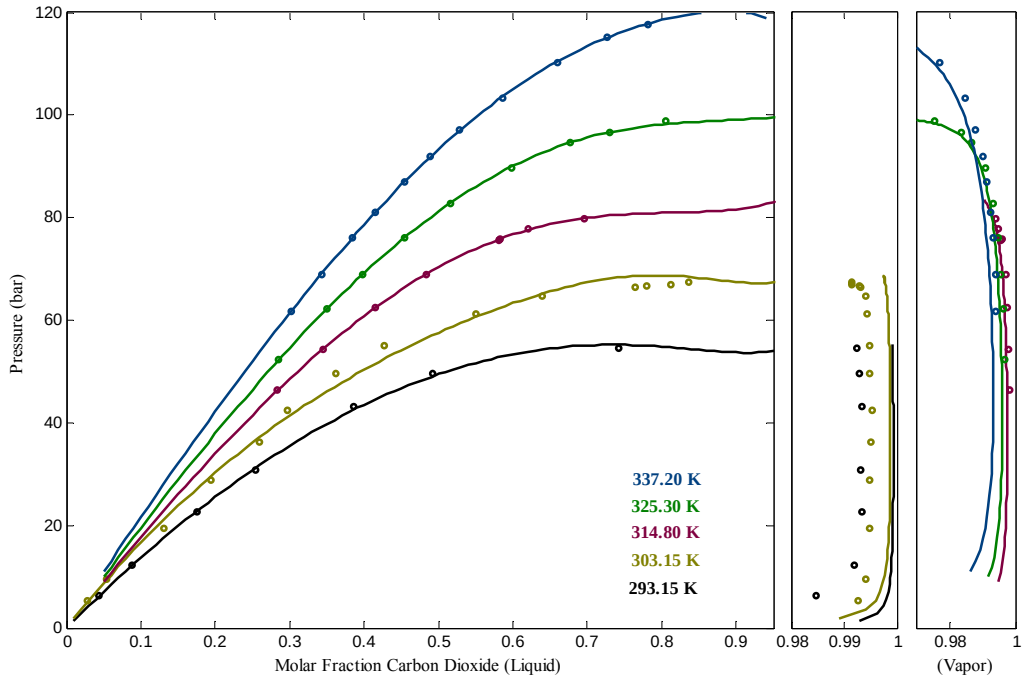

Fig. 5.5 Experimental and predicted VLE for carbon dioxide + 1–butanol binary system. Experimental data were taken from Secuianu *et al*. [37] and Jennings *et al*. [9].

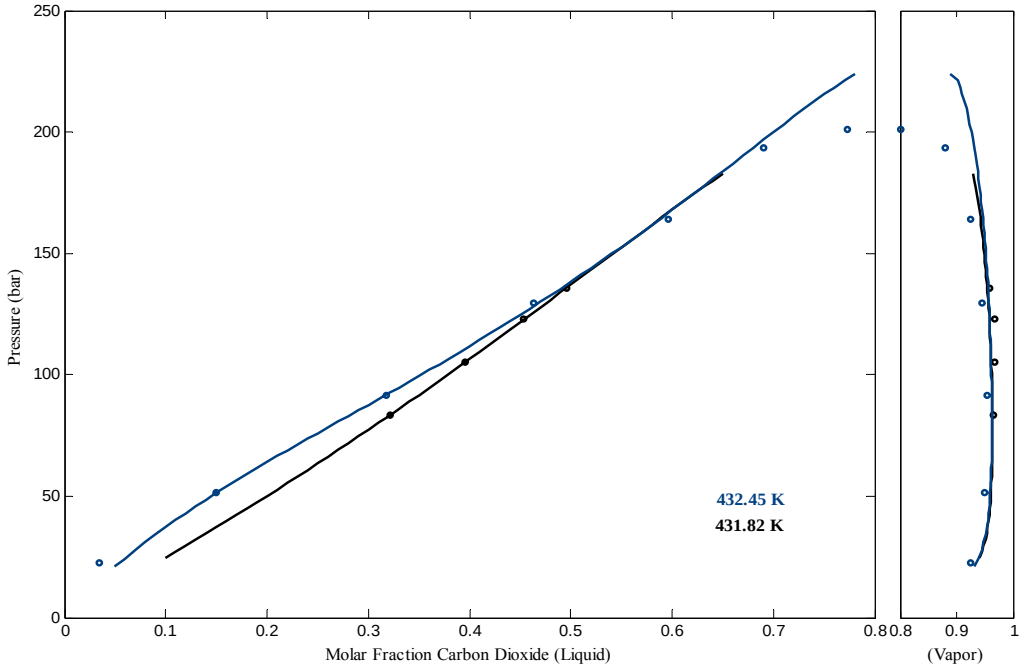

Fig. 5.6 Experimental and predicted VLE for carbon dioxide + 1–hexanol binary system. Experimental data were taken from Solis *et al*. [39].

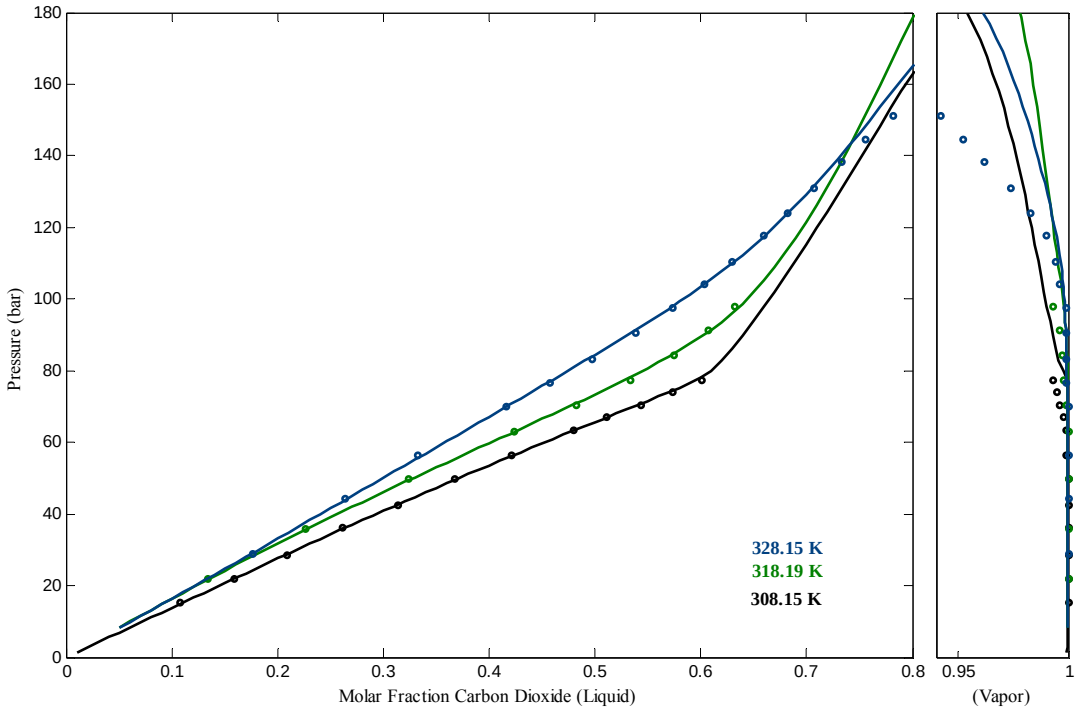

Fig. 5.7 Experimental and predicted VLE for carbon dioxide + 1–octanol binary system. Experimental data were taken from Chiehming *et al.* [34].

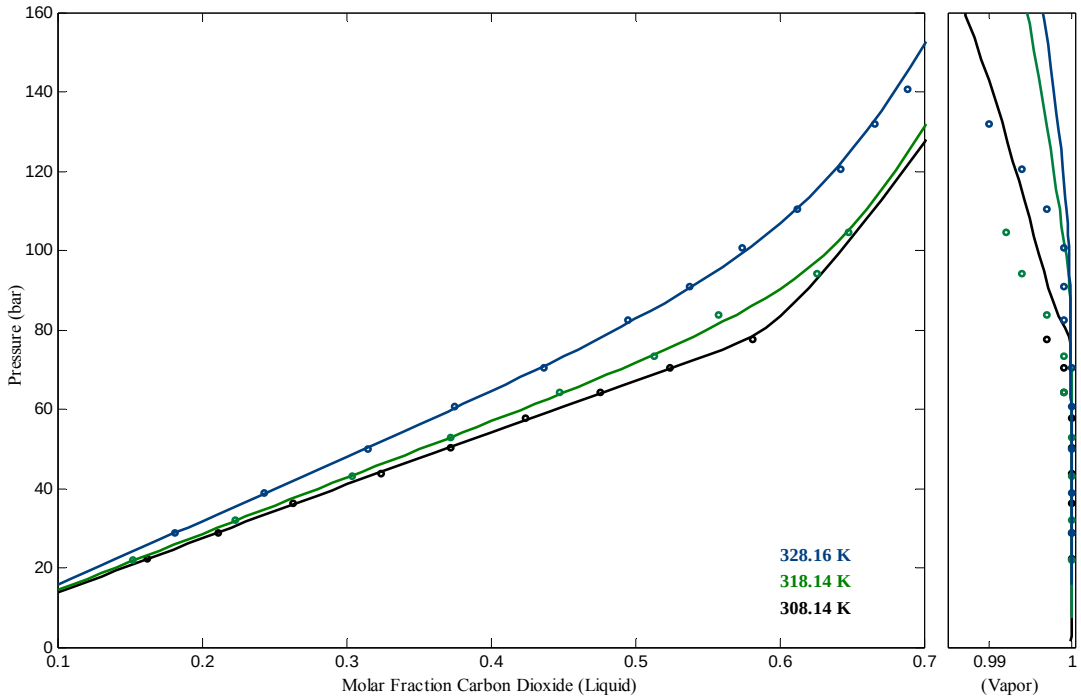

Fig. 5.8 Experimental and predicted VLE for carbon dioxide + 1–decanol binary system. Experimental data were taken from Chiehming *et al.* [34].

The parameters obtained from the minimization of the objective function eqn. (12) showed in Tables 5.2 and 5.3 were correlated as function of the *n*-alkanes and *n*-alkanols acentric factor and the equilibrium temperature as follows:

$$p_{ij} = T(K)\left(c_1 w^{c_2} + c_3\right) + w\left(c_4 + c_5 T(K)\right) + c_6 \tag{15}$$

where p_{ij} is any of the parameters obtained from optimization (τ_{12}, τ_{21} and k_{12}) and the constant values for each parameter are represented in Table 5.4.

Table 5.4 Coefficients c_1- c_6 for each interaction parameter represent for Eq. (15)

n-alkanes, p_{ij}	c_1	c_2	c_3	c_4	c_5	c_6
τ_{12}	0.1763	0.0008	-0.1818	9.0783	-0.0066	2.5005
τ_{21}	0.0419	0.7142	-0.0173	-10.677	-0.0150	4.4634
k_{12}	0.0022	-0.1135	-0.0004	3.1334	-0.0043	-0.6728
n-alkanols, p_{ij}	c_1	c_2	c_3	c_4	c_5	c_6
τ_{12}	6.8463	0.5669	-2.3576	-77.138	-4.6088	47.989
τ_{21}	0.1382	-0.3665	-0.2105	12.558	0.0711	-7.3326
k_{12}	0.4821	0.4546	-0.1690	22.034	-0.3560	-12.521

The optimal parameters presented in Table 5.4 have shown a uniform tendency correlating the equilibrium temperature and acentric factor as a function of for *n*-alkanes and *n*-alkanols

5.4 Conclusions

In the present work, the binary interaction parameter k_{12} of the second virial coefficient and the NRTL model parameters τ_{12} and τ_{21} were optimized for 20 binary mixtures containing carbon dioxide, *n*-alkanes (from methane to 1-decane) and *n*-alkanols (from methanol to 1-decanol). Phase equilibrium calculations were developed using the Peng–Robinson EOS coupled with the Wong–Sandler mixing rules. Excess Helmholtz free energy at infinite pressure was calculated using NRTL excess Gibbs free energy model. In total, 198 minimizations were carried out for the 20 mixtures at high pressures studied.

Here, the capability and efficiency of the objective function denoted by the Eq. (12) for minimizing VLE experimental data at high pressures has been demonstrated. The optimal parameters reported serve as a base to improve phase equilibria predictions in order to model and design chemical processes involving supercritical carbon dioxide *n*-alkanes and *n*-alkanols under non-ideal conditions. Then, the use of an adequate mixing rule containing a correction at infinite-pressure results convenient for the satisfactory representation of phase equilibrium of the highly asymmetric binary mixtures evaluated.

The optimal values of the binary interaction parameter of the second virial coefficient for all the mixtures studied were found to be in concordance with the statistical thermodynamic postulates considering that such values were in the acceptable range (0–1) and that it increases when the asymmetry of the mixtures also increases. Parallelly, we propose a

generalized correlation as function of the *n*-alkanes and *n*-alkanols acentric factor and the equilibrium temperature for mixing rule parameters, which gave good results in the vapor phase prediction.

List of symbols

$\underline{A}^E$	excess Helmholtz free energy
a, b	equation of state parameters
$(b\text{-}a/RT)_{ij}$	cross second virial coefficient
g_{ij}	parameter defined by Eq. 11
K_{ij}	distribution coefficient
k_{ij}	second virial coefficient interaction parameter
nc	number of components
np	number of experimental data points
P	pressure
R	gas constant
T	temperature
V	volume in molar units
X	liquid molar fraction
Y	vapor molar fraction
Z	molar fraction

Greek Letters

Δ	deviation
$\alpha(Tr)$	temperature-dependent alpha function
α_{ij}	NRTL model parameter
K	Peng-Robinson alpha function parameter
τ_{12}, τ_{21}	NRTL model binary interaction parameter.
Ω	acentric factor

Subscripts

c	critical point
m	mixture
r	reduced conditions
∞	infinite condition

Superscripts

E	excess property
exp	experimental
cal	calculated

References

[1] W.H. Hauthal, Advances with supercritical fluids, Chemosphere 43 (2001) 123–135.
[2] L.C. Gallego, C.A. Cardona, Supercritical fluids industrial applications I. Generalities and extraction processes, Ingeniería Química 411 (2004) 144–151 (in Spanish).
[3] L.C. Gallego, C.A. Cardona, Supercritical fluids industrial applications II. Extraction models, Ingeniería Química 412 (2004) 185–188 (in Spanish).
[4] L.C. Gallego, C.A. Cardona, Supercritical fluids industrial applications III. Supercritical conditions reactions, Ingeniería Química 413 (2004) 210–219 (in Spanish).
[5] L. Wang, C.L. Weller, Recent advances in extraction of nutraceuticals from plants, Trends in Food Science & Technology 17 (2006) 300–312.
[6] M.A. McHugh, V.J. Krukonis, Supercritical Fluid Extraction, Butterworth-Heinemann, Stoneham, 1994.
[7] A. Staby, J. Mollerup, Mutual solubilities of mono-alcohols and carbon dioxide: A review of experimental data, Fluid Phase Equilibria 89 (1993) 351–381.
[8] V. Brandani, G. Del Re, G. Di Giacomo, L. Gambacciani, Thermodynamic properties of polar fluids from a perturbed-dipolar-hard-sphere equation of state, Mixtures, Fluid Phase Equilibria 51 (1989) 23–36.
[9] D.W. Jennings, R. Lee, A.S. Teja, Vapor–liquid equilibria in the carbon dioxide + ethanol and carbon dioxide + l-butanol systems, Journal of Chemical and Engineering Data 36 (1991) 303–307.
[10] Z. Huanga, Y.C. Chiew, M. Feng, H. Miaoa, J.H. Li, L. Xua, Modeling aspirin and naproxen ternary solubility in supercritical CO2/alcohol with a new Peng–Robinson EOS plus association model, Journal of Supercritical Fluids 43 (2007) 259–266.
[11] D.Y. Peng, D.B. Robinson, A new two-constant equation of state, Industrial and Engineering Chemistry Fundamentals 15 (1976) 59–64.
[12] J.O. Valderrama, The state of the cubic equations of state, Industrial and Engineering Chemistry Research 42 (7) (2003) 1603–1618.
[13] J.A. López, V.M. Trejos, C.A. Cardona, Objective functions analysis in the minimization of binary VLE data for asymmetric mixtures at high pressures, Fluid Phase Equilibria 248 (2006) 147–157.
[14] J.A. López, C.A. Cardona, Phase equilibrium calculations for carbon dioxide + *n*-alkanes binary mixtures with the Wong–Sandler mixing rules, Fluid Phase Equilibria 239 (2006) 206–212.
[15] M.L. Michelsen, Amodified Huron–Vidal mixing rule for cubic equation of state, Fluid Phase Equilibria 60 (1990) 213–219.
[16] Dahl, M.L. Michelsen, High-pressure vapor–liquid equilibrium with a UNIFAC based equation of state, American Institute of Chemical Engineering Journal 36 (1990) 1829–1836.
[17] D.S.H.Wong, S.I. Sandler, Theoretically correct mixing rule for cubic equations of state, American Institute of Chemical Engineering Journal 38 (1992) 671–680.
[18] P. Coutsikos, N.S. Kalospiros, D.P. Tassios, Capabilities and limitations of the Wong–Sandler mixing rules, Fluid Phase Equilibria 108 (1995) 59–78.
[19] N.G. Voros, D.P. Tassios, Vapor–liquid equilibria in nonpolar/weakly polar systems with different types of mixing rules, Fluid Phase Equilibria 91 (1993) 1-29.
[20] H. Renon, J.M. Prausnitz, Local compositions in thermodynamic excess functions 1for liquid mixtures, American Institute of Chemical Engineering Journal 14 (1967) 135–144.
[21] S. Angus, B. Armstrong, K.M. de Reuck, International Thermodynamic Tables of the Fluid State, vol. 3, Carbon Dioxide, Pergamon Press, Oxford, 1976.
[22]API 44 Tables, Selected Values of Properties of Hydrocarbons and Related Compounds, Texas A & M University College Station.
[23] S.M. Palosaari, S. Parviainen, J. Hiironen, J. Reunanen, P. Neittaanmäki, A random search algorithm for constrained global optimization, in: Acta Polytech. Scand. Chem. Tech. Metall. Ser. No. 172, Helsinki, 1985.
[24] M.S.W. Wei, T.S. Brown, A.J. Kidnay, E.D. Sloan, Vapor + liquid equilibria for the ternary system methane + ethane + carbon dioxide at 230K and its constituent binaries at temperatures from 207 to 270 K, J. Chem. Eng. Data 40 (1995) 726–731.
[25] L.A. Webster, A.J. Kidnay, Vapor–liquid equilibria for methane– propane–carbon dioxide systems at 230K and 270 K, J. Chem. Eng. Data 46 (2001) 759–764.
[26] M Niesen Vicki G. (Vapor + liquid) equilibria and coexisting densities of (carbon dioxide + n-butane) at 311 to 395 K. J. Chem. Thermodynamics 21 (1989) 915-923.

[27] K. Tochigi, K. Hasegawa, N. Asano, K. Kojima, Vapor–liquid equilibria for the carbon dioxide + pentane and carbon dioxide + toluene systems, J. Chem. Eng. Data 43 (1998) 954–956.
[28] K. Ohgaki, T. Katayama, Isothermal vapor–liquid equilibrium data for binary systems containing carbon dioxide at high pressures: methanol–carbon dioxide, n-hexane–carbon dioxide and benzene–carbon dioxide systems, J. Chem. Eng. Data 21 (1976) 53–55.
[29] H. Kaira, H. Kubota, D.B. Robinson, H.-J. Ng, Equilibrium phase properties of the carbon dioxide–*n*-heptane system, J. Chem. Eng. Data 23 (1978) 317–321.
[30] W.L. Weng, M.J. Lee, Vapor–liquid equilibrium of the octane/carbon dioxide, octane/ethane, and octane/ethylene systems, J. Chem. Eng. Data 37 (1992) 213–215.
[31] D.W. Jennings, R.C. Schucker, Comparison of high pressure vapor–liquid equilibria of mixtures of CO_2 or propane with nonane and C_9 alkylbenzenes, J. Chem. Eng. Data 41 (1996) 831–838.
[32] Nagarajan N., R.L. Robinson, Equilibrium phase compositions, phase densities, and interfacial tensions for CO_2 + hydrocarbon systems. CO_2 + *n*-decane, J. Chem. Eng. Data 31 (1986) 168–171.
[33] K. Ohgaki, T. Katayama, Isothermal vapor–liquid equilibrium data for binary systems containing carbon dioxide at high pressures: methanol-carbon dioxide, *n*-hexane-carbon dioxide, and benzene-carbon dioxide systems, Journal of chemical and Engineering Data 21 (1976) 53–55.
[34] C.J. Chiehming, C.K. Lung, D.C. Yih, A new apparatus for the determination of *P–x–y* diagrams and Henry's constants in high pressure alcohols with critical carbon dioxide, Journal of Supercritical Fluids 12 (1998) 223–237.
[35] V. Vandana, A.S. Teja, Vapor–liquid equilibria in the carbon dioxide + 1-propanol system, Journal of chemical and Engineering Data 40 (1995) 459–461.
[36] K. Suzuki, H. Sue, M. Itou, R.L. Smith, H. Inomata, K. Arai, S. Saito, Isothermal vapor–liquid equilibrium data for binary systems at high pressures: carbon dioxide-methanol, carbon dioxide-ethanol, carbon dioxide- 1-propanol, methane-ethanol, methane-1-propanol, ethane-ethanol, and ethane-1-propanol systems, Journal of chemical and Engineering Data 35 (1990) 63–66.
[37] C. Secuianu, V. Feroiu, D. Geana, High-pressure vapor–liquid equilibria in the system carbon dioxide + 1-butanol at temperatures from (293.15 to 324.15) K, Journal of Chemical and Engineering Data 49 (2004) 1635–1638.
[38] G.S. Oliver, L.A.G. Luna, S.I. Sandler, Vapor–liquid equilibria and critical points for the carbon dioxide + 1-pentanol and carbon dioxide + 2-pentanol systems at temperatures from 332 to 432 K, Fluid Phase Equilibria 200 (2002) 161–172.
[39] O.E. Solis, L.A.G. Luna, S.I. Sandler, J.G.S. Hernández, Vapor–liquid equilibria and critical points of the CO_2 + 1-hexanol and CO_2 + 1-heptanol systems, Fluid Phase Equilibria 210 (2003) 215–227.
[40] C. Secuianu, V. Feroiu, D. Geana, Investigation of phase equilibria in the ternary system carbon dioxide + 1-heptanol + *n*-pentadecane, Fluid Phase Equilibria 261 (2007) 337–342.

CHAPTER 6

THERMODYNAMIC CONSISTENCY OF EXPERIMENTAL VLE DATA FOR ASYMMETRIC BINARY MIXTURES CONTAINING CO_2 AT HIGH PRESSURES

In this chapter, the thermodynamic consistency of isothermal vapor-liquid equilibrium data for 9 non-polar and 9 polar binary asymmetric mixtures containing carbon dioxide at high pressures has been evaluated. A method based on the isothermal Gibbs-Duhem equation was used for the test of thermodynamic consistency using an Φ–Φ approach. The Peng-Robinson equation of state coupled with the Wong-Sandler mixing rules were used for modeling the vapor-liquid equilibrium (VLE) within the thermodynamic consistency test. The VLE parameters calculations for asymmetric mixtures at high pressures were highly dependent on bubble pressure calculation, making more convenient to eliminate the data points yielding the highest deviations in pressure. However the results of the thermodynamic consistencies test of experimental data for many cases were found not fully consistent. As a result, the strategies for solving these problems were discussed in detailed.

6.1 Introduction

Information about high-pressure phase equilibrium is essential for many chemical processes and separation operations involving higher pressures. Simulation of petroleum reservoirs, transportation, natural gas storage and carbon dioxide sequestration, and the study of geological processes are some examples in which high-pressure phase equilibrium data are necessary [1]. Many of the asymmetric mixtures at high pressures containing carbon dioxide and isoamyl acetate, ethyl laureate, ethyl caproate, among others compounds, have great industrial importance. For instance in the field of the supercritical fluid extraction, designing and sizing equipments. These kind of binary mixtures are characterized by both high complexity and asymmetry, being the more common shortcoming for modeling vapor-liquid equilibrium (VLE). Therefore it is necessary to account models that provide good prediction for VLE [2].

There are many ways to obtain information about VLE for asymmetric mixtures. The direct experimental measurement of phase equilibrium data may be the preferred option, although these measurements can be difficult and expensive. There are some useful thermodynamic models that can be employed for predicting the VLE for binary mixtures at high pressures [3-11], especially when a minimum number of experimental data is available, helping to reduce the number of experimental data points needed for a special design problem.

With the aim of generating adequate thermodynamic models, an accurate set of VLE data is required. This set is commonly tested by a thermodynamic consistency test in order to verify the reliability of the experimental data, which are increasingly in importance to have more accuracy. Among the most employed thermodynamic relations requiring to be satisfied for testing thermodynamic consistency are the Gibbs-Duhem and Gibbs-Helmholtz equations. Some common consistency thermodynamic tests (e.g. the overall area test method) are based on different mathematical rearrangement of the Gibbs-Duhem equation, which, in some cases, consider constant both temperature and pressure. Although the Gibbs-Duhem equation is also employed in the calculation of the fugacity coefficient among other thermodynamic relationships [12]. Furthermore, these thermodynamic equations, carried out in a rigorous manner, are really useful to prove the accuracy of the experimental data set [13].

The study of thermodynamic consistency of a binary system at low pressures is generally based on the equal-area criterion [13-17]. However, it is conveniently to use models different to the equal-area criterion when mixtures at high pressures are studied. Remarkable studies on thermodynamic consistency tests for these mixtures have been presented by Chueh et al. [18] by developing an equal-area test, based on extension of the Redlich and Kister's method for isothermal VLE data at low pressure. Won and Prausnitz [19] by proposing a method for isothermal data based on extension of the Baker's method. Christiansen and Frendenslund [20] by considering an applicable model test to isothermal and isobaric data with a supercritical condition component. Bertucco et al. [21] proposed a method to find the consistency VLE data for mixtures containing fluid in supercritical state. Also, Jackson and Wilsak [22] presented a review of several common thermodynamic consistency tests used mainly for mixtures at high pressure.

In many cases, thermodynamic consistency tests figure out the reliability of experimental data taken from literature. These tests provide a valuable tool when the experimental data satisfies and follows strictly a thermodynamic relationship (e.g. Gibbs-Duhen equation) assessing the data as thermodynamically consistent or inconsistent. In order to obtain VLE binary interaction parameters of asymmetric mixtures at high pressures, a suitable set of experimental data is required to generate reliable parameters coming from the minimization of a particular objective function.

In the present work, the thermodynamic consistency test for experimental VLE data of polar and non-polar asymmetric binary mixtures containing carbon dioxide at high pressures proposed by Valderrama et al. [23] is analyzed. The Peng-Robinson (PR) equation of state [24] coupled with the Wong-Sandler mixing rules [25] has been used in thermodynamic consistency test and VLE estimation. NRTL model [26] was employed to predict the excess Helmholtz free energy into the Wong-Sandler mixing rules. The optimal parameters used in this work were calculated in previous works [27, 28], and those were used for testing the thermodynamic consistency for twenty three isothermal sets of non-polar mixtures and twenty five isothermal sets of polar mixtures. Likewise the Levenberg-Marquardt minimization algorithm was used in all cases.

6.2 Thermodynamic consistency model

The Gibbs-Duhem equation requires a general coupling of molar partial properties of the components in a specific mixture that provides a basis for most of the methods for testing thermodynamic consistency of VLE experimental data. The general Gibbs-Duhem equation is expressed in terms of residual properties as [29]:

$$d\left(\frac{\underline{G}^R}{RT}\right)=\frac{\underline{V}^R}{RT}dP-\frac{\underline{H}^R}{RT^2}dT+\sum_i\frac{\overline{G}_i^R}{RT}dz_i \tag{1}$$

where z_i is the molar fraction of *i*-component in the reference phase (either *x* for liquid or *y* for the vapor phase) and the molar residual Gibbs property is defined by the equation (2):

$$\underline{G}^R=\sum_i\overline{G}_i^R z_i \tag{2}$$

By replacing Eqs. (2) into (1):

$$\sum_i z_i\frac{d\overline{G}_i^R}{RT}=\frac{\underline{V}^R}{RT}dP-\frac{\underline{H}^R}{RT^2}dT \tag{3}$$

The residual Gibbs free energy properties can also be expressed in terms of fugacity coefficients $\left(\overline{\phi}_i\right)$ in the mixture.

$$\frac{\overline{G}_i^R}{RT}=\frac{\overline{G}_i-\overline{G}_i^{IGM}}{RT}=\ln\left(\overline{\phi}_i\right) \tag{4}$$

The fugacity coefficient can be replaced in equation (3), giving:

$$\sum_i z_i d\ln\left(\overline{\phi}_i\right)=\frac{\underline{V}^R}{RT}dP-\frac{\underline{H}^R}{RT^2}dT \tag{5}$$

where $\underline{V}^R$ and $\underline{H}^R$ are the molar residual volume and enthalpy of the mixture, respectively. Equation (5) for a binary mixture, at constant temperature *T*, can be rewritten as:

$$z_1\frac{d\ln\left(\overline{\phi}_1\right)}{dz_i}+z_2\frac{d\ln\left(\overline{\phi}_2\right)}{dz_i}=\frac{1}{P}\left(Z-1\right)\frac{dP}{dz_i} \tag{6}$$

Equation (6) is usually written in terms of solute concentration into a vapor phase mixture ($z_i=y_i$). Thus, solute is termed as component 2 in the binary mixture. Taking into account these considerations the above equation can be expressed as:

$$\frac{1}{P}\frac{dP}{dy_2}=\frac{y_2}{(Z-1)}\frac{d\ln\bar{\phi}_2}{dy_2}+\frac{(1-y_2)}{(Z-1)}\frac{d\ln\bar{\phi}_1}{dy_2} \tag{7}$$

An analogous expression to (7), in terms of fugacity coefficients, has been reported by Bertucco et al. [21]. Likewise Eq. (7) can be conveniently expressed in integral form, as follows:

$$\int\frac{1}{Py_2}dP=\int\frac{1}{(Z-1)\bar{\phi}_2}d\bar{\phi}_2+\int\frac{(1-y_2)}{y_2(Z-1)\bar{\phi}_1}d\bar{\phi}_1 \tag{8}$$

where P is the absolute pressure, y_2 is the molar fraction of solute in the vapor phase, Z is the compressibility factor of the vapor phase mixture, and $\bar{\phi}_1$ and $\bar{\phi}_2$ are the fugacity coefficients of species 1 and 2 in the vapor phase mixture. The equation (8) can also be written as:

$$A_p=\int\frac{1}{Py_2}dP=A_\phi=A_{\phi1}+A_{\phi2} \tag{9}$$

The right hand side of the equation (8) is designated by A_ϕ as follows:

$$A_\phi=A_{\phi1}+A_{\phi2}=\int\frac{1}{(Z-1)\bar{\phi}_2}d\bar{\phi}_2+\int\frac{(1-y_2)}{y_2(Z-1)\bar{\phi}_1}d\bar{\phi}_1 \tag{10}$$

The parameters A_ϕ and A_p are obtained using a convenient thermodynamic model and from *P-y* experimental data set, respectively. The PR EoS coupled with the Wong-Sandler mixing rules was used to evaluate eqn. (10). Note the advantageous manner of eqn. (10) which overcomes the inconvenience in evaluating excess volume effects on the activity coefficient. As can be seen, eqn. (10) is a non-defined integral equation which can be solved using any integrator numerical method. Finally, in order to qualify an experimental data ser, A_p must be equal to A_ϕ within the defined deviations range [23].

6.3 Equation of state and mixing rules

The PR EoS has the following form:

$$P=\frac{RT}{v-b}-\frac{a}{v(v+b)+b(v-b)} \tag{11}$$

where P is the absolute pressure, T is the absolute temperature, R is the ideal gas constant, a and b are the energy and size parameters. These last are calculated from the expressions:

$$a=0.457235\frac{R^2T_c^2}{P_c}\alpha(T_r) \tag{12}$$

$$b = 0.077796\frac{RT_c}{P_c} \tag{13}$$

where subscripts *c* and *r* denote critical and reduced conditions, respectively. The α function is calculated from equations (14) and (15):

$$\alpha\left(T_r\right) = \left[1 + \kappa\left(1 - \sqrt{T_r}\right)\right]^2 \tag{14}$$

$$\kappa = 0.37464 + 1.54226\omega - 0.26992\omega^2 \tag{15}$$

where ω is the acentric factor. The PR EoS can be extended to mixtures by using the Wong-Sandler [25] mixing rules for both vapor and liquid phases. The parameters a_m and b_m are obtained from:

$$a_m = b_m\left[\sum_i z_i\frac{a_i}{b_i} + \frac{\underline{A}^E_\infty}{\sigma}\right] \tag{16}$$

with

$$b_m = \frac{\sum_i\sum_j z_i z_j\left(b - \frac{a}{RT}\right)_{ij}}{1 - \sum_i z_i\frac{a_i}{b_i RT} - \frac{\underline{A}^E_\infty}{\sigma RT}} \tag{17}$$

$$\sigma = \frac{1}{\sqrt{2}}\ln\left(\sqrt{2} - 1\right) \tag{18}$$

and

$$\left(b - \frac{a}{RT}\right)_{ij} = \frac{\left(b - \frac{a}{RT}\right)_i + \left(b - \frac{a}{RT}\right)_j}{2}\left(1 - k_{ij}\right) \tag{19}$$

where k_{ij} is a binary interaction parameter of the second virial coefficient, *z* is the molar fraction and $\underline{A}^E_\infty$ is the excess Helmholtz free energy at infinite pressure which is calculated from NRTL model for binary mixtures according to equations:

$$\frac{\underline{A}^E_\infty}{RT} = \sum_i z_i\left(\frac{\sum_j z_j\tau_{ji}g_{ji}}{\sum_k z_k g_{ki}}\right) \tag{20}$$

$$g_{ij} = \exp\left(-\alpha_{ij}\tau_{ij}\right) \tag{21}$$

where α_{12} (=α_{21}), τ_{12} and τ_{21} are the three parameters of NRTL model. A constant value for α_{12} of 0.3 was used. The PR EoS coupled with the Wong-Sandler mixing rules, the fitted NRTL parameters (τ_{12} and τ_{21}), and the binary interaction parameters of the second virial coefficient (k_{12}) were employed. These parameters have been previously determined using experimental phase equilibrium data at isothermal conditions for each of nine non-polar and eight polar asymmetric mixtures [27, 28]. The corresponding fugacity coefficients and the values of *P*-*y* variables for *T*-*x* were calculated by using these fitted parameters in order to evaluate eqn. (10). The required variables to calculate eqn. (10), that are P, y_2, $\overline{\phi}_1$ and $\overline{\phi}_2$, were found by using the thermodynamic condition expressing an equality-of-partial-fugacities for any component in all coexisting phases. This condition can be written in term of fugacity as:

$$\overline{f}_i^L\left(T, P, x_i; \tau_{12}, \tau_{21}, k_{12}\right) = \overline{f}_i^V\left(T, P, y_i; \tau_{12}, \tau_{21}, k_{12}\right) \tag{22}$$

where superscripts L and V denote the liquid and vapor phases, respectively. The expression (22) is the starting point for VLE calculations. Furthermore, these parameters were obtained from sets of experimental data using the following objective function [27]:

$$f_{ob} = \sum_{i=1}^{np}\sum_{j=1}^{nc}\left[y_{i,j}^{\exp} - x_{i,j}^{\exp} K_{i,j}^{cal} \right]^2 \tag{23}$$

where K is the distribution coefficient between vapor and liquid phases, the superscripts *np* and *nc* denote the numbers of experimental data points and components, and y and x are the molar fraction in the vapor and liquid phases, respectively. This objective function has shown very acceptable performances for VLE of asymmetric binary mixtures at high pressures [27, 28].

6.4 Asymmetric binary mixtures

In the present work, 9 non-polar (gas + non-polar solute) and 9 polar (gas + polar solute) asymmetric binary mixtures containing carbon dioxide have been analyzed. The experimental conditions and their reference sources are shown in Tables 6.1 and 6.2. Data for 23 isotherms with 338 experimental points were studied for gas + non-polar mixtures and 25 isotherms with 238 experimental points were studied for gas + polar mixtures. Several asymmetric mixtures have widely been used in many applications and reported in literature [30-32].

Table 6.1 Experimental conditions for non-polar asymmetric binary mixtures

CO_2	np	T (K)	Pressure range (bar)	Ref.
Ethane	17	210.00	3.350-5.380	[33]
	16	230.00	7.010-8.910	[33]
	20	250.00	13.03-17.87	[33]
	6	270.00	22.08-33.44	[33]
Propane	25	230.00	8.9-71.1	[34]
	27	270.00	32.0–79.5	[34]
n-Pentane	12	310.15	5.6-73.1	[35]
	13	333.15	5.9-87.5	[35]
	16	363.15	9.4-96.7	[35]
n-Hexane	10	298.15	8.9–57.7	[36]
	10	313.15	14.8–77.5	[36]
Benzene	8	298.15	8.9–57.7	[36]
	9	313.15	14.8–77.5	[36]
n-Heptane	23	310.65	1.861-75.63	[37]
	17	352.59	4.240-116.1	[37]
	15	394.26	11.30-133.1	[37]
n-Decane	22	344.30	63.8–127.4	[38]
	26	377.60	103.4–164.8	[38]
Styrene	9	333.15	60.3-112.0	[39]
	10	343.15	60.0–131.0	[39]
	8	348.15	62.9–134.2	[39]
Limonene	8	313.18	8.30-84.5	[40]
	11	323.25	11.3-98.3	[40]

Table 6.2 Experimental conditions for polar asymmetric binary mixtures

CO_2	np	T (K)	Pressure range (bar)	Ref.
Methanol	8	298.15	7.89-59.52	[36]
	11	291.15	5.6-43.3	[41]
	16	303.18	8.9-63.2	[41]
	16	308.15	13.2-77.2	[41]
Isoamyl acetate	7	308.15	10.3–69.3	[42]
	8	318.15	10.0–80.3	[42]
	9	328.15	10.3–90.7	[42]
Ethanol	6	314.50	5.7-81.1	[43]
	9	325.20	62.74-93.49	[43]
	8	337.20	62.19-108.45	[43]
Butanol	9	325.30	52.26-98.73	[43]
	11	337.20	61.78-117.76	[43]
n-Heptanol	8	374.63	40.38-145.72	[44]
	8	298.15	6.80-60.9	[45]
n-Octanol	9	403.15	64.0-183.0	[46]
	7	453.15	64.0-188.0	[46]
Ethyl caproate	8	308.20	17.0-64.6	[47]
	10	318.20	17.0-78.2	[47]
	12	328.20	17.3-92.2	[47]
Decanal	10	288.20	19.3-48.1	[48]
	11	303.20	21.7-67.6	[48]
	12	313.20	82.2-16.8	[48]

Ethyl laurate	8	308.15	14.8–70.0	[49]
	8	318.15	14.8–83.1	[49]
	9	328.15	14.8–100.1	[49]

6.5 Thermodynamic consistency criteria

Asymmetric binary mixtures require a suitable thermodynamic model, such as PR coupled with Wong Sandler mixing rules. Model correlation could be within an acceptable deviation range of molar fraction in vapor phase and pressure for values of (-20 to +20%) and (-10% to +10%) for molar fraction and pressure, respectively. The model is accepted only in the case of the deviations falling within this range. These criteria were set up by Valderrama et al. [23], defining the individual percentage deviations in bubble point pressure and percentage of molar fraction deviation of vapor phase for each *i*-point as:

$$\%\,\Delta P_i = \frac{\left(P_i^{\exp} - P_i^{cal}\right)}{P_i^{\exp}} \cdot 100 \tag{24}$$

$$\%\,\Delta y_{2i} = \frac{\left(y_{2i}^{\exp} - y_{2i}^{cal}\right)}{y_{2i}^{\exp}} \cdot 100 \tag{25}$$

Once the results from thermodynamic model are in agreement with the criteria, the individual percent area deviations must be calculated from the equation (26).

$$\%\,\Delta A_i = \frac{\left(A_{\phi i} - A_{pi}\right)}{A_{pi}} \cdot 100 \tag{26}$$

In order to conclude that experimental data are thermodynamically consistent (TC), the individual area deviations (eqn. 26) must fall within the range (−20% to +20%), from here termed as criterion range. Valderrama et al. [23] summarize these referred criteria including the required minimum number of experimental data and the decision rules for consistency test.

Resuming, the calculation of pressure and solute concentration in the vapor phase (y_2), as the evaluation of the expressions for A_ϕ and A_p, requires a suitable EoS and any mixing rule. Furthermore, individual percentage deviations in the variables y_2 and P must be low to accept the thermodynamic model. In some cases in which percentage Δy_2 and percentage ΔP_i are outside the defined margins of errors, it is concluded that another model must be applied, being this case commonly known as “try a different model” (TDM).

The consistency method studied in this article has some important aspects about multiple solutions, objective function and the best paired combinations of them. With the aim of determining the optimal parameters in each minimization of the objective function, the Levenberg-Marquardt minimization algorithm was used. Hence, the parameters τ_{12}, τ_{21} and k_{12} for each isothermal temperature were calculated by

optimizing the objective function until VLE predictions showed low deviations in bubble point pressure and vapor phase composition [27]. A substantial reduction in the computing time requirements was observed. Multiple solutions coming from the experimental data set for each mixture could appear in each minimization. These solutions were obtained into an acceptable predefined range taking into account, for example, available values for τ_{12} and τ_{21} calculated at low pressures. The k_{12} must be in concordance with the statistical thermodynamic postulates considering that such values were in acceptable range (0-1). Considering this objective function, it is expected to find all possible solutions for these parameters within the predefined range. The optimal parameters are chosen to be those that show the lowest deviation both in bubble point pressure and vapor phase composition.

6.6 Results and discussion

The optimal parameters of the studied thermodynamic model, relative percentage deviations in bubble point pressure and absolute deviation in vapor phase molar fraction for polar and non-polar asymmetric mixtures have been previously reported in the supplementary material available in the preceding chapters. The parameters given in that material were used to predict the phase equilibrium and thermodynamic consistency test for the whole mixtures in the present study. Results of thermodynamic consistency test for the carbon dioxide + ethane experimental data were considered consistent only if some points of data set are eliminated according to the decision rules proposed by the authors [23].

Table 6.3 shows the summary results for carbon dioxide + ethane at 230K. The data set for this system was found to be thermodynamically inconsistent (TI), denoting that some points in the obtained area deviations were out of the range (see bold face on Table 6.3). In the case when three points were eliminated from the initial data set, the area deviations for the remaining 13 points were within the defined limits previously. Therefore, the initial set of 16 data points was declared as TI, but the remaining set of 13 data points was considered as TC.

The predicted VLE data was in agreement with the experimental data as shown for carbon dioxide + ethane system in Fig. 6.1. Good predictions in the bubble point pressure ($\Delta P = 0.189$, $\Delta P = 0.361$, $\Delta P = 0.3347$ and $\Delta P = 0.4281$) at the four evaluated temperatures (210, 230, 250 and 270K) were obtained. A good prediction was also obtained at the same temperatures for the absolute mean deviations in the vapor phase molar fraction for $\Delta y_1 = 0.0064$, $\Delta y_1 = 0.0032$, $\Delta y_1 = 0.0068$ and $\Delta y_1 = 0.0114$.

Residual deviations in the individual areas for the carbon dioxide + ethane system at 230K are shown in Figs. 6.2a, 6.2b and 6.2c. The margins of error were established by the calculation of individual area deviation percentage ($\%\Delta A_i$) by the eqn. (26). Fig. 6.2a shows the deviations in the individual areas for the first set of experimental data. On the other hand, Figs. 6.2b and 6.2c show the deviations for pressure and the vapor phase solute concentration. As can be seen in these figures, deviations in pressure and solute concentration were below 0.8% and 5% respectively. It can be concluded that binary interaction parameters were not enough good to predict the VLE for the studied system.

Table 6.3 Detailed results for the system carbon dioxide + ethane at 230 K found to be thermodynamically consistent (TC) using PR+WS/NRTL model

A_p	A_ϕ	$\%\Delta A_i$	P^{exp}	P^{cal}	$\%\Delta P$	$y_2^{\exp}$	y_2^{cal}	$\%\Delta y_{2i}$
0.0371	**0.0294**	**-20.721**	**7.01**	**7.0094**	**-0.008**	**1.0000**	**1.0000**	**-0.0003**
0.1044	0.1086	4.0472	7.27	7.2148	-0.759	0.9655	0.9666	0.1088
0.0621	0.0641	3.2221	7.99	7.964	-0.324	0.8487	0.8567	0.9400
0.0627	0.0645	2.9361	8.41	8.3981	-0.141	0.8018	0.8000	-0.2272
0.0572	0.0493	-13.873	8.83	8.8275	-0.027	0.7548	0.7477	-0.9471
0.0414	0.0490	18.3600	9.21	9.1504	-0.647	0.7180	0.7102	-1.0836
0.2199	0.2265	3.0338	9.48	9.4664	-0.144	0.6775	0.6748	-0.4059
0.0585	0.0602	2.8473	10.8	10.824	0.218	0.5218	0.5222	0.0774
0.0191	0.0190	-0.4823	11.12	11.153	0.299	0.4773	0.4767	-0.1356
0.0320	0.0320	-0.2906	11.22	11.253	0.294	0.4598	0.4599	0.0150
0.0159	**0.0088**	**-44.846**	**11.38**	**11.413**	**0.288**	**0.4250**	**0.4239**	**-0.2517**
-0.134	-0.134	-0.4366	11.45	11.45	0.001	0.3516	0.3538	0.6306
-0.368	-0.371	0.8392	11	10.991	-0.083	0.2597	0.2661	2.4712
-1.110	-1.104	-0.5685	10.23	10.182	-0.469	0.1611	0.1678	4.1485
-252.9	-65.35	-74.162	9.36	9.2648	-1.016	0.0549	0.0579	5.4351
------	-------	------	8.91	8.8205	-1.004	0.0001	0.0004	281.630

CO_2 + ethane, T=230 K, τ_{12}=1.8426, τ_{21}=0.7901, k_{12}=0.0907, 16 Points Result (*TI), $\%\Delta P_{av}$=0.3601, $\%\Delta y_{2av}$= 18.657%, $\%\Delta A_{av}$=12.711.

A_p	A_ϕ	$\%\Delta A_i$	P^{exp}	P^{cal}	$\%\Delta P$	$y_2^{\exp}$	y_2^{cal}	$\%\Delta y_{2i}$
0.0370	0.0307	-16.917	7.01	7.0094	-0.0092	1.0000	1.0000	0.0000
0.1043	0.1115	6.8627	7.27	7.2247	-0.6233	0.9655	0.9654	-0.0013
0.0621	0.0642	3.4026	7.99	7.9948	0.0594	0.8487	0.8548	0.7289
0.0626	0.0635	1.3767	8.41	8.4306	0.2447	0.8018	0.7992	-0.3152
0.0572	0.0479	-16.302	8.83	8.8551	0.2839	0.7548	0.7486	-0.8162
0.0414	0.0472	13.941	9.21	9.1704	-0.4297	0.7180	0.7127	-0.7362
0.2198	0.2168	-1.3818	9.48	9.4765	-0.0366	0.6775	0.6788	0.1902
0.0585	0.0599	2.3406	10.8	10.79	-0.0892	0.5218	0.5303	1.6441
0.0191	0.0194	2.0016	11.12	11.123	0.0228	0.4773	0.4834	1.2806
0.0320	0.0337	5.2038	11.22	11.226	0.0524	0.4598	0.4656	1.2622
-0.1057	-0.1104	4.3953	11.38	11.396	0.1383	0.4250	0.4266	0.3770
-0.3683	-0.3600	-2.2564	11.00	10.999	-0.0074	0.2597	0.2616	0.7619
--------	---------	---------	10.23	10.224	-0.0614	0.1611	0.1686	4.6918

CO_2 + ethane, T=230 K, τ_{12}=2.229, τ_{21}=1.0893, k_{12}=-0.0302, 13 Points Result (**TC), $\%\Delta P_{av}$= 0.15838, $\%\Delta y_{2av}$= 0.98507%, $\%\Delta A_{av}$= 6.3651.

*TI: Thermodynamically inconsistent. **TC: Thermodynamically consistent.

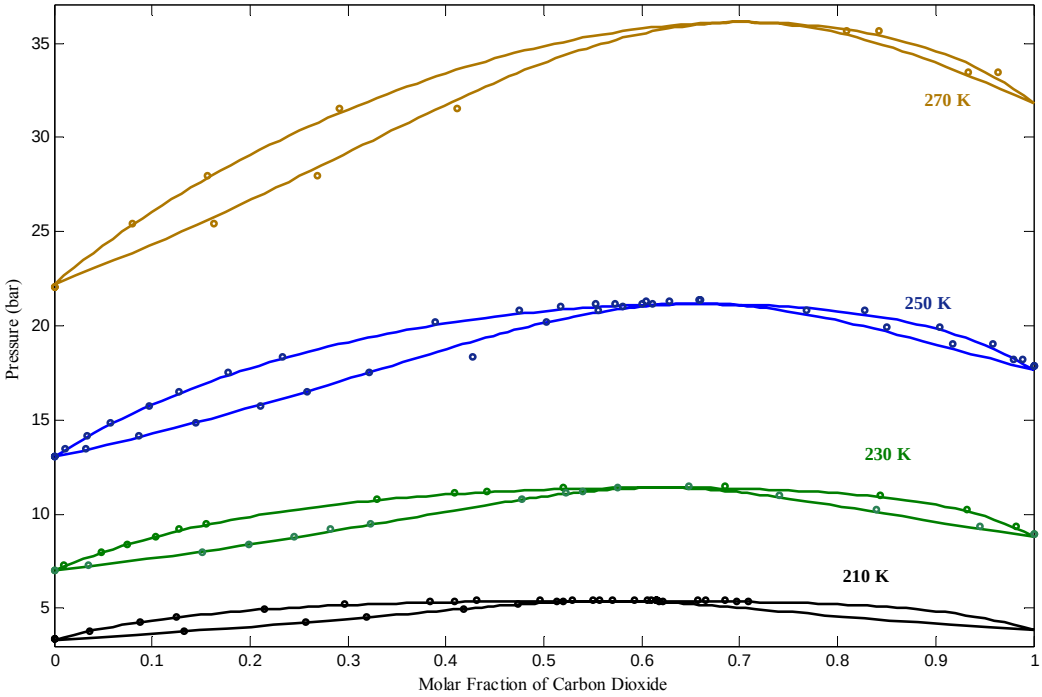

Fig. 6.1 Experimental and predicted VLE for carbon dioxide + ethane binary system. Experimental data were taken from Wei *et al*. [33].

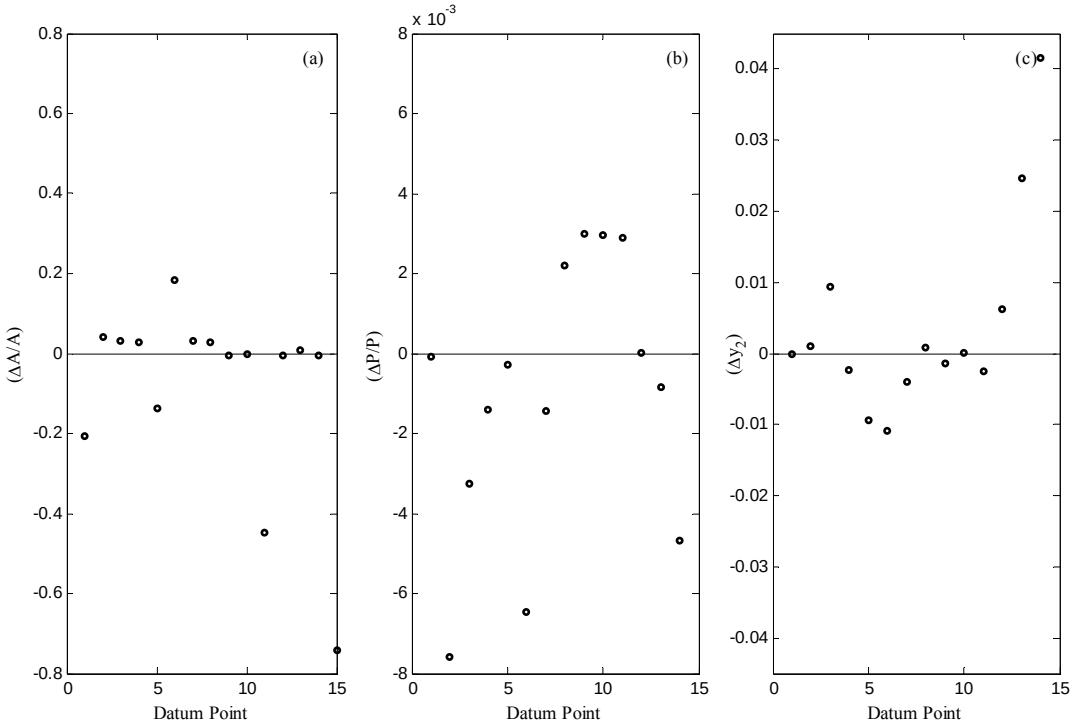

Fig. 6.2 Deviations in the individual areas for carbon dioxide + ethane binary system at 230K. Experimental data were taken from Wei *et al*. [33].

Table 6.4 Detailed results for the system carbon dioxide + 1-octanol at 403.15K found to be thermodynamically consistent (TC) using PR+WS/NRTL model

A_p	A_ϕ	$\%\Delta A_i$	P^{exp}	P^{cal}	$\%\Delta P$	$y_2^{\exp}$	y_2^{cal}	$\%\Delta y_{2i}$
38.024	32.089	-15.608	65	65.159	0.244	0.0055	0.00619	12.58
29.191	25.320	-13.260	80	79.852	0.184	0.0055	0.00659	19.90
26.671	24.269	-9.006	95	95.077	0.0813	0.0065	0.00732	12.69
13.249	13.451	1.525	115	115.210	0.182	0.0083	0.00879	5.928
9.310	9.103	-2.219	130	130.880	0.679	0.0107	0.0104	-2.868
6.675	7.081	6.070	145	144.960	0.0305	0.0132	0.0123	-7.160
3.362	**4.311**	**28.238**	**160**	**159.290**	**0.441**	**0.0170**	**0.0146**	**-13.83**
3.793	4.539	19.668	170	170.460	0.269	0.0193	0.0169	-12.21
--------	--------	-------	185	185.520	0.282	0.0269	0.0208	-22.66

CO_2 + 1-Octanol, T=403.15 K, τ_{12}=1.968, τ_{21}= -0.6095, k_{12}=0.7315, 9 Points Result (*TI), $\%\Delta P_{av}$=0.266, $\%\Delta y_{2av}$= -0.847%, $\%\Delta A_{av}$=11.95.

A_p	A_ϕ	$\%\Delta A_i$	P^{exp}	P^{cal}	$\%\Delta P$	$y_2^{\exp}$	y_2^{cal}	$\%\Delta y_{2i}$
38.024	32.090	-15.606	65	65.159	0.244	0.0055	0.00619	12.543
29.191	25.321	-13.259	80	79.852	0.185	0.0055	0.00659	19.875
26.671	24.267	-9.013	95	95.077	0.081	0.0065	0.00733	12.703
13.249	13.450	1.514	115	115.210	0.182	0.0083	0.00879	5.9784
9.310	9.106	-2.196	130	130.880	0.679	0.0107	0.0104	-2.805
10.341	11.487	11.085	145	144.960	0.031	0.0132	0.0123	-7.123
3.793	4.539	19.674	170	170.460	0.269	0.0193	0.0169	-12.110
--------	--------	-------	185	185.520	0.282	0.0269	0.0208	-22.550

CO_2 + 1-Octanol, T=403.15 K, τ_{12}=1.968, τ_{21}=-0.6081, k_{12}=0.7303, 8 Points Result (**TC), $\%\Delta P_{av}$= 0.244, $\%\Delta y_{2av}$= 0.813%, $\%\Delta A_{av}$= 10.33.

*TI: Thermodynamically inconsistent. **TC: Thermodynamically consistent.

Carbon dioxide + 1-octanol mixture data set at 403.15K was found to be thermodynamically inconsistent (TI). The values of $\%\Delta A_i$ were out of the adequate range (see bold face on Table 6.4). As a result, one point from the initial data set was not considered, and then $\%\Delta A_i$ was calculated for the remaining 8 points. This last set was considered TC because their $\%\Delta A_i$ were inside the range (Table 6.4).

According to the results obtained and showed in Fig. 6.3, the accuracy in VLE prediction for the experimental and predicted VLE for carbon dioxide + 1-octanol system was verified. The parameters obtained by minimization at 453.15K and 403.15K provided good predictions for pressure ($\Delta P = 0.23$ and $\Delta P = 0.266$). Furthermore, good predictions for vapor phase concentration were also obtained ($\Delta y_1 = 0.0017$ and $\Delta y_1 = 0.0045$).

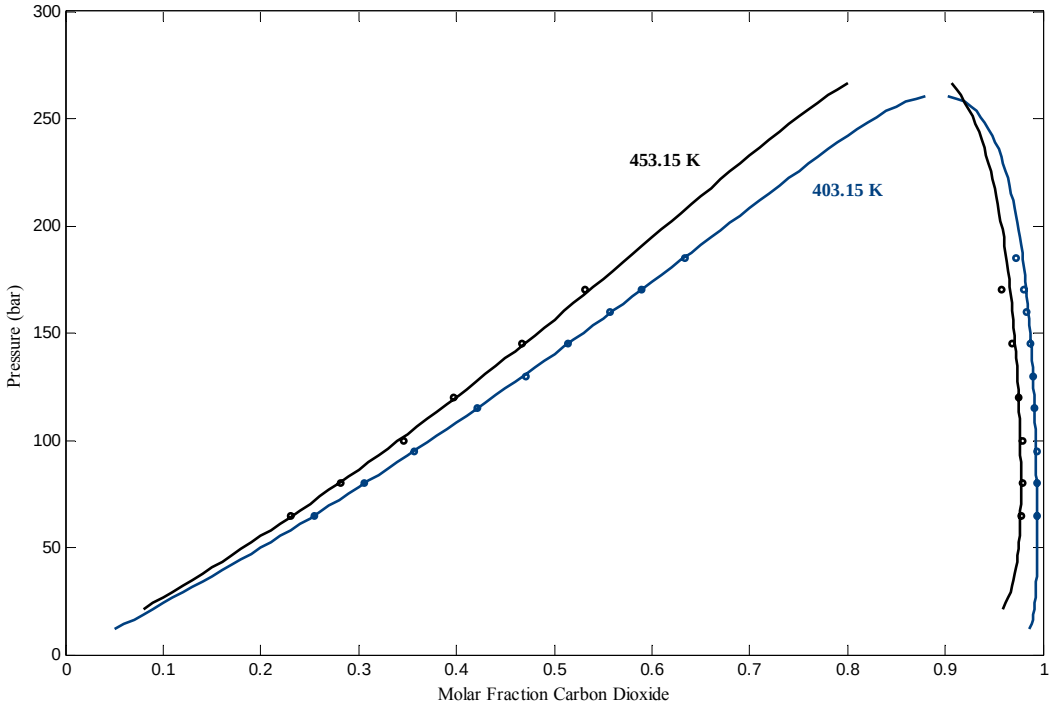

Fig. 6.3 Experimental and predicted VLE for carbon dioxide + 1-octanol binary system. Experimental data taken from Weng *et al.* [46]. Prediction with Peng-Robinson EOS coupled with the WS mixing rules.

Fig. 6.4 shows the deviations in the individual areas, pressure and the vapor phase solute concentration for the carbon dioxide + 1-octanol system at 403.15 K. As can be observed in Fig. 6.4a, there was only 1 point greater than 20% of area deviation from the initial data set. In the same way, deviations for pressure and the vapor phase solute concentration were less than 0.6% and 3%, respectively (see Figs. 6.4b and 6.4c). On the other hand, Fig. 6.5a, 6.5b and 6.5c shows the solution for each integral function in eqn.(8) corresponding to the carbon dioxide + 1-octanol mixture at 403.15K. Evaluation of the respective area under the curve for integral terms in this eqn. (8) was evaluated by inscribing *N-1* trapezoids under the curve for a set of *N* experimental points. Finally, the sum of trapezoid areas were then obtained. Additionally, the results from the trapezoidal method calculations were validated by the alternative method by fitting parameters in the polynomial expressions coming from experimental data. These referred methods were used to solve the integral expressions in eqn. (8), resulting in an area deviation below 1%. It was considered acceptable for our analysis.

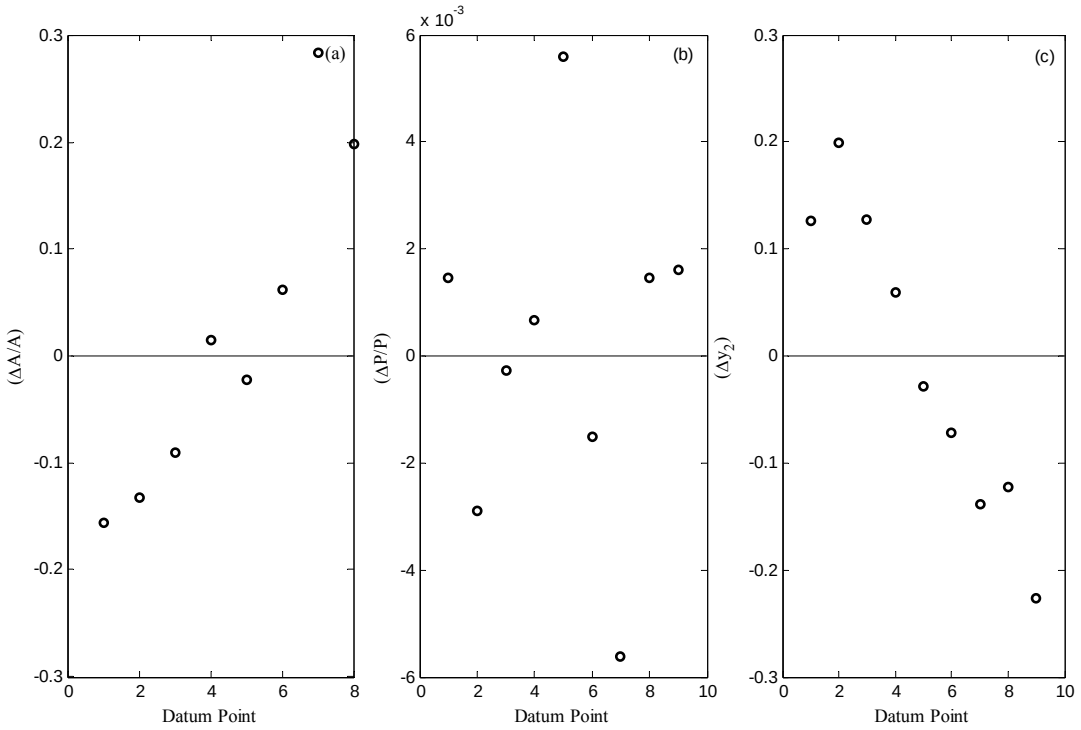

Fig. 6.4 Deviations in the individual areas for the carbon dioxide + 1-octanol binary system at 403.15 K. Experimental data were taken from Weng *et al.* [46].

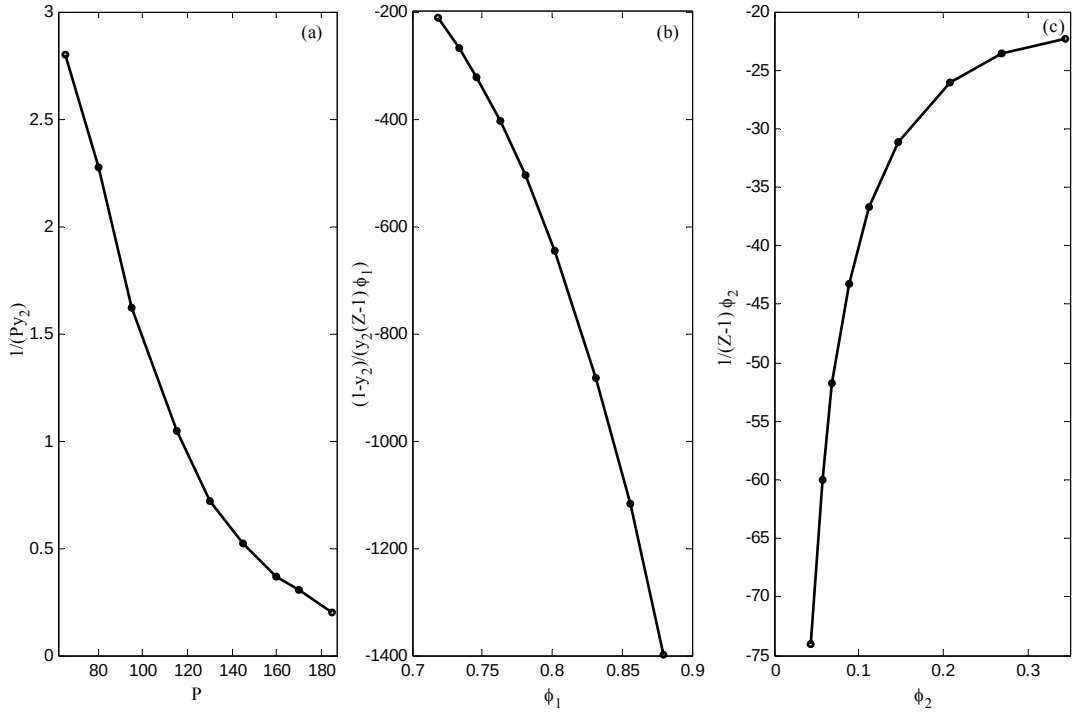

Fig. 6.5 Integral functions in Eq. (8) for the carbon dioxide + 1-octanol binary system at 403.15 K. Experimental data were taken from Weng *et al.* [46].

After developing the consistency test procedure for the carbon dioxide + ethyl laurate system at 308.15K, it was found to be NFC. Their $\%\Delta A_i$ were outside of the criterion range (see bold face on Table 6.5). Furthermore, total of $\%\Delta A_i$ obtained were higher than one quarter of the data points initially considered. As a result, two points from the initial data set were not considered, and then $\%\Delta A_i$ were calculated for the remaining 6 points.

Because of their $\%\Delta A_i$ were outside of the range, this last set of data was newly considered NFC. Fig. 6.6 shows the experimental and predicted VLE for the highly asymmetric carbon dioxide + ethyl laurate system. Not so good predictions for the data set parameters at 308.15K, 318.15K and 328.15K were obtained ($\Delta P = 0.611$, $\Delta P = 0.851$ and $\Delta P = 1.144$). However, good predictions for vapor phase concentration data $\Delta y_1 = 0.0001$, $\Delta y_1 = 0.0001$ and $\Delta y_1 = 0.0001$ were obtained.

Table 6.5 Detailed results for the system carbon dioxide + ethyl laurate at 308.15 K found to be not fully consistent (NFC) using PR+WS/NRTL model

A_p	A_ϕ	$\%\Delta A_i$	P^{exp}	P^{cal}	$\%\Delta P$	$y_2^{\exp}$	y_2^{cal}	$\%\Delta y_{2i}$
7070.5	**3.7x10^5**	**5240.6**	**14.8**	**14.843**	**0.2931**	**0.0001**	**1x10^{-6}**	**98.27**
2178.8	**1.1x10^5**	**5196.6**	**28.59**	**28.022**	**-1.986**	**0.0001**	**2x10^{-6}**	**98.091**
1783.6	**66354**	**3620.3**	**35.49**	**35.61**	**0.3392**	**0.0001**	**2x10^{-6}**	**97.615**
1514.1	**40131**	**2550.4**	**42.38**	**42.511**	**0.3089**	**0.0001**	**3x10^{-6}**	**96.857**
1312.4	**26246**	**1899.9**	**49.28**	**49.129**	**-0.306**	**0.0001**	**4x10^{-6}**	**95.631**
1161.2	**12912**	**1011.9**	**56.17**	**56.359**	**0.3369**	**0.0001**	**6x10^{-6}**	**93.199**
1038.6	**6943.7**	**568.54**	**63.07**	**62.745**	**-0.514**	**0.0001**	**1x10^{-5}**	**88.898**
------	--------	-------	69.96	69.364	-0.852	0.0001	2x10^{-5}	78.136
CO_2 + ethyl laurate, T=308.15 K, τ_{12}=3.358, τ_{21}=-0.808, k_{12}=0.817, 8 Points Result (*NFC), $\%\Delta P_{av}$=0.6112, $\%\Delta y_{2av}$=93.33%, $\%\Delta A_{av}$=2869.								
A_p	A_ϕ	$\%\Delta A_i$	P^{exp}	P^{cal}	$\%\Delta P$	$y_2^{\exp}$	y_2^{cal}	$\%\Delta y_{2i}$
7070.5	**3.6x105**	**5012.6**	**14.8**	**14.857**	**0.382**	**0.0001**	**1x10^{-6}**	**-98.2**
2178.8	**1.1x105**	**4751.7**	**28.59**	**28.162**	**-1.49**	**0.0001**	**2x10^{-6}**	**-97.9**
1783.6	**58614**	**3186.3**	**35.49**	**35.804**	**0.883**	**0.0001**	**2x10^{-6}**	**-97.3**
1514.1	**34126**	**2153.8**	**42.38**	**42.683**	**0.714**	**0.0001**	**3x10^{-6}**	**-96.4**
1312.4	**21502**	**1538.4**	**49.28**	**49.156**	**-0.25**	**0.0001**	**5x10^{-6}**	**-94.9**
-------	--------	--------	56.17	56.007	-0.29	0.0001	7x10^{-6}	-92.1
CO_2 + ethyl laurate, T=308.15 K, τ_{12}=3.581, τ_{21}=-0.805, k_{12}=0.809, 6 Points Result (**NFC), $\%\Delta P_{av}$= 0.67, $\%\Delta y_{2av}$= 96.16%, $\%\Delta A_{av}$= 3328.6.								

*NFC: Not fully consistent

Deviations in individual areas, pressure and the vapor phase solute concentration for this mixture at 308.15K are given in Fig. 6.7. Here, it is observed that the deviation in the areas for the initial data set was exceeded in 50%. These results come from the fact that ethyl laurate vapor phase concentration is close to 1. This fact made the term A_p from the integral in eqn. (9), and A_ϕ from the integral in eqn. (10) bigger as 7070.5 and 3.7x10^5, respectively (see Table 6.5). As a result, ΔA_i defined by the eqn. (26) turns bigger as the single terms turn equally bigger, obtaining results NFC. On the other hand, Figs. 6.7b, 6.7c show the deviations in the individual pressure and the vapor phase solute concentration. Complete consistency results for all systems studied are shown in Table 6.6.

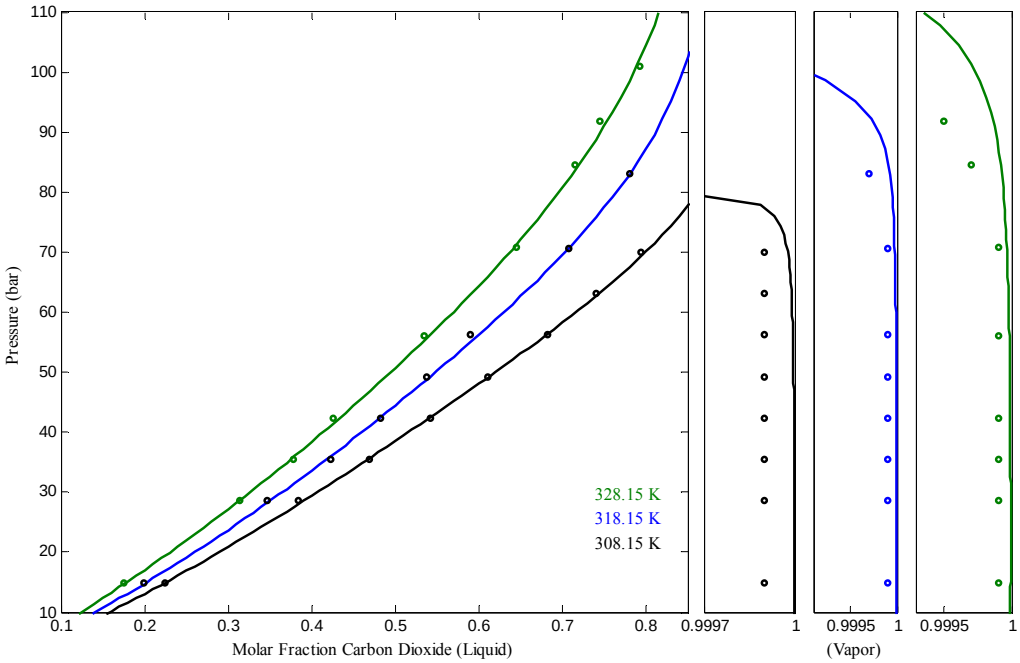

Fig. 6.6 Experimental and predicted VLE for carbon dioxide + ethyl laurate binary system. Experimental data were taken from Cheng et al. [49].

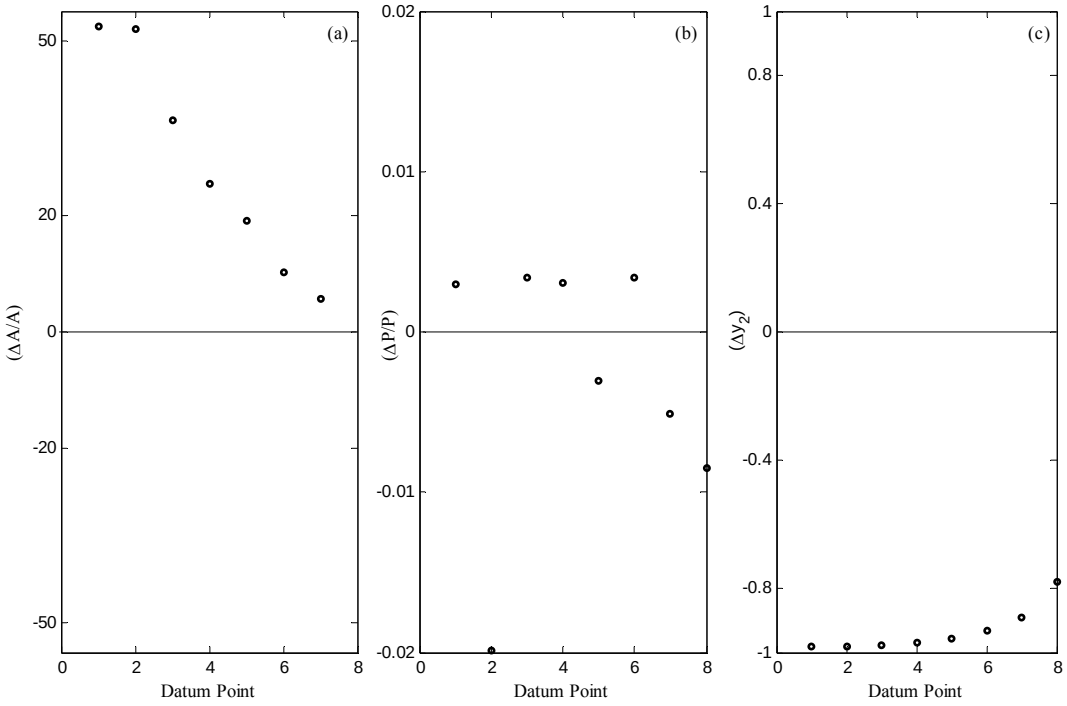

Fig. 6.7 Deviations in the individual areas for the carbon dioxide + ethyl laurate binary system at 308.15K. Experimental data were taken from Cheng et al. [49].

Experimental data for carbon dioxide + *n*-hexane system at 298.15 K and 313.15 K have been found thermodynamically inconsistent (TI). Some difficulties were found when a consistency test decision rules proposed by Valderrama and Alvarez [23] were applied. In this particular system, the initial data set was composed by 10 data points and the 25% of them with $\%\Delta A_i$ outside of the criterion range is 2.5 points. This last value is an integer number and had to be rounded to 2 or 3 points to apply the test again

for the remaining data set. Here the decision about TC, TI or NFC of the experimental data depends highly on this number.

Consequently, the reported decision rules [23] did not include a proper way to choice the suitable number of data that must be eliminated from the initial data set, suggesting that the points with the highest deviation in the vapor phase concentration must be eliminated as the best choice. After this, the method should be implemented again. However, in the systems studied, the above referred procedure was unsuitable to be used because the VLE parameters calculations were highly dependent on bubble pressure calculation. It becomes more convenient to eliminate the data points, and therefore yielded highest deviations in pressure. For example, the remaining 9 points of the initial data set of carbon dioxide + ethane at 230 K system were found to be TC according to the defined error ranges proposed by the authors [23]. Furthermore, to obtain this result, the points with the highest deviation in bubble pressure from the initial data set were necessarily eliminated. Additionally, the points with highest deviation of Δy_2 were eliminated from the initial data set and the consistency test was employed again using the remaining 13 points. The deviations in the obtained vapor phase solute concentration were not within the range (−20% to +20%). Therefore, TDM was the result of the test. Although the consistency test requires a high accuracy on the prediction of vapor phase solute concentration, for integral calculations in eqn. (8) is preferable to eliminate several points with the highest deviations in bubble point pressure from initial data set before applying the test again. Thus, the parameters obtained fitted better the remaining experimental data set when points with the highest deviations in bubble point pressure were eliminated. On the other hand, the y_2 deviations for asymmetric mixtures are usually high and commonly not reported in literature [2, 27-28, 53].

According to the decision rules proposed by the authors [23], 6 points is the minimum experimental data from initial data set considered to apply the consistency test. For example, the initial data set of carbon dioxide + ethanol at 314.50 K was found to be TC. Thus, the initial data set was composed by 6 data points and if one point from the initial data set would not considered, the thermodynamic test could not be applied and only one result could be obtained. Certainly, the thermodynamic consistency results and statistical analysis are improved when the availability of experimental data is big. In some cases, for example systems such as carbon dioxide + ethyl laurate at 308.15 K and 318.15 K, carbon dioxide + ethyl caproate at 308.20 K, the initial data set were considered NFC. As a result, two points from the initial data set were not considered, and the thermodynamic consistency test was applied again for the remaining 6 data points. Similar results were obtained. Therefore, the thermodynamic test cannot be applied again because the remaining data set was lees of six points. Additionally, the parameters obtained by the minimization using the current data set were very similar to those calculated from the initial data set, and the thermodynamic consistency results were identical in both cases. On the other hand, experimental data for systems such as carbon dioxide + octanol at 453.15 K, and carbon dioxide + ethanol at 337.20 K, were found to be TI. As a result, two points with the lowest deviation in pressure from the initial data set were not considered, and this last set was again analyzed and found as TC.

Table 6.6 Summary of the final results for all non-polar and polar asymmetric binary mixtures containing carbon dioxide

Non-polar systems				Polar Systems			
CO_2+	T (K)	np	Final result	CO_2+	*T* (K)	np	Final result
Propane	230.00	25	NFC	Isoamyl acetate	308.15	7	NFC
		22	NFC			6	NFC
		19	NFC		318.15	8	NFC
	270.00	27	NFC			6	NFC
		20	NFC		328.15	9	NFC
						6	NFC
n-Pentane	310.15	12	NFC	Ethyl caproate	308.20	8	NFC
		9	NFC			6	NFC
	333.15	13	TI		318.20	10	NFC
		10	TC			7	NFC
	363.15	16	NFC		328.20	12	NFC
		12	NFC			9	NFC
Benzene	298.15	8	TI	Butanol	325.30	9	TI
		6	TI			8	TC
	313.15	9	TC		337.20	11	TC
Styrene	333.15	9	NFC	Decanal	288.20	10	NFC
		6	NFC			7	NFC
	343.15	10	NFC		303.20	11	NFC
		7	NFC			8	NFC
	348.15	8	NFC		313.20	12	NFC
		6	NFC			8	NFC

n-Decane	344.30	22	NFC	Ethanol	314.50	6	TC
		17	NFC		325.20	9	TC
	377.60	26	NFC		337.20	8	TI
		19	NFC			6	TC
n-Hexane	298.15	10	NFC	Octanol	403.15	9	TI
		7	TI			8	TC
	313.15	10	NFC		453.15	7	TI
		7	TI			6	TC
Ethane	210.00	17	NFC	Methanol	291.15	11	NFC
		13	NFC			8	NFC
		10	NFC		298.15	8	NFC
	230.00	16	TI			6	TI
		13	TC		303.18	16	TI
	250.00	20	TI			12	TI
		16	TI		308.15	16	TI
	270.00	6	TC			12	TI
n-Heptane	310.65	23	NFC	Ethyl laurate	308.15	8	NFC
		18	NFC			6	NFC
	352.59	17	NFC		318.15	8	NFC
		13	TI			6	NFC
		11	TI		328.15	9	NFC
	394.26	15	NFC			6	NFC
		13	NFC				
Limonene	313.18	8	TDM	Heptanol	374.63	8	TI
	323.25	11	TDM			6	NFC
					298.15	8	NFC
						6	NFC

The consistency test proposed by the authors [23], do not take into account the cases when data sets of vapor phase concentration is close to 1 (i.e. 0.9998-0.9999). This fact made big the terms A_p and A_ϕ, and as a result, ΔA_i turns bigger than the single terms, obtaining results NFC. In this way, experimental data set for systems such as carbon dioxide + isoamyl acetate, carbon dioxide + ethyl caproate, carbon dioxide + decanal and carbon dioxide + ethyl laurate, were considered NFC. In the same way, for example, experimental data set for carbon dioxide + limonene at 313.18 K and 323.25 K, were considered as TDM.

According to the consistency test proposed by Valderrama [23], it is important to remark the necessity for carrying out several minimizations procedures looking for new parameters that allow calculating the right hand side in the eqn. (8). In the same way, the set of parameters fitted in each minimization, depend strongly of the objective function used. According to that, the computing time requirements can be increased considerably [27].

6.7 Conclusions

In this work, thermodynamic consistency test of nine non-polar and nine polar asymmetric binary mixtures at high pressure were analyzed. Additionally, the ability of Peng-Robinson EoS coupled with the Wong–Sandler mixing rules and the NRTL model for representing fluid phase equilibrium within the thermodynamic test was demonstrated. Results of bubble point pressure, vapor phase concentration and the individual areas of relative percentage deviations, have demonstrated the capability and efficiency of the objective function used for minimizing VLE experimental data at high pressures. Finally the studied method gives an answer about consistency or inconsistency of a set of experimental *P–T–x–y* data for the studied cases. A method to test the thermodynamic consistency of incomplete high-pressure VLE data in binary mixtures has been proved showing favorable results.

In some cases, the high asymmetry of these mixtures, is reflected in the way that the vapor phase concentration is close to 1, as a result of this, the left hand side of the eqn. (8) turns bigger than the other single terms, obtained as a result of the NFC test. Some difficulties with the experimental data set were analyzed and taken into account: 1. If the asymmetry of these mixtures makes grow the vapor phase concentration closer to 1, the left hand of the eqn. (8) turns into a big value. 2. The points which must be removed from the remaining experimental data set, with the aim of reduce the deviations for each *i*-point in bubble point pressure and vapor phase composition. Therefore some examples and strategies for solving these problems were discussed in detailed of the present work. In the same way, the calculations of the VLE parameters for asymmetric mixtures at high pressures were highly dependent on bubble pressure calculation, making more convenient to eliminate the data points yielding the highest deviations in pressure. Finally the results obtained using the thermodynamic consistency test is a necessary, but no sufficient, condition for accepting the experimental data set.

References

[1] R. Dohrn and G. Brunner. High-pressure fluid phase equilibria: experimental methods and Systems investigated (1988-1993). Fluid Phase Equilib. 106 (1995) 213-282.
[2] J.A. López, C.A. Cardona, Phase equilibrium calculations for carbon dioxide + *n*-alkanes binary mixtures with the Wong–Sandler mixing rules, Fluid Phase Equilib. 239 (2006) 206–212.
[3] J. Schwartzentruber, H. Renon, Extension of UNIFAC to high pressures and temperatures by use of a cubic equation of state, Ind. Eng. Chem. Res. 28 (1989) 1049–1055.
[4] S.K. Shibata, S.I. Sandler, Critical evaluation of equation of state mixing rules for the prediction of high-pressure phase equilibria, Ind. Eng. Chem. Res. 28 (1989) 1893–1898.
[5] S. Dahl, M.L. Michelsen, A high-pressure vapor–liquid equilibrium with a UNIFAC based equation of state, AIChE J. 36 (1990) 1829–1836.
[6] C.H. Twu, J.E. Coon, D. Bluck, Comparison of the Peng–Robinson and Soave–Redlich–Kwong equations of state using a new zero-pressure-based mixing rule for the prediction of high-pressure and high-temperature phase equilibria, Ind. Eng. Chem. Res. 37 (1998) 1580–1585.
[7] H. Orbey, S.I. Sandler, D.S.H.Wong, Accurate equation of state predictions at high temperatures and pressures using the existing UNIFAC model, Fluid Phase Equilib. 85 (1993) 41–54.
[8] H. Huang, S.I. Sandler, Prediction of vapor–liquid equilibria at high pressures using activity coefficient parameter obtained from low-pressure data: a comparison of two equations of state mixing rules, Ind. Eng. Chem. Res. 32 (1993) 1498–1503.
[9] H. Orbey, C. Balci, G.A. Gürüz, Phase equilibrium of asymmetric systems by predictive equations of state models, Ind. Eng. Chem. Res. 41 (2002) 963–967.
[10] T. Yang, G.J. Chen, W. Yan and T.M. Guo, Extension of the Wong–Sandler mixing rule to the three parameter Patel–Teja equation of state: application up to the near-critical region, Chem. Eng. J. 67 (1997) 26–36.
[11] K. Tochigi, T. Iizumi, H. Sekikawa, K. Kurihara and K. Kojima, High-pressure vapor–liquid and solid–gas equilibria using a Peng–Robinson group contribution method, Ind. Eng. Chem. Res. 37 (1998) 3731–3740.
[12] S. Malanowski, A. Anderko. Modelling phase equilibria: Thermodynamic background and practical tools, John Wiley and Sons, Inc., Canada, 1992.
[13] J. Wisniak, A New Test for the Thermodynamic Consistency of Vapor-Liquid Equilibrium, Ind. Eng. Chem. Res. 32 (1993) 1531-1533.
[14] L.C. Tao, New methods of testing thermodynamic consistency of isobaric, multicomponent vapor-liquid equilibrium data, Ind. Eng. Chem. Fundam. 8 (1969) 133-137.
[15] K. Kurihara, Y. Egawa, S. Iino, K. Ochi, K. Kojima, Evaluation of thermodynamic consistency of isobaric and isothermal binary vapor–liquid equilibrium data using the PAI test. Fluid Phase Equilib. 219 (2004) 75–85.
[16] K. Kurihara, Y. Egawa, S. Iino, K. Ochi, K. Kojima, Evaluation of thermodynamic consistency of isobaric and isothermal binary vapor–liquid equilibrium data using the PAI test II, alcohol + *n*-alkane, + aromatic, + cycloalkane systems, Fluid Phase Equilib. 257 (2007) 151–162.
[17] O. Redlich, and A.T. Kister, Algebraic representation of thermodynamic properties and the classification of solutions, Ind. Eng. Chem. Res. 40 (1948) 345-348.
[18] P.L. Chueh, N.K. Muirbrook, J. M. Prausnitz, Part II thermodynamic analysis, AIChE J. 11 (1965) 1097–1102.
[19] K.W. Won, J.M. Prausnitz, High-Pressure vapor–liquid equilibria. Calculation of partial pressures from total pressure data. Thermodynamic consistency, Ind. Eng. Chem. Fundam. 12 (4) (1973) 459–463.
[20] L.J. Christiansen, A. Fredenslund, Thermodynamic consistency using orthogonal collocation or computation of equilibrium vapor compositions at high-pressures, AIChE J. 21 (1975) 49–57.
[21] A. Bertucco, M. Barolo, N. Elvassore, Thermodynamic consistency of vapor–liquid equilibrium data at high-pressure, AIChE J. 43 (1997) 547–554.
[22] P.L. Jackson, R.A. Wilsak, Thermodynamic consistency tests based on the Gibbs–Duhem equation applied to isothermal, binary vapor–liquid equilibrium data: data evaluation and model testing, Fluid Phase Equilb. 103 (1995) 155–197.
[23] J.O. Valderrama, V.H. Alvarez, A versatile thermodynamic consistency test for incomplete phase equilibrium data of high-pressure gas–liquid mixtures, Fluid Phase Equilib. 226 (2004) 149–159.
[24] D.Y. Peng, D.B. Robinson, A new two constant equation of state, Ind. Eng. Chem. Fundam. 15 (1976) 59–64.
[25] D.S.H. Wong, S.I. Sandler, Theoretically correct mixing rule for cubic equations of state, AIChE J. 38 (1992) 671–680.

[26] H. Renon, J.M. Prausnitz, Local compositions in thermodynamic excess functions for liquid mixtures, AIChE J. 14 (1967) 135–144.
[27] J.A. López, V.M. Trejos, C.A. Cardona, Objective functions analysis in the minimization of binary VLE data for asymmetric mixtures at high pressures, Fluid Phase Equilibria 248 (2006) 147–157.
[28] J.A. López, V.M. Trejos, C.A. Cardona, Parameters Estimation and VLE Calculation in Asymmetric Binary Mixtures Containing Carbon Dioxide + *n*-Alkanols, Fluid Phase Equilibria 275 (2008) 1-7.
[29] J.M. Smith, M.M. Abbott, H.C. Van Ness, Introduction to Chemical Engineering Thermodynamics, fifth, McGraw-Hill, New York, USA, 2001.
[30] Z. Knez, M. Habulin, Compressed gases as alternative enzymatic reaction solvent. A short review, J. Supercrit. Fluids 23 (2002) 29–42.
[31] M. Christov, R. Dohrn, Review High-pressure fluid phase equilibria Experimental methods and systems investigated (1994–1999), Fluid Phase Equilib. 202 (2002) 153–218.
[32] W.H. Hauthal, Advances with supercritical fluids [review], Chemosphere 43 (2001) 123-135.
[33] M.S.W. Wei, T.S. Brown, A.J. Kidnay, E.D. Sloan, Vapor + liquid equilibria for the ternary system methane + ethane + carbon dioxide at 230K and its constituent binaries at temperatures from 207 to 270 K, J. Chem. Eng. Data 40 (1995) 726–731.
[34] L.A. Webster, A.J. Kidnay, Vapor–liquid equilibria for the methane–propane–carbon dioxide systems at 230 and 270 K, J. Chem. Eng. Data 46 (2001) 759–764.
[35] K. Tochigi, K. Hasegawa, N. Asano, K. Kojima, Vapor–liquid equilibria for the carbon dioxide + pentane and carbon dioxide + toluene systems, J. Chem. Eng. Data 43 (1998) 954–956.
[36] K. Ohgaki, T. Katayama, Isothermal vapor–liquid equilibrium data for binary systems containing carbon dioxide at high pressures: methanol– carbon dioxide, *n*-hexane–carbon dioxide, and benzene–carbon dioxide systems, J. Chem. Eng. Data 21 (1976) 53–55.
[37] H. Kaira, H. Kubota, D.B. Robinson, H.-J. Ng, Equilibrium phase properties of the carbon dioxide–n-heptane system, J. Chem. Eng. Data 23 (1978) 317–321.
[38] N. Nagarajan, R.L. Robinson, Equilibrium phase compositions, phase densities, and interfacial tensions for CO_2 + hydrocarbon systems. CO_2 + *n*-decane, J. Chem. Eng. Data 31 (1986) 168–171.
[39] M. Akgün, D. Emel, N. Baran, N.A. Akgûn, S. Deniz, S. Dincer, Styrene–carbon dioxide phase equilibria at high pressures, J. Supercrit. Fluids 31 (2004) 27–32.
[40] C.M. Chang, C.C. Chen, High-pressure densities and *P–T–x–y* diagrams for carbon dioxide + linalool and carbon dioxide + limonene, Fluid Phase Equil. 163 (1999) 119–126.
[41] C.J. Chiehming, C.K. Lung, D.C. Yih, A new apparatus for the determination of *P–x–y* diagrams and Henry's constants in high pressure alcohols with critical carbon dioxide, Journal of Supercritical Fluids 12 (1998) 223–237.
[42] L.C. Feng, K.W. Cheng, M. Tang, Y.P. Chen, Vapor–liquid equilibria of carbon dioxide with ethyl benzoate, diethyl succinate and isoamyl acetate binary mixtures at elevated pressures, J. Supercrit. Fluids 21 (2001) 111–121.
[43] D.W. Jennings, R. Lee, A.S. Teja, Vapor–liquid equilibria in the carbon dioxide + ethanol and carbon dioxide + l-butanol systems, J. Chem. Eng. Data 36 (1991) 303–307.
[44] O.E. Solis, L.A.G. Luna, S.I. Sandler, J.G.S. Hernández, Vapor–liquid equilibria and critical points of the CO_2 + 1-hexanol and CO_2 + 1-heptanol systems, Fluid Phase Equilibria 210 (2003) 215–227.
[45] C. Secuianu, V. Feroiu, D. Geana, Investigation of phase equilibria in the ternary system carbon dioxide + 1-heptanol + *n*-pentadecane, Fluid Phase Equilibria 261 (2007) 337–342.
[46] W.L. Weng, J.T. Chen and M.J. Lee. High-pressure Vapor-Liquid Equilibria for Mixtures Containing a Supercritical Fluid. Ind. Eng. Chem. Res. 33 (1994) 1955-1961.
[47] W.H. Hwu, J.S. Cheng, K.W. Cheng, Y.P. Chen, Vapor–liquid equilibrium of carbon dioxide with ethyl caproate, ethyl caprylate and ethyl caproate at elevated pressures, J. Supercrit. Fluids 28 (2004) 1-9.
[48] M. V. Silva, D. Barbosa, P.O. Ferreira, High pressure vapor–liquid equilibrium data for the system carbon dioxide + decanal at 288.2, 303.2, and 313 2K, J. Chem. Eng. Data 47 (2002) 1171–1172.
[49] K.W. Cheng, M. Tang, Y.P. Chen, Vapor–liquid equilibria of carbon dioxide with diethyl oxalate, ethyl laurate, and dibutyl phthalate binary mixtures at elevated pressures, Fluid Phase Equilib. 181 (2001) 1–16.
[50] J.O. Valderrama, The state of the cubic equations of state, Ind. Eng. Chem. Research. 42 (2003) 1603–1618.

List of captions

Figures

Fig. 2.1. (a). *P*-*T* phase diagram of a one-component fluid, with the vapor pressure curve and critical point. (b). Same diagram in *P*-*V* space coexistence curve and several isotherms. (c). Same diagram in *T*-*V* space coexistence curve and several isobar. The cross-hatched region is considered supercritical.
Fig. 2.2 Esquematic of supercritical extraction. P-Compressor, E- extraction vessel; Se-Separation vessel, V- expanssion valve; Sc- heat exchanger, G-ant-isolvent supply, G/SC-separator of anti-solvent and SCF; M- mixing port [73].
Fig. 2.3 Carbon dioxide temperature-pressure phase diagram showing the triple point and critical point of carbon dioxide. Experimental data taken from Span and Wagner [76] and Angus et al. [77].
Fig. 2.4 The *P*-*V* diagram and isotherms of pure carbon dioxide. Experimental data taken from Span and Wagner [76].
Fig. 2.5. The T-*V* diagram and isobars of pure Carbon Dioxide. Experimental data taken from Span and Wagner [91].
Fig. 2.6 The vapor pressure curves of pure carbon dioxide. Experimental data taken from Span and Wagner [76].

Fig. 3.1 Experimental and predicted VLE for CO_2 + limonene binary system. Comparison of accuracy of two objective functions. Experimental data taken from Iwai et al. [61].
Fig. 3.2 Experimental and predicted VLE for CO_2 + propane binary system. Comparison of accuracy of two objective functions. Experimental data taken from Webster and Kidnay [54].
Fig. 3.3 Experimental and predicted VLE for CO_2 + pentane binary system. Comparison of accuracy of two objective functions. Experimental data taken from Tochigi et al. [55].
Fig. 3.4 Experimental and predicted VLE for CO_2 + octane binary system. Comparison of accuracy of two objective functions (OF 2 and OF 5, identical predictions). Experimental data taken from Weng and Lee [58]. Prediction with PR EOS coupled with the WS mixing rules.
Fig. 3.5 Experimental and predicted VLE for CO_2 + ethyl caproate binary system. Comparison of accuracy of two objective functions. Experimental data taken from Hwu et al. [67].
Fig. 3.6 Experimental and predicted VLE for CO_2 + ethyl laurate binary system. Experimental data taken from Cheng et al. [69]. Parameters obtained from OF 2.
Fig. 3.7 Experimental and predicted VLE for carbon dioxide + 1-heptanol binary system. Experimental data taken from Elizalde-Solis et al. [64]. Parameters obtained from OF 3.
Fig. 3.8 Experimental and predicted VLE for CO_2 + linalool binary system. Comparison of accuracy of two objective functions. Experimental data taken from Iwai et al. [70].
Fig. 3.9. Experimental and predicted VLE for CO_2 + decanal binary system. Comparison of accuracy of two objective functions. Experimental data taken fromVázquez da Silva et al. [68].

Fig. 3.10 Deviations between experimental points and calculated values of *y* and *P* for CO_2 + *n*-pentane at 363.15 K. Parameters obtained from: ▽, OF 1; +, OF 2; ●, OF 3; □, OF 4; ○, OF 5.

Fig. 4.1 VLE correlation of the CO_2 + propane system by MHV1 and HVO mixing rules. Experimental data were taken from Webster and Kidnay [21].
Fig. 4.2 VLE correlation of the CO_2 + methane system by WS and MHV2 mixing rules. Experimental data were taken from Wei *et al*. [20].
Fig. 4.3 VLE correlation of the CO_2 + methanol system by WS and HVOS mixing rules. Experimental data were taken from Ohgaki and Katayama [22] and Chiehming *et al*. [23].
Fig. 4 .4 VLE correlation of the CO_2 + ethane system by WS MHV1 and MHV2 mixing rules. Experimental data were taken from Wei *et al*. [20].
Fig. 4.5 Deviations between experimental points and calculated values of *y* and *P* for CO_2 + methanol at 298.16K. Parameters obtained from: ▽, HVO; +, MHV1; ●, MHV2; □, WS; ○, HVOS

Fig. 5.1 Experimental and predicted VLE for carbon dioxide + methane binary system. Experimental data were taken from Wei *et al*. [24].
Fig. 5.2 Experimental and predicted VLE for carbon dioxide + ethane binary system. Experimental data were taken from Wei *et al*. [24].
Fig. 5.3 Experimental and predicted VLE for carbon dioxide + heptane binary system. Experimental data were taken from Kaira *et al*. [29].
Fig. 5.4 Experimental and predicted VLE for carbon dioxide + methanol binary system. Experimental data were taken from Ohgaki and Katayama [33] and Chiehming *et al*. [34].
Fig. 5.5 Experimental and predicted VLE for carbon dioxide + 1–butanol binary system. Experimental data were taken from Secuianu *et al*. [37] and Jennings *et al*. [9].
Fig. 5.6 Experimental and predicted VLE for carbon dioxide + 1–hexanol binary system. Experimental data were taken from Solis *et al*. [39].
Fig. 5.7 Experimental and predicted VLE for carbon dioxide + 1–octanol binary system. Experimental data were taken from Chiehming *et al*. [34].
Fig. 5.8 Experimental and predicted VLE for carbon dioxide + 1–decanol binary system. Experimental data were taken from Chiehming *et al*. [34].

Fig. 6.1 Experimental and predicted VLE for carbon dioxide + ethane binary system. Experimental data were taken from Wei *et al*. [33].
Fig. 6.2 Deviations in the individual areas for carbon dioxide + ethane binary system at 230K. Experimental data were taken from Wei *et al*. [33].
Fig. 6.3 Experimental and predicted VLE for carbon dioxide + 1-octanol binary system. Experimental data taken from Weng *et al.* [48]. Prediction with Peng-Robinson EOS coupled with the WS mixing rules.
Fig. 6.4 Deviations in the individual areas for the carbon dioxide + 1-octanol binary system at 403.15 K. Experimental data were taken from Weng *et al.* [48].
Fig. 6.5 Integral functions in Eq. (8) for the carbon dioxide + 1-octanol binary system at 403.15 K. Experimental data were taken from Weng *et al.* [48].

Fig. 6.6 Experimental and predicted VLE for carbon dioxide + ethyl laurate binary system. Experimental data were taken from Cheng et al. [52].
Fig. 6.7 Deviations in the individual areas for the carbon dioxide + ethyl laurate binary system at 308.15K. Experimental data were taken from Cheng et al. [52].

Tables

Table 3.1 Experimental conditions for non-polar asymmetric binary mixtures.
Table 3.2 Experimental conditions for polar asymmetric binary mixtures.
Table 3.3 Average deviations in the VLE prediction of the parameters obtained from each objective functions for both non-polar and polar binary systems.

Table 4.1. Combination of equation of state with excess free energy models, (EOS-G^{ex}), matching conditions
Table 4.2 Experimental conditions for asymmetric binary mixtures containing CO_2.
Table 4.3 Optimal parameters and deviations values for asymmetric mixtures using EOS-G^{ex} mixing rules
Table 4.4 Average deviations in the VLE prediction of the parameters obtained from each mixing rules for asymmetric systems.

Table 5.1 Properties of pure substances for *n*-akanols and *n*-alkanes
Table 5.2 Optimal parameters obtained from optimization and deviations between calculated and experimental values for *n*-alkanes.
Table 5.3 Optimal parameters obtained from optimization and deviations between calculated and experimental values for *n*-alkanols.
Table 5.4 Coefficients c_1- c_6 for each interaction parameter represent for Eq. (15)

Table 6.1 Experimental conditions for non-polar asymmetric binary mixtures
Table 6.2 Experimental conditions for polar asymmetric binary mixtures
Table 6.3 Detailed results for the system carbon dioxide + ethane at 230 K found to be thermodynamically consistent (TC) using PR+WS/NRTL model
Table 6.4 Detailed results for the system carbon dioxide + 1-octanol at 403.15K found to be thermodynamically consistent (TC) using PR+WS/NRTL model
Table 6.5 Detailed results for the system carbon dioxide + ethyl laurate at 308.15 K found to be not fully consistent (NFC) using PR+WS/NRTL model
Table 6.6 Summary of the final results for all non-polar and polar asymmetric binary mixtures containing carbon dioxide

APPENDIX A

OPTIMAL PARAMETERS AND DEVIATIONS

Table 1. Optimal parameters and deviations obtained from minimization of each objective function. Non-polar asymmetric binary mixtures.

	Carbon dioxide + Methane (230 K)					Carbon dioxide + Methane (250 K)				
OF	τ_{12}	τ_{21}	k_{12}	ΔP	Δy	τ_{12}	τ_{21}	k_{12}	ΔP	Δy
f_1	n.a.	n.a.	n.a.	n.a.	n.a.	n.a.	n.a.	n.a.	n.a.	n.a.
f_2	0.9231	0.7099	0.1563	1.1070	0.0029	1.0580	0.4165	0.1428	0.6750	0.0046
f_3	0.9503	0.8522	0.1208	1.1881	0.0084	0.9291	0.8409	0.0899	1.3067	0.0122
f_4	0.9329	0.8553	0.1225	1.1231	0.0078	0.9826	0.8519	0.1107	2.6093	0.0161
f_5	0.9543	0.8428	0.1385	1.6859	0.0084	0.8984	0.8602	0.0996	1.3132	0.0113
	Carbon dioxide + Methane (270 K)					Carbon dioxide + Propane (230 K)				
f_1	n.a.	n.a.	n.a.	n.a.	n.a.	0.9685	0.1057	0.5207	9.2611	0.0389
f_2	0.9347	0.0846	0.2039	0.7432	0.0092	4.3311	1.3291	0.0169	1.5120	0.0213
f_3	0.0089	1.8986	0.1262	0.7186	0.0054	3.2663	0.7848	0.1098	5.1561	0.0306
f_4	0.0072	1.8987	0.1393	0.9864	0.0039	3.5644	1.4472	0.2576	22.8445	0.0329
f_5	0.0100	1.9000	0.1357	0.8962	0.0042	3.5028	0.8678	0.1816	3.6790	0.0165
	Carbon dioxide + Propane (270 K)					Carbon dioxide + *n*-Pentane (310.15 K)				
f_1	2.8232	-0.5610	0.2964	4.8409	0.0243	1.2178	0.4877	0.4654	4.9428	0.0058
f_2	2.4946	0.2091	0.1908	0.4002	0.0112	0.2957	0.9251	0.5603	2.9072	0.0110
f_3	1.9999	0.1791	0.2445	0.4432	0.0081	1.6536	0.0601	0.5129	2.5907	0.0078
f_4	2.8092	0.3984	-0.0326	7.8272	0.0345	1.3045	0.4152	0.5385	4.7811	0.0101
f_5	1.8959	-0.2978	0.2802	5.4351	0.0223	1.4812	0.1455	0.5170	2.4947	0.0080
	Carbon dioxide + *n*-Pentane (333.15 K)					Carbon dioxide + *n*-Pentane (363.15 K)				
f_1	1.1840	0.2327	0.4978	2.4231	0.0096	1.1471	0.0855	0.5214	1.5926	0.0115
f_2	1.0449	0.2109	0.5287	1.2980	0.0137	0.3094	0.6142	0.5597	2.7394	0.0250
f_3	2.2578	-0.2436	0.4963	1.9966	0.0064	1.1818	0.0603	0.5282	1.4261	0.0126
f_4	1.4816	0.1494	0.4885	3.1560	0.0068	1.1480	0.0827	0.5403	1.9755	0.0152
f_5	2.4919	-0.4043	0.5025	2.6703	0.0091	3.0600	-0.5589	0.4859	2.7869	0.0106
	Carbon dioxide + *n*-Hexane (298.15 K)					Carbon dioxide + *n*-Hexane (313.15 K)				
f_1	2.6804	0.0551	0.4316	5.5960	0.0023	-0.2086	1.3930	0.5283	7.0402	0.0035
f_2	1.5917	0.0557	0.5676	2.5149	0.0053	1.4805	-0.0728	0.5449	1.8079	0.0044
f_3	2.1977	-0.0959	0.5354	2.2323	0.0046	1.7766	-0.1732	0.5345	1.7432	0.0044
f_4	2.6002	0.0189	0.3503	15.2695	0.0007	1.7667	-0.1722	0.5030	4.4108	0.0036
f_5	2.2502	-0.0935	0.5329	2.2134	0.0045	2.0217	-0.2191	0.5230	1.7282	0.0045
	Carbon dioxide + *n*-Heptane (310.65 K)					Carbon dioxide + *n*-Heptane (352.59 K)				
f_1	3.2651	-0.5358	0.6677	8.7835	0.0087	2.7463	-0.6698	0.6425	5.0226	0.0078
f_2	3.8381	-0.3973	0.5774	2.0079	0.0095	2.8376	-0.6426	0.6095	1.0223	0.0103
f_3	3.7560	-0.4149	0.5831	1.8931	0.0094	2.7152	-0.6378	0.6155	0.7592	0.0096
f_4	2.7723	-0.4522	0.6566	5.8580	0.0081	2.8715	-0.6432	0.6026	1.6607	0.0109
f_5	3.7722	-0.4136	0.5816	1.9168	0.0095	2.7141	-0.6471	0.6145	0.8143	0.0097
	Carbon dioxide + *n*-Heptane (394.26 K)					Carbon dioxide + *n*-Octane (313.15 K)				
f_1	2.9334	-1.0642	0.6711	8.0907	0.0109	3.5540	-0.2443	0.7155	17.3215	0.0147
f_2	4.9407	-0.8718	0.5613	2.4930	0.0414	3.1397	-0.1264	0.6726	0.4398	0.0019
f_3	1.6291	-0.6214	0.6406	2.6516	0.0154	3.2246	-0.1291	0.6698	0.3778	0.0020
f_4	1.6348	-0.6037	0.6422	2.6233	0.0153	3.2209	-0.1752	0.6751	1.2423	0.0019
f_5	1.6332	-0.6041	0.6414	2.6291	0.0154	3.2618	-0.1305	0.6687	0.3623	0.0020

(Continued)

OF	τ_{12}	τ_{21}	k_{12}	ΔP	Δy	τ_{12}	τ_{21}	k_{12}	ΔP	Δy
	Carbon dioxide + *n*-Octane (328.15 K)					Carbon dioxide + *n*-Octane (348.15 K)				
f_1	4.6574	-0.3775	0.7134	33.6827	0.0191	3.5709	-0.3778	0.7069	12.2447	0.0096
f_2	3.8866	-0.2908	0.6512	1.0694	0.0047	3.5901	-0.3804	0.6641	1.0491	0.0078
f_3	3.8285	-0.2979	0.6520	0.8904	0.0046	3.5091	-0.3901	0.6682	0.9245	0.0072
f_4	3.8466	-0.3481	0.6531	1.6301	0.0044	3.5824	-0.3881	0.6664	1.0043	0.0077
f_5	3.8324	-0.2979	0.6541	1.0762	0.0046	2.8264	-0.3134	0.6839	1.1750	0.0051
	Carbon dioxide + *n*-Decane (344.30 K)					Carbon dioxide + *n*-Decane (377.60 K)				
f_1	1.3091	1.8841	0.7514	11.9594	0.0065	1.7132	0.7094	0.7687	3.8156	0.0149
f_2	4.3681	-0.4012	0.7321	0.3955	0.0105	3.7302	-0.7114	0.7521	0.5231	0.0064
f_3	1.3303	1.7550	0.7592	6.5327	0.0098	3.2951	-0.8412	0.7335	0.6671	0.9624
f_4	1.3079	1.8664	0.7511	7.1367	0.0107	3.3244	-0.8600	0.7333	0.6533	0.0095
f_5	1.4398	1.6485	0.7556	6.2568	0.0099	3.3279	-0.8554	0.7326	0.6586	0.0093
	Carbon dioxide + Benzene (298.15 K)					Carbon dioxide + Benzene (313.15 K)				
f_1	0.7277	0.2921	0.3831	6.5783	0.0006	1.7718	-0.3162	0.3696	4.8809	0.0016
f_2	1.2600	-0.2334	0.4547	1.0113	0.0013	2.7770	-0.6341	0.3816	1.0199	0.0011
f_3	1.2929	-0.2493	0.4537	1.0044	0.0012	1.7441	-0.4283	0.4279	1.5903	0.0026
f_4	0.7098	0.2500	0.3864	6.6045	0.0007	1.7298	-0.4285	0.3921	4.1354	0.0023
f_5	1.2840	-0.2454	0.4541	1.0057	0.0012	2.0791	-0.5393	0.4166	1.2940	0.0023
	Carbon dioxide + Styrene (333.15 K)					Carbon dioxide + Styrene (338.15 K)				
f_1	3.3829	-1.1976	0.5680	11.890	0.0226	1.3101	-0.5327	0.5686	2.4809	0.0017
f_2	1.6272	-0.7473	0.5675	1.5912	0.0025	1.4069	-0.4262	0.5694	0.9506	0.0047
f_3	1.7120	-0.7010	0.5633	1.5142	0.0019	1.6997	-0.6414	0.5664	1.2026	0.0018
f_4	1.6957	-0.6952	0.5527	2.3620	0.0010	1.6895	-0.6897	0.5645	1.7287	0.0017
f_5	1.7143	-0.6924	0.5636	1.5501	0.0019	1.7394	-0.6679	0.5660	1.2495	0.0018
	Carbon dioxide + Styrene (343.15 K)					Carbon dioxide + Styrene (348.15 K)				
f_1	3.9315	-1.3768	0.5676	17.3974	0.0249	3.0270	-1.1745	0.5775	1.1852	0.0120
f_2	0.8976	-0.2259	0.5830	2.2814	0.0063	0.3073	0.3707	0.5823	1.0783	0.0028
f_3	1.4976	-0.6354	0.5714	1.8610	0.0032	1.3257	-0.5103	0.5710	1.2507	0.0029
f_4	1.6698	-0.6799	0.5598	2.4776	0.0026	1.6599	-0.6700	0.5703	1.7530	0.0032
f_5	1.4918	-0.6332	0.5715	1.8755	0.0032	1.6549	-0.6774	0.5670	1.5669	0.0032
	Carbon dioxide + Limonene (313.20 K)					Carbon dioxide + Limonene (323.20 K)				
f_1	3.2233	-0.4286	0.6478	3.4899	0.0005	1.3927	8.1598	0.6934	9.6353	0.0014
f_2	1.3877	2.8917	0.7146	2.6556	0.0005	2.6576	-0.2289	0.6773	0.4877	0.0008
f_3	4.2029	-0.8194	0.6421	0.9746	0.0003	2.4918	-0.1682	0.6804	0.7661	0.0009
f_4	0.6934	-0.8370	0.6065	24.6656	0.0016	2.3973	-0.1948	0.6962	1.5435	0.0008
f_5	3.4295	-0.6431	0.6584	0.1373	0.0004	2.6632	-0.2281	0.6770	0.4836	0.0008
	Carbon dioxide + Limonene (333.20 K)									
f_1	1.4071	8.0690	0.7131	6.8599	0.0010					
f_2	2.5526	-0.3420	0.6777	0.4400	0.0005					
f_3	2.5269	-0.3355	0.6785	0.4609	0.0005					
f_4	0.0375	-0.0368	0.7771	32.2878	0.0021					
f_5	2.5555	-0.3442	0.6777	0.4327	0.0005					

[a] not available value.

Table 2. Optimal parameters and deviations obtained from minimization of each objective function. Polar asymmetric binary mixtures

	Carbon dioxide + *n*-Butanol (293.15 K)					Carbon dioxide + *n*-Butanol (303.15 K)				
OF	τ_{12}	τ_{21}	k_{12}	ΔP	Δy	τ_{12}	τ_{21}	k_{12}	ΔP	Δy
f_1	n.a.	n.a.	n.a.	n.a.	n.a.	n.a.	n.a.	n.a.	n.a.	n.a.
f_2	1.5861	0.1655	0.5787	0.8935	0.0073	1.0752	0.4405	0.5812	3.2506	0.0042
f_3	1.6729	0.1397	0.5734	0.8555	0.0073	1.4746	0.2519	0.5641	2.5683	0.0041
f_4	1.6432	0.1899	0.6043	7.5348	0.0074	1.4649	0.5133	0.5191	8.6025	0.0041
f_5	1.6738	0.1395	0.5733	0.8552	0.0073	1.3624	0.3026	0.5675	2.6377	0.0041
	Carbon dioxide + *n*- Butanol (314.80 K)					Carbon dioxide + *n*- Butanol (325.30 K)				
f_1	1.7155	0.0532	0.5626	8.6940	0.0098	2.0216	-0.1319	0.5418	10.4003	0.0300
f_2	1.9301	-0.0051	0.5273	0.0881	0.0008	1.8663	-0.0445	0.5244	0.1412	0.0012
f_3	1.9294	-0.0047	0.5274	0.0852	0.0008	1.8319	-0.0311	0.5257	0.1284	0.0011
f_4	1.9420	-0.0047	0.5223	1.0250	0.0007	1.9797	-0.0438	0.5114	1.4429	0.0019
f_5	1.9638	-0.0173	0.5257	0.0918	0.0008	1.8598	-0.0435	0.5247	0.1427	0.0012
	Carbon dioxide + *n*-Hexanol (431.82 K)					Carbon dioxide + *n*-Hexanol (432.45 K)				
f_1	0.1021	0.0894	0.6677	0.6395	0.0018	-0.8788	3.0671	0.6515	7.0524	0.0275
f_2	1.4259	-0.7219	0.6310	0.1367	0.0058	-0.5979	1.8222	0.6773	2.6389	0.0332
f_3	1.4617	-0.7317	0.6287	0.1347	0.0062	-0.6016	1.8206	0.6706	6.5588	0.0294
f_4	1.4452	-0.7259	0.6290	0.1370	0.0061	-0.5755	1.9225	0.6576	6.6885	0.0262
f_5	1.4433	-0.7298	0.6305	0.1329	0.0058	-0.5760	1.9222	0.6570	6.7287	0.0261
	Carbon dioxide + *n*-Nonanol (308.14 K)					Carbon dioxide + *n*-Nonanol (318.13 K)				
f_1	n.a.	n.a.	n.a.	n.a.	n.a.	n.a.	n.a.	n.a.	n.a.	n.a.
f_2	2.9503	-0.1062	0.7564	0.4157	0.0017	1.9111	-0.0169	0.7926	0.7922	0.0040
f_3	3.0110	-0.1069	0.7527	0.3109	0.0017	2.0028	-0.0371	0.7865	0.4139	0.0040
f_4	3.0583	-0.1090	0.7471	0.9204	0.0018	1.9987	-0.0336	0.8013	6.3893	0.0038
f_5	3.0481	-0.1088	0.7510	0.3211	0.0017	2.0237	-0.0440	0.7858	0.4060	0.0040
	Carbon dioxide + *n*-Nonanol (328.14 K)					Carbon dioxide + 1-Heptanol (374.63 K)				
f_1	n.a.	n.a.	n.a.	n.a.	n.a.	0.8849	-0.3711	0.7226	3.4060	0.0007
f_2	2.4344	-0.2631	0.7704	0.8896	0.0055	2.3674	-0.8955	0.6597	0.6572	0.0029
f_3	2.4985	-0.2663	0.7661	0.7065	0.0054	2.5686	-0.9301	0.6459	0.6186	0.0031
f_4	2.4867	-0.2644	0.7645	1.0750	0.0055	2.0090	-0.7395	0.6237	6.1403	0.0030
f_5	2.4864	-0.2641	0.7662	0.7013	0.0054	2.2968	-0.8824	0.6582	0.7144	0.0025
	Carbon dioxide + 1-Heptanol (431.54 K)					Carbon dioxide + Isoamyl acetate (308.15 K)				
f_1	0.7192	-0.7073	0.7364	8.5509	0.0027	5.0369	-0.9454	0.5748	7.1793	0.0005
f_2	3.9066	-1.0822	0.5106	2.0066	0.0459	1.9020	-0.7950	0.6370	1.2463	0.0007
f_3	1.7788	-0.9949	0.6449	0.6353	0.0131	1.7653	-0.7402	0.6395	1.1573	0.0006
f_4	0.9992	-0.9996	0.6517	10.6156	0.0069	1.7616	-0.8100	0.6000	8.8384	0.0006
f_5	1.8366	-1.0176	0.6436	0.6377	0.0132	1.7127	-0.7157	0.6401	1.2379	0.0006
	Carbon dioxide + Isoamyl acetate (318.15 K)					Carbon dioxide + Isoamyl acetate (328.15 K)				
f_1	2.2067	-0.8087	0.6844	15.3626	0.0041	3.0783	-1.0001	0.6832	22.2260	0.0065
f_2	2.0043	-0.7443	0.6283	0.7811	0.0007	2.1070	-0.8124	0.6257	0.9701	0.0013
f_3	2.4544	-0.8741	0.6184	1.0085	0.0008	2.6090	-0.9459	0.6146	1.5658	0.0014
f_4	1.7615	-0.8098	0.6024	9.2620	0.0007	1.7609	-0.8100	0.6019	8.5587	0.0011
f_5	2.4720	-0.8794	0.6181	1.0463	0.0008	2.4037	-0.8856	0.6182	1.0639	0.0013

(Continued)

	Carbon dioxide + Ethyl caproate (308.20 K)					Carbon dioxide + Ethyl caproate (318.20 K)				
OF	τ_{12}	τ_{21}	k_{12}	ΔP	Δy	τ_{12}	τ_{21}	k_{12}	ΔP	Δy
f_1	0.4213	8.4396	0.6341	9.5667	0.0001	-0.3727	1.4896	0.6220	10.3996	0.0003
f_2	1.7591	-0.8709	0.6502	0.8014	0.0003	1.6555	-0.7516	0.6569	1.3483	0.0004
f_3	1.9534	-0.9439	0.6471	0.8208	0.0003	2.1234	-0.9119	0.6479	1.0344	0.0003
f_4	1.7613	-0.8098	0.6020	8.1464	0.0003	1.7613	-0.8098	0.6020	10.8042	0.0003
f_5	2.0923	-0.9983	0.6453	0.9398	0.0003	2.4458	-1.0250	0.6433	1.1992	0.0003
	Carbon dioxide + Ethyl caproate (328.20 K)					Carbon dioxide + Decanal (288.20 K)				
f_1	-0.7055	1.7045	0.6407	7.4077	0.0005	n.a.	n.a.	n.a.	n.a.	n.a.
f_2	1.2842	-0.6342	0.6589	1.3482	0.0004	-0.2234	-0.5930	-0.7619	0.9137	0.0052
f_3	2.0602	-0.9647	0.6477	0.9749	0.0004	0.7944	-1.2777	-0.7168	0.8768	0.0052
f_4	1.7613	-0.8098	0.6020	9.4405	0.0004	1.8196	-1.6948	-0.4629	12.1508	0.0052
f_5	2.1343	-0.9937	0.6468	1.0405	0.0004	-1.6127	0.8944	-0.8243	1.1779	0.0052
	Carbon dioxide + Decanal (303.20 K)					Carbon dioxide + Decanal (313.20 K)				
f_1	0.6547	6.2089	-1.6845	n.a.	n.a.	-1.6337	0.2020	1.1287	n.a.	n.a.
f_2	-0.3870	-0.6353	-0.8042	0.8513	0.0042	-1.0785	0.9250	-1.0117	4.9734	0.0066
f_3	0.8309	-1.3790	-0.7558	1.3866	0.0042	0.9906	-1.3529	-0.8057	2.9873	0.0066
f_4	1.8196	-1.6951	-0.4631	19.9799	0.0041	1.8257	-1.7132	-0.6448	9.5582	0.0061
f_5	-0.8538	-0.2310	-0.8389	0.9832	0.0042	-0.5903	-0.2327	-0.8619	3.9869	0.0066
	Carbon dioxide + Ethyl laurate (308.15 K)					Carbon dioxide + Ethyl laurate (318.15 K)				
f_1	4.4475	-1.6424	0.6782	n.a.	n.a.	-3.2890	1.9588	1.2838	n.a.	n.a.
f_2	3.3581	-0.8088	0.8175	0.6112	0.0001	3.1643	-0.8583	0.8219	0.8511	0.0001
f_3	3.1934	-0.7836	0.8206	0.6136	0.0001	3.1799	-0.8555	0.8211	0.7627	0.0001
f_4	2.8229	-0.8713	0.8645	16.5831	0.0002	2.8244	-0.8699	0.9004	38.1695	0.0001
f_5	5.9610	-0.7735	0.7735	4.0380	0.0001	5.9378	-0.8272	0.7722	3.8081	0.0001
	Carbon dioxide + Ethyl laurate (328.15 K)					Carbon dioxide + Linalool (313.20 K)				
f_1	3.7104	-1.2227	0.7597	22.2162	0.0002	3.9931	-0.6832	0.6702	2.5222	0.0001
f_2	2.8508	-0.8386	0.8257	1.1437	0.0002	3.2507	-0.6839	0.6857	0.6512	0.0001
f_3	3.1090	-0.8866	0.8210	1.0955	0.0002	3.3055	-0.6904	0.6841	0.6448	0.0001
f_4	2.8229	-0.8713	0.8645	16.8960	0.0001	2.8228	-0.6712	0.6452	13.2394	0.0003
f_5	6.1805	-0.8513	0.7664	5.7884	0.0001	3.4382	-0.7192	0.6815	0.6950	0.0001
	Carbon dioxide + Linalool (323.20 K)									
f_1	9.2219	-0.1278	0.6499	n.a.	n.a.					
f_2	2.6831	-0.5911	0.6936	1.8436	0.0011					
f_3	3.4088	-0.7461	0.6774	1.5854	0.0003					
f_4	2.8229	-0.6713	0.6454	11.2993	0.0012					
f_5	3.4007	-0.7438	0.6775	1.5751	0.0003					

[a] not available value.

APPENDIX B

SUMMARY OF ALGEBRAIC DETAILS FOR THE VARIOUS MIXING RULES

In this appendix is shown the summary of algebraic expressions for the EOS parameters *a* and *b* and for the fugacity coefficient expressions for mixtures for each of the various mixing rules considered in the Chapter 3. The expressions presented in this Appendix are used in VLE calculations.

1. Equations of state models for vapor-liquid phase equilibrium calculations

The criterion of fugacity of vapor and liquid must be equal for a VLE calculation. This equilibrium relation is expressed as:

$$\overline{f}_i^L\left(T,P,x_i\right)=\overline{f}_i^V\left(T,P,y_i\right) \tag{1}$$

where $\overline{f}_i$ is the fugacity of species *i* in homogeneous liquid or vapor mixtures, the overbar to indicate a property of a species in a mixture, and the superscripts *L* and *V* represent the liquid and vapor phases, respectively. Also T and P are the absolute temperature and pressure and *x* and *y* are mole fractions (of species *i*) in the liquid and vapor, respectively. The eqn. (1) can be conveniently expressed for both phases in fugacity coefficient form, as follows:

$$x_i\overline{\phi}_i^L\left(T,P,x_i\right)=y_i\overline{\phi}_i^V\left(T,P,y_i\right) \tag{2}$$

Here the fugacity coefficient for specie *i* in a mixture from an equation of state can be obtain as:

$$\ln\left(\overline{\phi}_i\right)=\ln\left[\frac{\overline{f}_i\left(T,P,z_i\right)}{z_iP}\right]=\frac{1}{RT}\int_{V=\infty}^{V}\left[\frac{RT}{V}-\left(\frac{\partial P}{\partial N_i}\right)_{T,V,N_{i\neq j}}\right]dV-\ln\left(Z\right) \tag{3}$$

where z_i is the molar fraction for both phases and when the eqn. (3) is applied to the vapor phase y_i, is substituted; for the liquid x_i is used instead.

The PR EOS is used to obtain $\underline{V}$ or, equivalently, Z in the eqn. (3).

$$P=\frac{RT}{\underline{V}-b}-\frac{a\left(T\right)}{\underline{V}\left(\underline{V}+b\right)+b\left(\underline{V}-b\right)} \tag{4}$$

When the eqn. (4) is solved at a selected *T,* and *P*, and composition, three volumes roots are obtained at temperatures less than the critical temperature.

2. Huron-Vidal Mixing Rule (HVO)

In the Huron-Vidal mixing rule the mixture EOS parameters are given as:

$$b = \sum_i z_i b_i \tag{5}$$

the eqn. (5) is identical to van der Waals mixing rule parameter and for the *a* parameter is giving as:

$$a = b\left[\sum_i z_i \frac{a_i}{b_i} + \frac{G_\gamma^{ex}(T, z_i)}{C}\right] \tag{6}$$

In this case the fugacity coefficient of species *i* in a mixture become:

$$\ln\left(\bar{\phi}_i\right) = \frac{b_i}{b}(Z-1) - \ln(Z-B) - \frac{1}{2\sqrt{2}}\left(\frac{a_i}{b_i RT} + \frac{\ln\gamma_i}{C}\right)\ln\left(\frac{Z+\left(1+\sqrt{2}\right)B}{Z+\left(1-\sqrt{2}\right)B}\right) \tag{7}$$

In the eqn. (7) the compressibility factor *Z* is computed from the PR EOS.

3. The modified Huron-Vidal first order mixing rule (MHV1)

In this mixing rule the expressions for the *b* parameter is the same as the HVO mixing rule presented in the eqn. (5). The parameter *a* is giving as:

$$a = bRT\left\{\sum_i z_i \frac{a_i}{b_i RT} + \frac{1}{q_1}\left[\frac{G_\gamma^{ex}(T, z_i)}{RT} + \sum_i z_i \ln\left(\frac{b}{b_i}\right)\right]\right\} \tag{8}$$

where q_1 is an empirical parameter obtained by fitting pure component information. The fugacity coefficient of species *i* in a homogeneous solution is:

$$\ln\left(\bar{\phi}_i\right) = \frac{b_i}{b}(Z-1) - \ln(Z-B) - \frac{1}{2\sqrt{2}}\left(\frac{a_i}{b_i RT} + \frac{\ln\gamma_i}{q_1} + \frac{1}{q_1}\ln\left(\frac{b}{b_i}\right) + \frac{1}{q_1}\left(\frac{b_i}{b} - 1\right)\right)\ln\left(\frac{Z+\left(1+\sqrt{2}\right)B}{Z+\left(1-\sqrt{2}\right)B}\right) \tag{9}$$

4. Modified Huron-Vidal second order mixing rule (MHV2)

In this mixing rule the eqn. (5) is used again for the *b* parameter. The parameter *a* is obtained by solving the following expression for $\alpha = a/bRT$:

$$q_1\alpha^2 + q_1\alpha + \left[-q_1 \sum_i z_i\alpha_i - q_2 \sum_i z_i\alpha_i^2 - \frac{G_\gamma^{ex}(T, z_i)}{RT} \right] - \sum_i z_i \ln\left(\frac{b}{b_i}\right) = 0 \tag{10}$$

The eqn. (10) is quadratic function and have 2 roots, the larger of the two real roots is used for obtain α. In the eqn. (10), q_1 and q_2 are empirical constants obtained by fitting pure component properties. The fugacity expression for *i* in a homogeneous mixtures is:

$$\ln\left(\bar{\phi}_i\right) = \frac{b_i}{b}(Z-1) - \ln(Z-B) - \frac{1}{2\sqrt{2}}\left(\frac{\partial N\alpha}{\partial N_i}\right)\ln\left(\frac{Z+\left(1+\sqrt{2}\right)B}{Z+\left(1-\sqrt{2}\right)B}\right) \tag{11}$$

where

$$\frac{\partial N\alpha}{\partial N_i} = \frac{q_1\alpha_i + q_2\left(\alpha^2 + \alpha_i^2\right) + \ln\gamma_i + \ln\left(b/b_i\right) + \left(b/b_i\right) - 1}{q_1 + 2q_2\alpha} \tag{12}$$

5. Orbey-Sandler modification of the Huron-Vidal mixing rule (HVOS)

Again eqn. (5) is used, and the *a* parameter relation is:

$$a = bRT\left\{\sum_i z_i \frac{a_i}{b_i RT} + \frac{1}{C}\left[\frac{G_\gamma^{ex}(T, z_i)}{RT} + \sum_i z_i \ln\left(\frac{b}{b_i}\right)\right]\right\} \tag{13}$$

The fugacity coefficient of species *i* in a mixture become:

$$\ln\left(\bar{\phi}_i\right) = \frac{b_i}{b}(Z-1) - \ln(Z-B) - \frac{1}{2\sqrt{2}}\left(\frac{a_i}{b_i RT} + \frac{\ln\gamma_i}{C} + \frac{1}{C}\ln\left(\frac{b}{b_i}\right) + \frac{1}{C}\left(\frac{b_i}{b} - 1\right)\right)\ln\left(\frac{Z+\left(1+\sqrt{2}\right)B}{Z+\left(1-\sqrt{2}\right)B}\right) \tag{14}$$

6. Wong-Sandler mixing rule (WS)

In the Wong-Sandler mixing rule the EOS parameters for a homogeneous liquid or vapor mixture is computed from:

$$b = \frac{\sum_i \sum_j z_i z_j \left(b - \frac{a}{RT}\right)_{ij}}{1 - \sum_i z_i \frac{a_i}{b_i RT} - \frac{G_\gamma^{ex}(T, z_i)}{CRT}} \tag{15}$$

with

$$\left(b-\frac{a}{RT}\right)_{ij}=\frac{\left(b-\frac{a}{RT}\right)_i+\left(b-\frac{a}{RT}\right)_j}{2}\left(1-k_{ij}\right) \tag{16}$$

and

$$a=b\left[\sum_i z_i\frac{a_i}{b_i}+\frac{\underline{G}_\gamma^{ex}\left(T,z_i\right)}{C}\right] \tag{17}$$

In these equations, $\underline{G}_\gamma^{ex}$, the molar excess Gibbs free energy obtained from any excess free energy model, is a function of temperature and composition only. The *C* term is the EOS-dependent constant, for the PR EOS $C=\ln\left(\sqrt{2}-1\right)\Big/\sqrt{2}$. The fugacity coefficient expressions for species *i* in a mixture for the WS mixing rule is:

$$\ln\left(\bar{\phi}_i\right)=\frac{1}{b}\left(Z-1\right)\left(\frac{\partial Nb}{\partial N_i}\right)-\ln\left(Z-B\right)+\frac{a}{2\sqrt{2}bRT}\left(\frac{1}{a}\left(\frac{1}{N}\frac{\partial N^2a}{\partial N_i}\right)-\frac{1}{b}\left(\frac{\partial Nb}{\partial N_i}\right)\right)\ln\left(\frac{Z+\left(1-\sqrt{2}\right)B}{Z+\left(1+\sqrt{2}\right)B}\right) \tag{18}$$

The partial derivatives of a_m and b_m are:

$$\left(\frac{\partial Nb}{\partial N_i}\right)=\frac{1}{\left(1-D\right)}\left(\frac{1}{n}\frac{\partial N^2Q}{\partial N_i}\right)-\frac{Q}{\left(1-D\right)^2}\left(1-\frac{\partial ND}{\partial N_i}\right) \tag{19}$$

$$\frac{1}{RT}\left(\frac{1}{N}\frac{\partial N^2a}{\partial N_i}\right)=D\left(\frac{\partial Nb}{\partial N_i}\right)+b \tag{20}$$

with the partial derivates of Q and D given by:

$$\left(\frac{1}{N}\frac{\partial N^2Q}{\partial N_i}\right)=2\sum_j z_j\left(b-\frac{a}{RT}\right)_{ij} \tag{21}$$

$$\left(\frac{\partial ND}{\partial N_i}\right)=\frac{ai}{biRT}+\frac{\ln\gamma_i}{C} \tag{22}$$

$$l\,\mathrm{n}\,\gamma_i=\frac{1}{RT}\frac{\partial N\underline{A}^{ex}}{\partial N_i} \tag{23}$$